MODELING AND CONTROL OF A THREE-EVAPORATOR AIR CONDITIONING (TEAC) SYSTEM WITH AN EMPHASIS ON IMPROVED INDOOR HUMIDITY CONTROL

YAN HUAXIA

Ph.D

The Hong Kong Polytechnic University

2016

The Hong Kong Polytechnic University

Department of Building Services Engineering

Modeling and Control of a Three-evaporator Air Conditioning (TEAC) System with an Emphasis on Improved Indoor Humidity Control

YAN Huaxia

A thesis submitted in partial fulfillment of the requirements for the Degree of Doctor of Philosophy

May 2016

Certificate of Originality

I hereby declare that this thesis is my own work and that, to the best of my knowledge and belief, it reproduces no material previously published or written, nor material that has been accepted for the award of any other degree or diploma, except where due acknowledgement has been made in the text.

YAN Huaxia

Department of Building Services Engineering

The Hong Kong Polytechnic University

Hong Kong SAR, China

May 2016

Abstract

Multi-evaporator air conditioning (MEAC) systems featuring variable refrigerant flow, with a three-evaporator air conditioning (TEAC) system being a typical example, have increasingly become attractive. This is because MEAC systems have a number of advantages such as higher energy efficiency and system design and installation flexibility.

Although both a single-evaporator air conditioning (SEAC) system and an MEAC system are operated based on the same vapor compression cycle, there exist a number of noticeable differences between the two. Usually in an MEAC system, there are two or more indoor units (IU) installed in parallel without any pressure regulators, which results in strongly coupled operational parameters in each IU. Although there have been studies on the relationships among the coupled operating parameters in an MEAC system, most of them were simulation based. No previous experimental based studies on the operating characteristics of MEAC systems having more than two evaporators may be identified in the open literature. On the other hand, for buildings located in hot and humid climates such as Hong Kong, controlling indoor air humidity at an appropriate level is critically important since this directly affects building occupants' thermal comfort, indoor air quality and the operating efficiency of the building air conditioning

installations. Although MEAC systems worth many billions of dollars are sold worldwide, only a very limited number of capacity control algorithms for MEAC systems can be identified in the open literature, with most of them focusing on the control of indoor air temperature only. Furthermore, there is a lack of experimentally validated dynamic mathematical MEAC models which can better understand the complex coupled operating characteristics and develop novel capacity controller for MEAC systems for improved control accuracy and higher energy efficiency.

Therefore, a programmed research work on the modeling and control of a TEAC system, with an emphasis on improved indoor humidity control, has been carried out and the study results are presented in this thesis.

This thesis begins with reporting the development of an experimental TEAC system, consisting of three indoor spaces (IS) and one outdoor space. The experimental TEAC system was operated by a computerized logging and control supervisory system. All its major operating parameters can be real-time measured and recorded using high precision measuring devices. The availability of the experimental TEAC system would help facilitate studying the operating characteristics of a TEAC system, experimentally validating a dynamic TEAC mathematical model to be developed and developing novel capacity controllers for a TEAC system with an emphasis on indoor humidity control.

Secondly, the thesis presents the results of two Sets of specifically designed experiments on the operating characteristics of the experimental TEAC system. In the first Set, changes in the operating parameters in one of the three IUs/ ISs were introduced, but that in two of the three IUs/ ISs in the second. Similar coupling effects of mutual influences reported in previous dual-evaporator air conditioning (DEAC) systems may also be observed in the first Set. However, when the operating parameters in two of the three IUs/ ISs were varied, the coupling effects became more complicated, with mutual influences being more remarkable than that in the first Set with even less variation magnitude. Furthermore, the operating characteristics on both the refrigerant side and air side of each IU/ IS in the experimental TEAC system were also studied, which is the first of its kind in the open literature.

Thirdly, the development of a dynamic mathematical model for the experimental TEAC system is presented. The model was built based on the sub-models of major system components in the TEAC system, including a variable speed compressor, an air-cooled condenser, three electronic expansion valves, three IUs and ISs. Unlike all other reported TEAC models, both sensible and latent heat balances on the air side of all IUs were specifically taken into account in the TEAC model developed. The model was experimentally validated using the experimental TEAC system. Model predictions were found to be within ±6% of the measured values, suggesting that the model developed

was capable of simulating both the steady state and dynamic operation of a TEAC system with an acceptable accuracy.

Finally, the development of a novel capacity controller for the experimental TEAC system for improved indoor humidity control is reported. The novel controller was developed by integrating two previously developed control algorithms, one for a DEAC system for temperature control and the other for an SEAC system for improved indoor humidity control. Both simulative and experimental controllability tests were carried out, using the validated TEAC model and the experimental TEAC system, respectively. The controllability test results showed that, with the novel controller, improved control over indoor air humidity and better energy efficiency for the TEAC system could be obtained, as compared to the use of traditional On-Off controllers extensively used in MEAC systems.

Acknowledgements

I must express my sincere grateful thanks to my Chief Supervisor, Professor Deng Shiming from Department of Building Services Engineering (BSE), The Hong Kong Polytechnic University, for his readily available supervision, invaluable suggestions, patient guidance and continuous helps throughout the course of my study.

My special thanks go to the Research Grant Council (RGC) of Hong Kong and the Hong Kong Polytechnic University for financially supporting this research work (PolyU 5146/12E). I would like to thank Dr. Chan Ming-yin, Dr. Pan Dongmei, Dr. Li Zhao, Mr. Xia Yudong and Ms. Wang Yan for their helps during my study. I would like also to thank the technicians in the heating, ventilation and air conditioning (HVAC) Laboratory of the BSE Department for their assistances in the experimental work.

I also wish to thank Professor Wang Xinlei of University of Illinois at Urbana-Champaign, USA, for accepting me as a visiting student to his research laboratory in February to May, 2016.

Last but not the least I wish to express my gratitude and love to my family for their supports, patience and understandings.

Table of Contents

List of Figures

List of Tables

Nomenclature

Variable	Description	unit
A	Opening area of an EEV; or the transfer area	m^2
C_d	Flow coefficient of an EEV	DL
Cp	Specific heat at constant pressure	kJ/(kg·K)
D	Tube diameter	m
E	Control signal	DL
f	Friction factor coefficient for refrigerant pipe	DL
g	Air moisture content	kg/(kg dry-air)
g_r	Refrigerant mass flux	kg/(s·m^2)
h	Enthalpy	kJ/kg
j	Colburn factor	DL
K_{EEV}	Valve opening per unit of pulse output	m^2/Pulse
l	Tube length	m
$LMTD$	Log mean temperature difference	K
m	Mass flow rate	kg/s
M	Mass	kg
n	Compressor speed	r/min
P	P-ressure	Pa
ΔP	Pressure difference	Pa
Pr	Prandtl number	DL
Q	Heat transfer	W

Q_l	Latent cooling load	kg/s
Q_s	Sensible cooling load	W
q	Heat transfer flux	W/m^2
t	Time	s
T	Temperature	ºC
ΔT	Dead-band for temperature control	ºC
v	Velocity	m/s
V	Space volume	m^3
$\dot{V}_d$	Theoretical displacement volumetric of a compressor	m^3/rec
w_{com}	Indicated specific work to the compressor	J/kg
x_i	The ratio of refrigerant mass flow rate at a L-period to that at an H-period	DL
Z	Refrigerant void fraction	DL
α	Convective heat transfer coefficient	$W/(m^2 \cdot K)$
β	Compression index	DL
η_i	Indicated coefficient of compressor	DL
λ	Displacement coefficient	DL
ρ	Density	kg/m^3
ξ	Dehumidifying augmentation factor	DL

Note: DL: Dimensionless

Subscripts

a	Air
c	Condenser/ condensing
com	Compressor
ds	De-superheating region
dry	Dry-cooling
e	Evaporator/ evaporating
fl	Fittings and pipeline
i	Inside tube
l	Liquid refrigerant
m	Metal
o	Outside tube
r	Refrigerant
set	Setting point
sb	Sub-cooled region/ degree of sub-cooling
sh	Superheated region/ degree of superheat
tp	Two-phase region
tu	Tube
v	Vapor refrigerant
wet	Wet-cooling
$\__i$	The i^{th} evaporator

List of Abbreviations

A/C	Air-conditioning
ANN	Artificial neural networks
A SHR	Application sensible heat ratio
COP	Coefficient of performance
DDC	Direct digital control
DEAC	Dual-evaporator air-conditioning
DS	Degree of superheat
DX	Direct-expansion
EER	Energy efficiency ratio
EEV	Electronic expansion valve
E SHR	Equipment sensible heat ratio
HVAC	Heating, ventilation and air conditioning
H-L	High-low
IAQ	Indoor air quality
IS	Indoor space
IU	Indoor unit
LGU	Load generating unit
LMTD	Log mean temperature difference
MEAC	Multi-evaporator air-conditioning
MIMO	Multi-input multi-output
PMV	Predicted mean vote and

PPD	Predicted percentage of dissatisfied
RAC	Refrigeration and air conditioning
RH	Relative humidity
SEAC	Single-evaporator air conditioning
SHR	Sensible heat ratio
SISO	Single-input single-output
TEAC	Three-evaporator air-conditioning
TEV	Thermostatic expansion valve
VRF	Variable refrigerant flow
VRV	Variable refrigerant volume

Chapter 1

Introduction

With the improvement in living standards, air conditioning (A/C) technology has been extensively applied to buildings to provide occupants with a thermally comfortable environment. Consequently, energy use for A/C has significantly increased over the last few decades. It is therefore very important to develop energy conscious A/C technology to achieve energy saving and contribute to sustainability. Multi-evaporator air conditioning (MEAC) system, which may also be called multi-split air conditioning systems or variable refrigerant flow/ variable refrigerant volume (VRF/ VRV) systems in the open literature, may be regarded as one of the energy conscious A/C technologies.

Although both a single-evaporator air conditioning (SEAC) system and an MEAC system are operated based on the same vapor compression cycle and both are of direct expansion (DX) type, there exists a number of noticeable differences between the two. Usually in an MEAC system, there are two or more evaporators (or indoor units) installed in parallel without any pressure regulators, which results in strongly coupled operating parameters in each indoor unit (IU). Although the coupling effects of the operating parameters in dual-evaporator air conditioning (DEAC) systems have been extensively studied, no detailed experimental studies on operating characteristics of an

MEAC system with more than two IUs may be identified in the open literature. However, the operating characteristics are important references for the optimization of design and developments of appropriate capacity controllers for MEAC systems.

On the other hand, only a limited number of reported studies on the modeling and control of MEAC systems may be identified in the open literature. Currently, most MEAC systems are operated for controlling indoor air temperature only without appropriately controlling indoor air humidity. The potential of MEAC technology in achieving energy saving has not yet been fully explored. Therefore, it is necessary to develop a novel capacity controller for an MEAC system, not only to control indoor air temperature but also to achieve an improved indoor humidity control, when compared to using On-Off based temperature control by most current MEAC systems.

Therefore, a study on the modeling and control of a TEAC system, with an emphasis on improved indoor humidity control, has been carried out and the study results are presented in this thesis. To begin with, a comprehensive literature review on a number of important issues related to the modeling and control of MEAC systems is presented in Chapter 2. Firstly, detailed configurations for an MEAC system with respect to its components are described. A review on the previous studies on the operating performances of MEAC systems is then presented. This is followed by reporting the

previous studies on the modeling of MEAC systems and their major components. Fourthly, previous studies on various control strategies for MEAC systems and indoor humidity control issues related to the use of DX A/C systems are reviewed. Furthermore, the issues related to the indoor thermal comfort control and energy consumption when using MEAC systems are also discussed. Several important issues, where further in-depth research studies relating the use of MEAC systems are required, have been identified and are summarized in Conclusion.

In Chapter 3, following the required further research work identified in the comprehensive literature review presented in Chapter 2, a proposal for the research work presented in this thesis is presented, including background, objectives and the methodologies to be used in the research work.

Chapter 4 presents the development of an experimental three-evaporator air conditioning (TEAC) system. The experimental TEAC system consisted of three indoor spaces (IS) and one outdoor space. A schematic diagram for the experimental TEAC system and the detailed specifications for its major components and the instrumentation used are included. The availability of the experimental TEAC system is considered essential in carrying out the research work proposed in Chapter 3.

Chapter 5 presents an experimental study on the operating characteristics on both the refrigerant side and air side of the experimental TEAC system described in Chapter 4. Two specially designed test Sets were carried out to study the influences of step changes in certain operating parameters in one or two of the three IUs/ ISs on the operating characteristics of the TEAC system. Coupling effects among operating parameters were observed. When the operating parameters in two of the IUs/ ISs were varied, coupling effects became more complicated as compared to that varied in only one IU/ IS.

Chapter 6 reports on the development of a dynamic mathematical model for the experimental TEAC system. The TEAC model was built on sub-models of major system components in the TEAC system, including a compressor, an air-cooled condenser, three electronic expansion valves (EEV), three IUs and ISs. Unlike all other reported TEAC models, both sensible and latent heat balances on the air side of all IUs were specifically taken into account in the TEAC model developed. The TEAC model was experimentally validated using the experimental TEAC system, with an acceptable modeling accuracy.

In Chapter 7, the development of a novel capacity controller for the experimental TEAC system for improved indoor humidity control is reported. The novel controller was developed by integrating two previously developed control algorithms, one for a DEAC

system for temperature control only and the other for an SEAC system for improved indoor humidity control. Both simulative and experimental controllability tests were carried out and the controllability test results showed that, with the novel controller, improved control over indoor air humidity and better energy efficiency for the TEAC system could be achieved, as compared to the use of a traditional On-Off controller extensively used in MEAC systems.

Finally, the Conclusions of the thesis and the proposed future work are presented in Chapter 8.

Chapter 2

Literature review

2.1 Introduction

A/C systems have been extensively used in buildings to provide occupants with thermally comfortable environment. Consequently, energy use for A/C has significantly increased over the last few decades. It has been reported that energy used for building cooling and heating accounted for more than half of the total energy use in commercial and public buildings in many parts of the world [Lam 2000]. It is therefore very important to develop energy conscious A/C technology to achieve energy saving and contribute to sustainability.

DX based MEAC systems may be regarded as one of the energy conscious A/C technologies. The use of DX A/C systems has become widespread in buildings, in particular in small- to medium-scaled buildings. Compared to chilled-water based central A/C systems, DX A/C systems are simpler, energy efficient and generally cost less to own and maintain [Amarnath and Blatt 2008]. No air duct or chilled water piping is required for a DX A/C system. Its DX evaporator is used directly as a cooling and dehumidifying coil to simultaneously cool and dehumidify the air passing through it.

For an MEAC system, there will be at least two IUs but only one outdoor unit. Consequently, the use of MEAC systems can help reduce the space requirement and complexity for installing an outdoor unit and help improve the appearance of buildings' external facade. Moreover, an MEAC system could be operated with some of its IUs providing cooling and others providing heating, implying a greater flexibility.

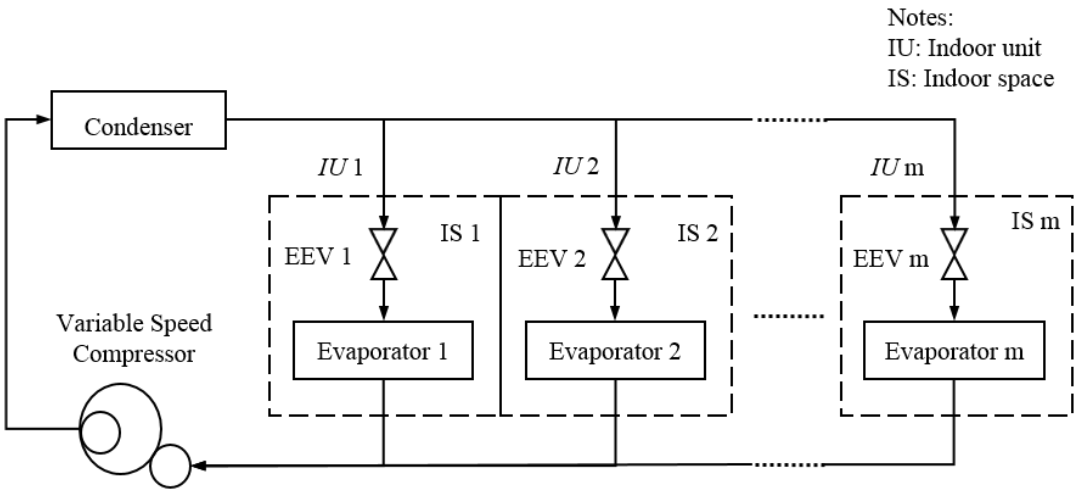

Fig. 2.1 Configuration of an MEAC system

Fig. 2.1 shows schematically the configuration of a typical MEAC system, which consists of an outdoor unit and multiple IUs. Inside each IU, there are a DX evaporator, an EEV and a supply fan. The outdoor unit houses a compressor which is usually of variable speed type, and a condenser, usually air cooled.

A detailed literature review on a number of issues related to MEAC systems has been

carried out and the review outcomes are presented in this chapter. Firstly, a detailed description of the configuration of an MEAC system as well as its major components is presented. A review on the previous studies on the operating characteristics of MEAC systems is then reported. This is followed by reviewing the previous modeling developments for MEAC systems and their major components. Fourthly, previous studies on developing various control strategies for MEAC systems and issues related to indoor humidity control using DX A/C systems are reviewed. Furthermore, the issues related to indoor thermal comfort and energy consumption when using MEAC systems are also discussed. Several important issues, where further in-depth research work for operating and controlling MEAC systems is required, have been identified and are summarized in Conclusion.

2.2 Configuration of MEAC systems

There are a number of IUs and one outdoor unit in an MEAC system. The IUs are located in each IS and connected to the outdoor unit in parallel using insulated refrigerant pipelines. The refrigerant leaving all the IUs mixes before being sucked into compressor. In this section, the detailed configurations of both an outdoor unit and IUs in an MEAC system, as well as the connection between the outdoor unit and IUs to form a complete system will be firstly described. Furthermore, the MEAC systems equipped

with certain special features will also be covered in this section.

2.2.1 Outdoor unit

An outdoor unit in an MEAC system mainly consists of two parts: a compressor and a condenser.

A variable-speed compressor is usually used in an MEAC system to meet cooling or heating needs in multiple ISs. Normally, its speed variation is achieved by using a frequency inverter [Aynur 2010]. As compared to On-Off operated compressors, inverter-driven compressors offer better control performances in terms of continuous temperature control. Compressor speed and thus its discharge refrigerant mass flow rate can be continually modulated to match varying space cooling loads [Afify 2008]. Furthermore, variable speed operation for a refrigerating compressor can also lead to better energy efficiency [Qureshi and Tassou 1996, Cuevas and Lebrun 2009].

Although the use of inverter technology can help achieve better capacity control in MEAC systems, an inverter may emit electronic noise into an electric system and, therefore, interfere the normal operation of electronic equipment [Hu and Yang 2005]. In addition, the cost of variable speed compressors is usually high. Recently, digital scroll compressors were increasingly utilized in MEAC systems [Vakiloroaya et al.

2014]. The performances of MEAC systems with a digital compressor have been widely examined [Hu and Yang 2005, Huang et al. 2008, Tu et al. 2011, Zhang and Zhang 2011]. Hu and Yang [2005] developed an MEAC system using a variable refrigerant volume digital scroll compressor. Both cost effectiveness and energy efficiency ratio (EER) of the developed system were compared with that of an inverter-driven system and a 20% energy saving was concluded when five IUs were handled. At a fixed input power, the digital scroll compressor based MEAC system could output 17–100% of its rated cooling capacity, which was wider than a frequency inverter based MEAC system (48–104%). The maximum EER in an inverter-driven MEAC system usually occurred at a partial output point. However, the EER for systems using digital scroll compressor peaked at a full output point, and was lower than that of inverter-driven MEAC systems. Zhang and Zhang [2011] developed and validated a dynamic model for an MEAC system with a digital scroll compressor to evaluate its efficiency. Key factors were suggested when evaluating the system efficiency under part-load conditions.

Twin rotary compressors were also used in MEAC systems for capacity regulation. Fujita et al. [1992] studied the capacity control of a DEAC system using EEVs as throttling devices. Two single-speed rotary compressors were connected in parallel to regulate refrigerant flow rates in order to handle the cooling loads in two ISs. Strategies to improve indoor thermal comfort and achieve energy saving were also reported.

Okuzawa [1992] used a horizontal twin rotary compressors in an MEAC system to improve the responses to load variations from four to six ISs, and an optimized degree of superheat (DS) control for the MEAC system was obtained by using a PI control method. Xia et al. [2004] studied the performance of an MEAC system having two rotary compressors when only dealing with sensible cooling. It was found that under part load conditions, the system's coefficient of performance (COP) did not vary much because the two compressors were installed in parallel, with one variable speed operated and the other constant speed operated.

Basically, all condensers in MEAC systems are air-cooled, with most of them using constant speed condenser fans. Recently, MEAC systems with water-cooled condensers are being introduced [Aynur 2010].

Generally, an air-cooled condenser, which is usually a fin-and-tube type heat exchanger, is cooled by the ambient air, but a water-cooled condenser, usually a plate type heat exchanger, by cooling water. A water pump and an additional cooling tower are thus required to form a condenser water loop for water-cooled outdoor units. A plate-type condenser connects the condenser loop and the refrigerant circuit. Since water piping is connected indirectly with a refrigerant circuit, there is no restriction on the length of water pipe [Li et al. 2009]. There have been studies on the energy performance of water-

cooled condensers used in MEAC systems. For example, Wang [1997] concluded that the condensing temperature was the main factor affecting the performance difference between an air-cooled condenser and a water-cooled condenser. In an air-cooled condenser, its condensing temperature is mainly influenced by ambient air dry-bulb temperature but in a water-cooled condenser, by ambient air wet-bulb temperature, respectively.

2.2.2 Indoor unit

The IU in an MEAC system mainly consists of an evaporator, an EEV and a circulating air fan.

In an MEAC system, a number of IUs may be connected in parallel to one single outdoor unit. In the 1950s, when ductless-type A/C products were first introduced in Japan, there was only one IU. The number of IUs was increased to eight in 1990s when inverter technology was incorporated into MEAC systems [Dyer 2006]. In around 2015, with the advancement of technology, an MEAC system could operate with up to 128 IUs connected to a single outdoor unit [Daikin 2015].

IUs of different capacities and installation methods can be found. Cooling or heating capacities of IUs range from 1.4 to 17.5 kW. There are different configuration types of

IUs depending on building type and layouts, including window/ wall-mounted type, roof-top type and floor standing type. It is also possible to combine multiple types of IUs with a single outdoor unit [Afify 2008].

Appropriate sensors for measuring air temperature can be found at IUs' supply air outlet for control purpose. The refrigerant mass flow rate passing through an IU is regulated by adjusting its corresponding EEV's opening according to a fixed setting of DS. The function of an EEV in a refrigeration system is similar to that of a thermostatic expansion valve (TEV), except that the refrigerant temperature at the exit of an evaporator is sensed electronically. Although EEVs are more expensive than other types of expansion valves, they gain more and more acceptance due to their advantages, such as a faster response to load variation, a wider range of flow rate regulation and a higher control precision [He et al. 1997, Aprea and Mastrullo 2002]. A further benefit of using EEVs in an MEAC system is that EEVs could be opened or shut down during operation, so it is possible to have individual control of providing A/C in different ISs.

In most cases, a supply fan is used to provide a constant mass flow rate of air in MEAC systems [Koeln et al. 2012]. The supply air fan in an IU in both SEAC and MEAC systems can also be of variable speed type [Li and Deng 2007a, Deng et al. 2009].

2.2.3 Refrigerant piping connecting on outdoor unit and indoor units

The outdoor unit and IUs in an MEAC system are connected to each other through refrigerant pipes and fittings. At present, with improved refrigerant charge and oil management, the total piping length in an MEAC system can be up to 1000m [Daikin 2015]. However, the longer the lengths of refrigerant pipes, the higher the initial and operating costs of an MEAC system. Afify [2008] provided a list of piping lengths and height limits between IUs and an outdoor unit for better design and performances. In buildings where several locations are available for the installation of an outdoor unit, it should be placed as close as possible to the IUs it serves.

2.2.4 MEAC systems with special features

Special features may be incorporated into an MEAC system to meet different requirements at different operating conditions.

2.2.4.1 Ventilation provisions

Since MEAC systems do not usually have any ventilation provisions as required by ASHRAE Standards [Goetzler 2007], additional ventilation measures are usually necessary to be provided to ensure adequate indoor air quality (IAQ), which will increase the cost of MEAC systems. Despite the large number of previous studies on

MEAC systems, there are limited studies on providing ventilation provisions in MEAC systems. This is understandable since most studies focused on the operating and control performances of MEAC systems.

Although Aynur et al. [2006] considered the variation of outdoor air temperature on the performance of an MEAC system, the focus was not on the ventilation provisions of the MEAC system. Performance evaluation of a VRV system integrated with a heat recovery ventilation system was carried out both experimentally [Aynur et al. 2008a and 2008b] and numerically [Aynur et al. 2008c] under various outdoor conditions and operating modes. It was observed that the availability of ventilation provision did not affect indoor air temperature control; instead, it increased indoor moisture content when outdoor air was humid. The cooling load due to ventilation contributed to an increase in system energy consumption; however, the use of heat recovery could achieve 17%–28% energy savings.

Ventilation provisions may be incorporated into an MEAC system in different ways. In humid climates, an additional air handling unit or one of IUs in the MEAC system may be used to pre-condition outdoor air to remove ventilation load. Therefore, an MEAC system would have to only deal with space load and conditioned outdoor air is provided to each IU to ensure satisfactory IAQ [Afify 2008].

However, often a fixed rather than variable outdoor air flow rate is introduced into conditioned zones, resulting in low energy efficiency for MEAC systems as the number of occupants in different rooms may frequently vary. Less attentions were paid to combining the control of both an MEAC system and ventilation provisions. Karunakaran et al. [2010] and Parameshwaran et al. [2010] indicated that both improved thermal comfort and energy saving may be achieved using demand controlled ventilation for MEAC systems, as compared to using normal ventilation. To take the advantages of MEAC systems, an additional DX A/C system was employed to pre-treat outdoor air and then the pre-treated air was supplied to air conditioned zones [Zhu et al. 2013, Zhu et al. 2014a and Zhu et al. 2014b]. As outdoor air flow rate and indoor CO_2 level in all zones were continuously monitored and controlled, over ventilation was avoided and eventually energy use could be reduced.

2.2.4.2 Simultaneous heating and cooling

Generally, an MEAC system can only provide either heating or cooling. A two-pipe (a high pressure refrigerant gas pipe and a low pressure liquid refrigerant pipe) MEAC system can be used for heating and cooling by way of a 4-way valve depending on seasons. However, an MEAC system that can provide simultaneous heating and cooling used three-pipe (a low pressure gas refrigerant pipe in addition to the two-pipe) and

could therefore supply heating and cooling to different zones at the same time [Joo et al. 2011]. An example of zones that may require simultaneous heating and cooling was that in a large building; its exterior zones required heating at cold outdoor weather condition while its interior zones may have cooling load to be removed because of internal heat gain [Amarnath and Blatt 2008].

A three-pipe MEAC system can operate at four modes: cooling-only, heating-only, cooling-principal and heating-principal. It has been shown that the COP of a heat recovery MEAC system is about two times as many as that of a three-pipe system at cooling-only or heating-only mode [Hai et al. 2006]. A 4-way valve is also needed to determine the refrigerant flow direction according to operating modes. Three-pipe and a gas-liquid separator may be also combined as a junction connecting an outdoor unit and several IUs [Lijima et al. 1991]. A further operating mode, called entire heat recovery mode, was also introduced [Joo et al. 2011]. In this mode, the number of IUs providing cooling was the same as that providing heating. All the heat absorbed from cooling-operated IUs was used for heating in heating-operated IUs.

2.3 Operating performances of MEAC systems

Fig. 2.2 shows the typical configurations of an MEAC system and a multi-evaporator

refrigeration system. The main difference between the two lies in that in a multi-evaporator refrigeration system, refrigerant pressure regulators are installed in each evaporator branch, as shown in Fig. 2.2b, enabling different evaporators to be operated at different evaporating pressures. However, the evaporators or IUs in an MEAC system are directly connected in parallel without pressure regulators. Because air humidity in different conditioned rooms severed by an MEAC system is usually not controlled, no pressure regulator is therefore needed to maintain different evaporating temperatures for humidity control.

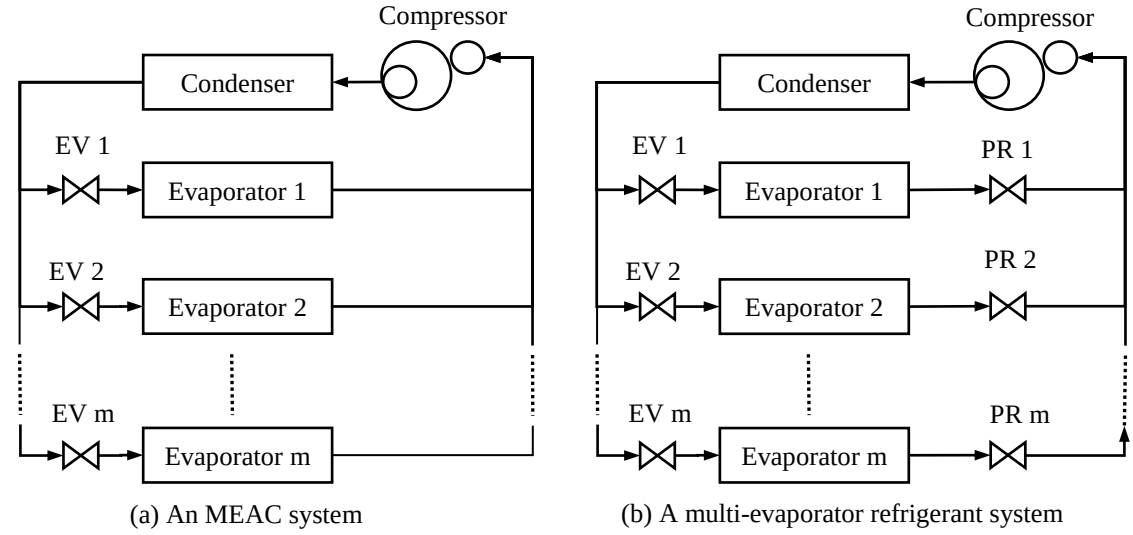

(a) An MEAC system (b) A multi-evaporator refrigerant system

Notes:
EV: Expansion valve PR: Pressure regulator

Fig. 2.2 Schematics of an MEAC system and a multi-evaporator refrigeration system

Consequently, the absence of pressure regulators in an MEAC system makes the cross-coupling effects among different evaporators complicated and a change in the thermal condition in one room may cause changes in the operating parameters such as evaporating pressures and temperatures in all other evaporators in an MEAC system [Lijima et al. 1991]. Therefore, the relationships among operating parameters in an MEAC system, including refrigerant flow distribution, evaporating pressure or temperature and energy efficiency under different cooling load fractions in different conditioned rooms, are highly coupled. This has thus attracted a great deal of research attentions.

2.3.1 Operating characteristics of MEAC systems

The operating characteristics of variable speed DX A/C systems were extensively studied through experiments by Li and Deng [2007a] and Xu et al. [2010]. Experimental results demonstrated that varying compressor and supply fan speeds would directly affect the output cooling capacity and sensible heat ratio (SHR) of a DX A/C system. The air side heat and mass transfer in an IU of an MEAC system is similar to that in the cooling coil in a SEAC system. Therefore, the advancements in SEAC systems may be applicable to IUs in MEAC systems.

He et al. [1997 and 1998] demonstrated that there were strong cross-coupling effects

among various operating parameters in a vapor compression refrigeration system, such as evaporating temperature, condensing temperature and DS, etc. Therefore, a proper coordination between the openings of an EEV and compressor speed would improve the control behavior for DS, and the ability to withstand external disturbances while effectively modulating the system cooling capacity. As the number of evaporators increased, the coupling effects in an MEAC system would become more complicated [Meissner et al. 2014].

Extensive studies have been carried out to investigate the influences of varying compressor speeds and varying indoor cooling loads on the operating performances of MEAC systems. It has been commonly acknowledged that coupling is strong in MEAC systems having two or more evaporators, which is the main hurdle in studying the operating characteristics of MEAC systems [Lee et al. 2002, Xia et al. 2004, Aprea et al. 2004, Shah et al. 2004, Koeln et al. 2012, Koeln and Alleyne 2013]. The experimental study by Choi and Kim [2003] on open-loop response clearly indicated that a change in one IU would definitely affect the operating parameters of others.

Other studies evaluated the operating efficiency of MEAC systems in terms of COP. Park et al. [2001] studied by simulation the operating performances of a DEAC system and found that the compressor power consumption increased with an increased

difference in space load between two rooms, although the total cooling load handled by the DEAC system remained unchanged. Zhou et al. [2007] investigated the operating characteristics of an MEAC system using EnergyPlus, a well-known dynamic building energy simulation program. It was found that the COP of the system increased when it worked at part load conditions. The performances of an MEAC system, which could provide cooling or heating at any time, were tested using three types of evaluating methods and the compressor curve method was suggested as the most effective one [Fujimoto et al. 2011a]. A modified controller was also proposed to improve system's COP [Fujimoto et al. 2011b]. Experimental [Lijima et al. 1991, Hai et al. 2006, Kang et al. 2009 and Joo et al. 2011] and numerical [Shi et al. 2003, Li and Wu 2010] studies suggested a higher COP at heating and cooling principal modes as compared to that at heating or cooling only mode, because both evaporating and condensing capacities were used.

2.3.2 The effects of the refrigerant pipework length of an MEAC system on its operating performance

While the cross-coupling effects among evaporators in an MEAC system have been extensively studied, less attention has been paid to the influence of pressure drop along the refrigerant pipeline in an MEAC system on its operating performance. The pipework in an MEAC system may affect its operating performance in the form of refrigerant

pressure drop along the pipework, which may be ignored or assumed at a fixed value in a SEAC system. However, due to a more complicated pipeline configuration with more fittings, refrigerant pressure drops should be taken into consideration in designing and operating an MEAC system.

Often, due to different pipe lengths used in actual installation, the actual COP value of an MEAC system obtained from field measurements was lower than its theoretical value. The effects of tube length and height difference of pipework were modeled and added to a heat pump system model to predict its steady-state and transient performances [Hirao et al. 1992]. Shao et al. [2008] and Shi et al. [2008] presented a generic model for refrigeration systems based on a two-phase flow network. The model consisted of four basic individual components and connecting pipes, aiming at analyzing the performances of three complex refrigeration systems, i.e., an MEAC system, a heat pump for producing domestic hot water and a multi-unit heat pump dehumidifier. However, the model for pipework was mainly used for predicting refrigerant flow direction and heat transfer, but not on the influence of refrigerant pipelines on system performances.

A dual-evaporator heat pump system was simulated by Cheung and Braun [2014]. The refrigerant pressure drops across heat exchangers and refrigerant pipelines were

evaluated using correlations. Based on previous modeling work of a DX A/C system, a steady-state mathematical model of a DEAC system considering the influence of refrigerant pipeline length on system operational performances was developed and validated [Pan et al. 2012]. Numerical results indicated that the system's COP decreased with an increase in the refrigerant pipeline length. Results of the layout optimization for the DEAC system also suggested that for a DEAC system, its highest COP would be resulted in when the outdoor unit was located equally between the two IUs and its lowest COP when the outdoor unit was located close to either of the IUs. Furthermore, an optimization layout of a DEAC system was recommended for the best possible system efficiency [Pan et al. 2014]. However, the study focused on a DEAC system, and the height differences of pipework were not considered. Hirao et al. [1992] found that the height differences of pipework in an SEAC system could cause serious refrigerant flashing. Therefore, it has been suggested that height differences of pipework should be taken into consideration when evaluating the actual operating performances of an MEAC system.

2.3.3 The operating characteristics of EEVs on the performances of an MEAC system

Currently, it still remains problematic to provide each evaporator in an MEAC system with the correct amount of refrigerant mass flow. In an MEAC system, its expansion

valves not only work as throttle devices but also distribute refrigerant mass flow to each evaporator. In many cases, EEVs are preferred in comparison with TEVs, especially when dealing with varying space load [Choi and Kim 2003]. The measured performance data of EEVs used in variable-speed MEAC systems were however limited in the literature.

Park et al. [2001] numerically studied the impacts of varying compressor speed and EEV openings on the output cooling capacity of a DEAC system. The total output cooling capacity of the DEAC system was controlled by the supply operating frequency of compressor. The simulation results showed that, at a fixed compressor speed, the DEAC system could provide variable cooling capacity by changing EEV openings to satisfy the cooling load in each IU. If the cooling loads in two rooms were different, the main control parameters of the system were EEV openings for varying the refrigerant mass flow rate to the two evaporators. Park et al. [2007] further noticed that for an MEAC system, the lowest operating compressor speed satisfying the imposed cooling load on the system should be selected in order to achieve the highest possible COP. A set of equations obtained using linear regression were given by Hu and Yang [2005], who tested and obtained the relationship between the opening of EEVs and the percentage output capacity of a variable-capacity scroll compressor in an MEAC system having five IUs.

Choi and Kim [2003] studied the coupled operating performances of a DEAC system when changing EEV openings. It was shown that at a constant compressor speed, the cooling capacity of one IU was increased when the opening of its matching EEV was increased. However, the cooling capacity of the other IU was lowered even the opening of its matching EEV remained unchanged. Therefore, it was suggested that two EEVs should be simultaneously controlled to obtain an appropriate capacity balance between the two IUs in a DEAC system, even though the cooling load variation only occurred in one IS. It was also suggested that the maximum cooling capacity could be achieved when the DS was maintained at 4 °C. Therefore, the DS should be controlled within a narrow range by adjusting both EEVs, but the compressor speed should be adjusted according to cooling load in each IS.

In practice, there can be two choices for locating an EEV, next to an IU or within an outdoor unit together with all other EEVs. Since refrigerant status would undergo significant phase change when passing through an EEV, different pressure drops may result in for these two different locations, even with the same pipe lengths and diameters. However, the impacts of the two different EEV locations on the operating performances of an MEAC system have not been addressed in the open literature.

2.4 Modeling of MEAC systems

As mentioned earlier, a large number of previous studies on MEAC systems can be identified in the open literature. These studies are either experimental or simulation based. While most simulation studies dealt with multi-evaporators, all experimental studies used a limited number of evaporators (up to 5), with two being the most common number. Simulation has become increasingly popular because it could not only save the research cost, but also help understand the operating characteristics of a physical system under study over its entire operating range.

A large number of published studies in the open literature are available on modeling both the steady state and dynamic behaviors of A/C systems. A number of steady state models were built based on popular building simulation software packages, such as EnergyPlus [Li and Wu 2010, Raustad 2013 and Wang 2014] and TRNSYS [Shen and Rice 2012, Shen et al. 2013, Zhu et al. 2013 and 2014a], to investigate the operating performances of MEAC systems. With an additional module to represent transient system responses, an MEAC system could also be dynamically modeled. Dynamic models were extensively used to develop control strategies and to diagnose system faults.

It should be noted that MEAC systems have been simulated in different methods with however few of them being experimentally validated. For those validated steady-state models, their validations were usually based on comparing the simulation results with experimental data in terms of cooling capacity [Li et al. 2010, Raustad 2013], power consumption [Aynur et al. 2008c and Zhou et al. 2008] or COP [Zhou et al. 2008, Li et al. 2010 and Raustad 2013]. Validation for dynamic MEAC system models was based on comparing the measured and simulated system transient responses following a step change in system operating parameters, such as compressor speed, IS cooling load and EEV opening [Shah et al. 2004 and Shao et al. 2012].

On the other hand, existing models can be classified into physical and empirical. A physical model, which can reflect the physical insight of a real system, is built based on physical principles and expressed using mathematic equations. An empirical model can be established using different modeling methods such as regression analysis, polynomial curve fit, artificial neural networks (ANN) and system identification, with possibly high adaptability. There exist however some unsolvable problems in an empirical modeling method because of the imperfection of the method itself and the limitation of a model developer's understandings of the input-output relationships of a process to be modeled [Ding 2007].

The complete model for a typical MEAC system is usually made of sub-models for both its refrigeration cycle and conditioned ISs. Decentralized method is commonly adopted in developing modules for individual component in a vapor compression refrigeration cycle so as to form a sub-model for the complete refrigeration cycle [Shah et al. 2004].

2.4.1 Sub-models for the refrigeration cycle of an MEAC system

Both an SEAC system and an MEAC system are operated based on vapor compression refrigeration cycle, and consist of four key cycle components, i.e., a compressor, one or more evaporators, the same number of expansion valves as that of evaporators and finally a condenser. Hence, modular-based modeling for the refrigeration cycle in an MEAC system is possible. Essentially, the same component modules might be used for either an SEAC system or an MEAC system. It is commonly acknowledged that the mathematical sub-model of a complete refrigeration cycle in an MEAC system is more complicated than that in an SEAC system due to the fact that two or more evaporators are connected in parallel so that system operating parameters are mutually affected and thus highly coupled.

By linking the modules of key cycle components and the connecting piping, a sub-model for the refrigeration cycle in an MEAC system may therefore be derived, and expressed by a set of ordinary differential equations and algebraic correlations. An

extensive survey of earlier developments of both dynamic and steady-state modules of key components in refrigeration systems was reported by Welsby et al. [1988]. In this section, the modeling for the key components in a refrigeration cycle is separately reviewed as follows.

2.4.1.1 Compressor modeling

Compressor modeling plays an important role in the simulation of A/C and refrigeration systems. Typically, a compressor simulation module calculates the refrigerant mass flow being circulated in a vapor compression cycle. Compressor speed should be taken into consideration when modeling a variable speed compressor.

Compressor modules have been reviewed and categorized [Rasmussen and Jakobsen 2000]. Compared to heat exchangers, the dynamics of a compressor may be negligible so that quasi-steady modeling is usually adopted [Rasmussen and Alleyne 2004]. This is achieved by assuming that a compressor reaches its specified operating speed instantly. A compressor may also be represented dynamically, where the changes in compression chamber volume and refrigerant properties are described as the continuous functions of time. A parametric analytical module for a centrifugal compressor was developed to predict its operating performances from geometric information [Jiang et al. 2006].

Generally, a polytropic compression process can be assumed and a mathematical module for a compressor established by using the traditional thermodynamic approach [Browne and Banasal 1998]. It assumes that a polytropic compression could represent all the processes from suction to discharge in a compressor.

On the other hand, a compressor may also be represented by an empirical correlation using the actual performance data based on curve fitting or regression analysis. This approach can achieve a better approximation but a set of detailed tested compressor performance data from manufacturers or in-situ tests is required. Li [2013a] proposed a semi-empirical compressor module which was suitable for both single speed compressor and variable speed compressors. The method required an integration of physical based modeling and experimental data.

2.4.1.2 Heat exchanger modeling

Various approaches have been employed to establish modules for heat exchangers used in refrigeration systems, including the distributed-parameter modeling approach [MacArthur and Grald 1987, Jia et al. 1995], the lumped-parameter approach [Chi and Didion 1982, Rasmussen and Alleyne 2004] and partial lumped-parameter approach [Deng 2000].

Generally, to achieve a high modeling accuracy for a heat exchanger, distributed-parameter modeling approach may be used, because it can reflect well the distributed nature of the operating parameters in a heat exchanger [Chen 2005]. However, because of distributed nature, using such a modeling approach is time-consuming with a potentially poor calculation stability.

In the lumped-parameter modeling approach, a heat exchanger is allowed to have time-varying lengths of different regions, which are distinguished according to the refrigerant status. Thus, the refrigerant flow in an evaporator can be divided into two regions since it enters as two-phase liquid and leaves as superheated vapor. The point of transition between the two regions changes dynamically [Rasmussen and Alleyne 2004]. Similarly, a condenser can be divided into three regions, i.e., de-superheating, two-phase and subcooled. The refrigerant properties, and thus heat transfer coefficients, are typically assumed to be constant in each region of a heat exchanger. These regions can be modeled separately based on the refrigerant mass and energy conservation equations. Zhang and Zhang [2006] developed a lump-parameter model for a DX A/C system, using moving boundary approach to describe the transient behavior in its DX evaporator. This model allowed the superheated region in the evaporator to be included or excluded. A time-variant, rather than a constant, mean void fraction was employed to improve the robustness of a traditional moving boundary model under larger disturbances.

2.4.1.3 EEV modeling

In a vapor compression cycle, an EEV acts as a throttling device where the expansion of refrigerant takes place. Mass flow rate of refrigerant passing through an EEV is usually modulated by adjusting its opening area. Commonly, an expansion valve can be represented by a steady-state model due to its small thermal inertia. Refrigerant expansion is generally treated as an isenthalpic process so that the expansion valve can be modeled using an isenthalpic orifice equation [MacArthur and Grald 1987].

One representative model for EEVs was developed by Damasceno et al. [1990], based on the specifications given by EEVs' manufacturers and the empirical fittings for one set of distributor nozzle and tube size.

Although the throttling mechanism in an EEV is identical to that of a short orifice valve, the flow coefficient is much more complex for an EEV than an orifice because the opening area of the EEV is dynamically adjusted. The characteristics of EEVs are usually obtained through experimental data for different refrigerant fluids. Park et al. [2007] developed an empirical correlation for predicting the mass flow rate passing through an EEV by modifying a single-phase orifice equation with the consideration of EEV's geometries parameters and operating conditions. Li [2013b] modified the

Bernoulli Equation for a short orifice to develop a mass flow coefficient correlation for an EEV by introducing an expansion factor. Only two key parameters (EEV opening and DS) were used to develop the coefficient correlation. Experimental analysis showed that the use of the mass flow coefficient correlation could well describe the refrigerant flow behavior through the EEV with negligible errors.

2.4.1.4 Refrigerant pipework modeling

Fluid resistance in the refrigerant pipework in an SEAC system was usually ignored in previous studies. However, in an MEAC system, since its refrigerant pipework is actually more complex, the fluid resistance must not be simply ignored. When considering the fluid resistances from pipework and fittings, a fluid network theory, which was analogous to an electric network, was employed to model refrigerant distribution characteristics in an MEAC system with 5 IUs [Lu et al. 2009]. It was concluded that the closer an IU was to the center of a fluid network, the less its mass flow rate was deviated from its design value, and vice versa. Pan et al. [2012] reported a numerical study on the effects of refrigerant pipeline length differences in a DEAC system on its operating performances. Similar to the study reported by Lu et al. [2009], refrigerant pipelines were divided into single-phase and two-phase types according to the refrigerant state, and the two types were analyzed separately using the fluid network

theory. The famous Darcy-Weisbach Equation was applied to calculating pressure losses along the pipelines. For the two-phase pipeline, its pressure drops were evaluated not only based on the friction losses similar to that in single-phase pipelines, but also the kinetic energy change caused by refrigerant phase change.

There was a further refrigerant pipeline model developed by Cheung and Braun [2014]. The model assumed that the liquid line and suction line were adiabatic, while the significant heat loss between the hot gas line and surroundings was modeled based on the effectiveness-NTU method.

2.4.1.5 Supply fan modeling

Supply fans move air by forced convection through conditioned spaces for air distribution to achieve the control over indoor air temperature, humidity and air velocity. For HVAC systems, the pressure-volume flow characteristics of a fan can be represented in many different ways. In general, they are described by a set of constant-speed curves for pressure rise versus volume flow rate. For a variable speed blower, fan characteristics at different speeds are obtained through using the performance data from manufacturers or the fan performance law (fan pressure rises being proportional to the square of the change in fan speed). It is noted that ANN method may be used to generate

a polynomial differential equation describing the non-linear characteristics of fans, which proved to be suitable for developing fan control strategies [Mei and Levermore 2002].

2.4.2 Sub-models for indoor spaces in an MEAC system

Real-time control of an HVAC system very often requires the back up of a dynamic model of ISs severed by the HVAC system. Early models available in the literature usually focused on indoor air temperatures under the assumption that room air was well mixed, i.e., a single air node to represent the whole air status in a room. Therefore, air temperature distribution in a zone/ room is uniform and the dynamics of the zone can be modeled using the lumped parameter modeling approach. Kasahara [2000] derived a simplified dynamic model for an air-conditioned space for control analysis, which can provide an indicative temperature distribution inside the space. The whole space under study was divided into five zones and the dynamics of each zone described by a lumped-parameter model.

Yao et al. [2013] developed a lumped-parameter model to investigate the thermodynamic behaviors of indoor air temperature and humidity. Each conditioned space was divided into three typical zones (an air-supply zone, an occupied zone and an air-return zone), and each zone was separately modeled based on energy and mass

conservation equations. Compared to previous single-zone models, a simplified multi-zone room model was much closer to reality.

2.5 Control strategies for MEAC systems

Generally, A/C systems and their control are designed to provide the required capacity control at a higher system efficiency. From the literature to date, there have been limited studies conducted on the control of MEAC systems. Most current research efforts focused on control against indoor air dry-bulb temperature or DS but no studies involving control of indoor air humidity using MEAC systems may be identified.

2.5.1 On-Off control

The most commonly used capacity control method for DX A/C systems was to intermittently run its compressor, e.g., On-Off cycling [Okuzawa 1992], so it was operated either at its full or zero capacity. A number of compressors of different sizes may be connected in parallel to provide different combinations of output capacity options [Fujita et al. 1992].

Early studies on the control of MEAC systems were carried out by Okuzawa [1992]. Constant-speed compressors were On-Off controlled, which was not difficult to

implement. However, its disadvantages were that it was difficult to maintain indoor air temperatures within a suitable range, and refrigerant mass flow rate cannot be distributed precisely.

2.5.2 Advanced control strategies applied to MEAC systems

Recently, the successful application of a variable-speed compressor, EEV and variable speed fan to SEAC systems has opened up the opportunity to incorporate these technologies into MEAC systems. Advanced control strategies, such as fuzzy logic control, system identification and model based predictive control, etc., have also been increasingly applied to MEAC systems.

However, the control scenario in an MEAC system is very different from that in an SEAC system. For example, the precise refrigerant mass flow rate in an SEAC system could be achieved by both adjusting EEV opening based on the DS at evaporator exit and modulating compressor speed according to the IS temperature or evaporating temperature. However, it is much more difficult to apply this control strategy to an MEAC system, since the operating parameters in an MEAC system are strongly coupled and a change in the operating condition in one IU/ IS would significantly affect that in other IUs/ ISs. Therefore, in a number of studies on controlling MEAC systems, Multiple-Input Multiple-Output (MIMO) control strategies were adopted.

The design of a MIMO controller usually requires an accurate dynamic model for an MEAC system. A model-based feedback linearization part was introduced to compensate for the nonlinearity in the dynamics of MEAC systems [He and Asada 2003]. Simulation results showed good control performances in evaporator temperatures and DS under the feedback linearization control approach. Using moving boundary approach, an MEAC system model was developed to investigate both the open-loop behaviors and the closed-loop responses of the MEAC system [Shah et al. 2003 and Shah et al. 2004]. Model validation against data from an experimental DEAC system was also presented. It was shown that, due to the cross-coupling effect among operating variables of different evaporators, the use of an MIMO control strategy led to a better control performance than the use of Single-Input Single-Output (SISO) control strategy in term of DS and evaporating pressure control.

It should be noted that the studies mentioned above were mainly focused on vapor compression cycles of MEAC systems alone. Indoor temperatures in multiple ISs were usually regarded as being constant rather than variable. One of the exceptions was the simulation work by Chen et al. [2005], in which a fuzzy control algorithm was proposed to control indoor temperatures at different operating conditions for an MEAC system with three evaporators and a variable-speed compressor. To improve the control performance using fuzzy logic, a self-tuning modifying factor was incorporated into an

MEAC model. However, the model used for control design was not experimentally validated. A fuzzy logic based controller was also applied to an MEAC system to achieve stable indoor air temperature control and energy savings [Chiou et al. 2009]. But the control algorithms involved were usually complicated and thus costly to develop [Li et al. 2013 and Li et al. 2015].

A novel capacity control algorithm for a DEAC system, which was based on On-Off control of a compressor in an SEAC system, was developed for temperature control [Xu et al. 2013b]. The compressor speed and EEV openings were adjusted according to the indoor air temperatures in two ISs. Experimental tests validated the accuracy and robustness of the control algorithm. However, indoor air temperature may still be subjected to fluctuations under certain operating conditions due to the use of temperature dead-band and time delay for compressor start-up. The controller was further improved to avoid frequent On-Off operation of compressor so as to restrain the temperature fluctuations.

Lin and Yeh [2007a, 2007b, 2009a and 2009b] reported a modeling study on designing a cascade control structure for a TEAC system. The compressor speed and the three EEVs openings were selected as the inputs and the metal temperature of the two-phase region in each evaporator and the associated DS as outputs. It was shown that the

proposed controller could regulate indoor air temperatures and maintain the steady-state DS at acceptable levels. One concern was that the mathematical model was obtained through system identification and the controller developed based on the model may not be applicable to other MEAC systems having different configurations and/ or being operated under other operating conditions.

Elliott and Rasmussen [2009 and 2013] proposed a two-level structure controller for a TEAC system using model predictive control method. A supervisor level sub-controller was developed to regulate indoor air temperatures and calculate set points for cooling capacities and evaporating pressures. A local level sub-controller was developed to regulate the fan speed and EEV openings to meet the set points as required in the supervisor level sub-controller. The controller could be used to trade between the energy efficiency and the fluctuation of air temperatures.

2.6 Humidity control using DX A/C systems

Controlling indoor air humidity at an appropriate level is very important since this affects IAQ and occupants' thermal comfort. Traditionally, a DX A/C system focuses only on the control of space air temperature, with air humidity in the space being passively controlled. Dehumidification is usually the by-product of a cooling process, so

that the indoor air relative humidity (RH) can fluctuate. In this section, several issues related to humidity control using DX A/C systems are reviewed.

2.6.1 The fundamental issues about indoor humidity control

For indoor humidity control, it is important to understand the sources of indoor moisture, since the amount of moisture to be removed from an IS should be equal to that introduced into the space, to maintain a stable indoor air humidity level.

2.6.1.1 Source of indoor moisture

The sources of indoor moisture can be categorized into external and internal. External sources may cover outdoor air ventilation and infiltration. Most residential buildings require the ASHRAE-recommended minimum ventilation rate to ensure IAQ and occupants' thermal comfort [McGahey 1998]. The effects on indoor air humidity level due to ventilation and infiltration are significantly dependent on the moisture content of outdoor air. Generally, the higher the moisture content of outdoor air, the higher the IS latent cooling load an A/C system would have to deal with. In particular, during part load conditions in hot and humid subtropics, the latent cooling load from ventilation air would have greater influences on indoor air humidity than that at full load conditions [Aynur et al. 2008a], and therefore should receive more attentions.

On the other hand, internal sources for indoor moisture load mainly include the moisture gains from occupants and other indoor activities, such as washing and cooking.

There are two causes for possible high indoor air humidity when using an On-Off temperature only control scheme in DX A/C systems: the absence of dehumidification and re-evaporation of residual moisture on the surface of an IU during an Off period. When a preset air temperature is reached, compressor is stopped, and dehumidification is also stopped. If supply fan is still on when the compressor cycles off, moisture on the wet surface of a cooling coil and drain pan may be reintroduced into air stream due to constant air circulation, resulting in an increased RH level in a conditioned space [Amrane et al. 2003]. Therefore, indoor air humidity may remain at a high level in the space served by an On-Off controlled DX A/C System, which can cause discomfort to occupants, lower IAQ and decrease energy efficiency of an A/C system. Other related work has also concluded that even when a supply fan is cycled On-Off intermittently with a compressor, there is a degradation of latent capacity at part load [Shirey et al. 2003].

2.6.1.2 The effects of indoor air humidity level on thermal comfort

It was found in previous studies [Toftum and Fanger 1999] that the level of indoor air

humidity could affect the skin humidity and respiratory comfort of a human being.

Low humidity level (RH < 30%) in inhabited dwellings is associated with dryness of mucous membrane and the dryness of eyes and skin. Indoor air humidity is closely related to human health as well as the problem of static electricity [Paasi et al. 2001]. Reinikainen and Jaakkola [2003] conducted a study on assessing the effects of absolute humidity and RH on skin and upper airway symptoms. On-site investigation results showed that skin and nasal symptoms were deteriorated when air dry-bulb temperature rose, but improved when air RH was increased. Dryness in a heated space could be alleviated by lowering room temperature or through humidification. Sunwoo et al. [2006] studied the physiological and the subjective responses to low RH, and showed that eyes and skin became dry at 30% RH, whereas nasal cavity became dry at 10% RH.

On the other hand, Toftum et al. [1998a and 1998b] pointed out that there should be also an upper limit for indoor RH since a high humidity environment directly influences the perceived IAQ and also induces the growth of mold, leading to respiratory discomfort and allergies. Kishi et al. [2009] carried out a survey in various climate regions and concluded that the risk of sick building syndrome was increased when several dampness indicators were observed concurrently. In addition to lowering IAQ, an increased moisture level of indoor air in buildings would also deteriorate building materials and

impacted energy use performance in buildings [Osanyintola and Simonson 2006], leading to either oversizing of HVAC equipment in dry climates or underestimating the energy consumption in humid regions.

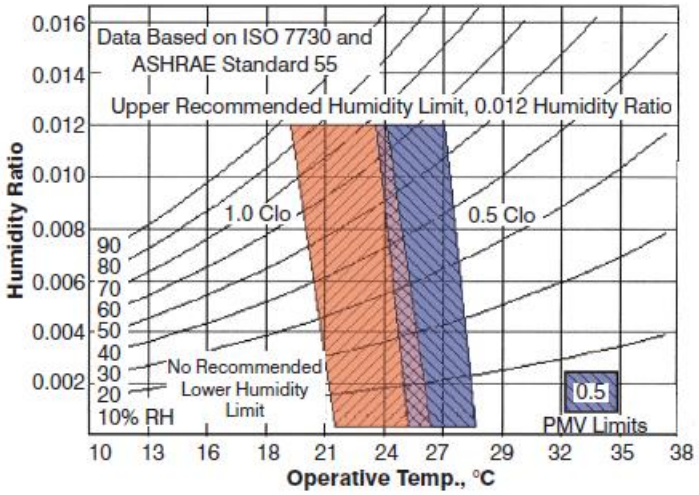

Fig. 2.3 Acceptable range of operative temperature and humidity [ASHRAE 2004]

Indoor thermal comfort for occupants is influenced by a number of factors. According to the "comfort zone" [Olesen and Brager 2004] shown in Fig. 2.3 for air speeds not greater than 0.2 m/s, a majority of people would feel thermally comfortable when the indoor air state is within the zone. This diagram has been used by researchers worldwide for the evaluation of indoor thermal environment. Besides, predicted mean vote (PMV) and predicted percentage of dissatisfied (PPD) indexes can be used to specify the recommended thermal environment for general comfort.

ASHRAE Standard [ASHRAE 2001] recommends that an optimum indoor air humidity zone be maintained between 30% and 60% RH to minimize the growth of allergenic or pathogenic organisms and avoid respiratory difficulties.

2.6.2 Existing strategies for DX A/C systems to control air humidity

In order to maintain an adequate level of indoor thermal comfort, space moisture loads must be removed through dehumidification. However, while indoor air temperature can be easily controlled by A/C technology, indoor humidity control remains relatively problematic. In this section, various strategies currently available for DX A/C systems to control indoor air humidity are reviewed.

Traditionally, the principal method for indoor humidity control is via mechanical cooling and reheating, i.e., to overcool air to below its dew point to remove moisture and then reheat it to a suitable supply temperature. However, this method has been known to be energy inefficient [Henderson et al. 1993] and thus rarely applied to DX A/C systems.

Several enhanced dehumidification technologies may be incorporated into DX A/C systems, including pre-conditioning ventilation air, evaporator bypass, heat pipe technology and the use of desiccant based supplementary equipment systems, etc.

A dual-path system that pre-treated ventilation air may be an attractive alternative dehumidification approach [Zhao et al. 2011]. This method introduced pre-conditioned outdoor air into a conditioned space at the dew point of indoor air, which was sufficient to deal with the entire space latent cooling load. At the same time, its main cooling coil was operated to only handle sensible cooling load with an Equipment SHR (E SHR) at 1.0. Such a control strategy could provide a comfortable indoor environment and higher system efficiency, but it would increase the initial cost of A/C systems.

Evaporator bypass is one of the approaches that can enhance dehumidification and ensure indoor air distribution at the same time. In many cases, a minimum air flow or supply duct pressure is required to make sure adequate air circulation in a conditioned space. One common method to reduce airflow passing through a cooling coil without affecting the total supply airflow is to bypass part of the total airflow using a modulating damper. While there would be no additional savings for fan power, a reduced airflow can help save energy by providing a better match between application SHR (A SHR) and E SHR [Huh and Brandemuehl 2008]. Such a system must incorporate safety measures to prevent the evaporator from being frosted under wet cooling conditions.

A standalone dehumidifier with desiccant is an example of supplementary equipment [Mazzei et al. 2005]. Drying agents used in a standalone dehumidifier can be solid or

liquid desiccants. A solid-desiccant based dehumidifier is more compact, but presents a higher pressure drop for both the air to be dehumidified and the air for regeneration. Therefore, a higher fan power is required. The final temperature of the processed air is always high, leading to a decrease in the adsorption capacity of desiccant. In addition, heat generated by a solid desiccant dehumidifier would cause thermal discomfort [Alpuche et al. 2005]. On the other hand, the use of a liquid desiccant based system could help control more easily air temperature during absorption, resulting in a lower temperature of the processed air. One more advantage of using liquid desiccant is air cleaning. For instance, the washing effect of liquid desiccant in a hospital environment would both reduce airborne bacteria and remove particulate matter [Elsarrag et al. 2005]. However, the operating costs using desiccants can be higher when compared to other indoor humidity control strategies [Harriman et al. 2000].

As Kosar [2006] concluded, who compared three enhanced dehumidification methods integrated with a conventional DX A/C system, augmenting a conventional DX cooling coil with enhanced dehumidification components can substantially increase an integrated system's moisture removal capacity, resulting in a lower E SHR that can better match higher latent loading applications. For the selection of a humidity control method, it may depend on the application of HVAC systems, which determines the load characteristics, operating conditions and system constraints.

2.6.3 Simultaneous control of indoor temperature and humidity using DX A/C systems

It is very challenging to precisely control both air temperature and humidity simultaneously using DX A/C systems, since it is difficult to control two coupled parameters using a single DX cooling coil.

New A/C systems have been proposed for independent temperature and humidity control, by integrating a solid-based or liquid-based desiccant dehumidification sub-system into a DX A/C system [Nagaya et al. 2006, Angrisani et al. 2012]. Under different sensible and latent loads in different spaces, a DX A/C / heat pump system controlled air temperature through sensible cooling or heating while a desiccant dehumidification sub-system dealt with air humidity, respectively. The warm airflow across the condenser in the DX A/C system can be used to regenerate the desiccant, so that both reduced condensing pressure and improved COP could be achieved [Ling et al. 2011]. In order to achieve the precise temperature and humidity control using a desiccant assisted air conditioner, Nayaga et al. [2006] presented an adaptive control algorithm with the consideration of control delays. The experimental results suggested that using the adaptive control would lead to better control performance and higher energy efficiency than using PD control. However, additional low-temperature heat source (waste thermal heat or renewable energy such as solar energy) was needed to

thermally regenerate liquid / solid desiccant, making the desiccant assisted air conditioner more complicated and requiring more space for installation.

It has been experimentally demonstrated that varying the speed of both a compressor and a supply fan in a DX A/C system could help control indoor air humidity. Andrade and Bullard [1999] conducted a detailed simulation work on controlling indoor air humidity using variable-speed compressors and blowers. Simulation results explained how indoor air humidity could be lowered by decreasing evaporator air flow rate due to a lower fin temperature. However, the associated control systems and hardware were both complicated and costly.

A computerized feedforward controller for a DX A/C system has been developed to control the air enthalpy at coil exit [Deng 2002]. Li and Deng [2007b and 2007c] developed a novel direct digital control (DDC)-based capacity controller for a variable speed DX A/C system to control indoor air temperature and humidity simultaneously. The controller development was based on a numerical calculation algorithm using a number of real-time measured system operating parameters. However, using this control strategy, it would take time for the controller to obtain the information required if the space cooling loads were changed, leading to an unacceptable control sensitivity. Besides, the controller's disturbance rejection ability was also poor because there was

no any feedback loop to reflect changes in the controlled process.

Qi and Deng [2009] developed a MIMO control strategy for simultaneously controlling the indoor air temperature and humidity by regulating compressor and supply fan speeds for an experimental DX A/C system. This MIMO controller took into account the coupling effects among multiple operating parameters of the DX A/C system, based on a dynamic mathematical model for the DX A/C system which was developed using system identification [Qi and Deng 2009]. This MIMO controller could however only perform as expected near the operating point where the governing equations in the model were linearized.

Xu et al. [2008] developed a new control algorithm, the so-called high-low (H-L) control strategy, for a variable speed SEAC system to enable both compressor and supply air fan to operate at high speeds when the indoor air dry-bulb temperature setting was not satisfied and at low speeds otherwise. This control strategy would achieve an improved indoor air humidity level and higher energy efficiency when compared to the use of the traditional On-Off control. The H-L control strategy was much simple and less costly, as compared to those based on variable speed technology. However, since indoor air humidity was indirectly controlled, its control accuracy was not as good as those based on variable speed technology.

To realize this H-L control method, two single speed compressors can be employed in parallel [Xu et al. 2013a]. This was technically feasible, since in an SEAC system under H-L control, a variable-speed compressor only needed to operate at two speeds (high-speed and low-speed). Experimental results showed that similar control performances when using two single speed compressors were achieved to those when using a variable speed compressor [Xu et al. 2008].

2.7 Indoor thermal comfort control and energy consumption using MEAC systems

Currently, maintaining a stable indoor thermal comfort level and minimizing energy use in buildings are two crucial issues in connection with the use of HVAC systems. These two issues are however conflicting as minimizing energy use may impair indoor thermal comfort and vice versa.

2.7.1 Indoor thermal comfort control emphasizing on controlling indoor air humidity

Occupants' thermal comfort is essentially their subjective response to their environment, and influenced by a number of factors including four environmental parameters (air temperature, radiant temperature, air speed and RH) and two personal parameters

(metabolic rate, clothing insulation) [ASHRAE 2001].

Simulation studies by Andrade and Bullard [2002] evaluated the trade-offs between indoor thermal comfort and the energy efficiency for a split-type air conditioner equipped with a variable-speed compressor and air blower. It was pointed out that varying the speed of the indoor air fan could provide the necessary humidity control by adjusting the evaporator surface temperature to meet latent loads at any compressor speeds. Therefore, maximized system efficiency could be obtained by varying the compressor speed to maintain a desired indoor dry-bulb temperature and the air blower speed to achieve a desired indoor air humidity level. Deng et al. [2009] carried out an experimental study using Fanger's comfort index [Fanger 1982] to evaluate the indoor thermal comfort characteristics when a DX A/C unit was used to deal with a fixed total space cooling load but with three different SHRs. The results of the experimental study suggested the potential of using indoor thermal comfort indexes, rather than indoor environmental parameters, such as indoor air dry-bulb temperature, for control purpose.

In a variable speed MEAC system, many zones are possible and individual temperature control can be achieved with individual set point control [Goetzler 2007]. In each IS, an EEV can be installed to adjust refrigerant flow rate or to shut down refrigerant supply during operation so that it is possible to have individual supply of A/C in different

spaces.

Chen et al. [2005] developed a dynamic model for a TEAC system. A novel control strategy, which incorporated a self-tuning modifying factor to express the system's cross-coupling effect characteristic, was proposed. The results of simulation-based controllability tests showed that the use of fuzzy logic control could help achieve acceptable air temperature control accuracy in all ISs. However, no humidity control and experimental validation of control algorithms were involved. Lijima et al. [1991] described the basic configuration and operating modes of an MEAC system with concurrent heating and cooling, so that thermal load in different rooms could be removed through heating or cooling. Individual room air temperature control using MEAC systems have been widely studied, however, no previous studies on indoor humidity control or thermal comfort control using an MEAC system may be identified in the open literature.

2.7.2 Energy consumption

Although A/C and refrigeration technologies emerged in late 1800's, there still remained huge interest in reducing energy consumption by A/C and refrigeration systems by means of increasing system efficiency. Efficiency improvements can be accomplished through optimizing the design of system components, the use of

refrigerants of best thermal properties and advanced control strategies. For example, the application of EEVs and variable speed technology to A/C systems has made immense impacts on the ability to regulate system parameters, resulting in important strides towards efficiency improvement [Otten 2010].

In developed countries, building energy consumption has steadily increased. Building energy consumption contributed between 20% and 40% to the total national energy use in many parts of the world. Growth in population, increased demand for building services provisions and better comfort levels, etc., lead to that the upward trend in energy demand will continue in the future. For this reason, increasing energy use efficiency in buildings is a prime objective for energy policy [Pérez-Lombard and Pout 2008].

Energy efficiency of DX A/C systems are affected by several factors. Firstly, without any air ducting, a DX A/C system essentially eliminates air flow losses through air duct, which are often estimated to be ranged from 10% to 20% of total airflow in a ducted system [Goetzler 2007]. Therefore, less energy will be needed to operate the supply fans in DX A/C systems than their ducted counterparts due to less pressure drop along air flow path.

Secondly, MEAC systems typically include a variable speed compressor or several parallel-connected single speed compressors, enabling a wide capacity modulation. Unitary A/C systems mainly use On-Off for temperature control, which causes unstable room temperatures [Chiou et al. 2008]. The changes in IS thermal conditions and various IUs working at the same time create large surges in energy consumption. Therefore, MEAC systems typically operate in the range of 40% to 80% of their maximum capacity for most of their operating hours. Various studies [Zhou et al 2007, Xu et al. 2008, Changenet et al. 2008] indicated that a lower compressor speed would result in a higher system efficiency due to a better load matching. Furthermore, if humidity control can be introduced into MEAC systems to improve indoor humidity control, indoor air dry bulb temperature may then be set at a higher level, leading to a lower space sensible cooling load because of a reduced indoor-outdoor air temperature difference.

Thirdly, for buildings requiring simultaneous heating and cooling, a heat recovery MEAC system can be considered. The system circulates refrigerant in various zones, transferring heat from the IUs serving the zones being cooled to those severing the zones being heated [Joo et al. 2011].

2.8 Conclusions

Since the first MEAC system was introduced in Japan more than 30 years ago, MEAC technology has been widely studied. Most existing research and development efforts related to MEAC systems focused on three main areas: (a) system operating performances evaluation; (b) optimal operation in terms of higher system efficiency and better indoor thermal comfort; (c) developing control strategies for variable speed compressors and EEVs used in MEAC systems.

A large number of previous studies on either modeling or controlling MEAC systems can be identified in the open literature. These studies are either experimental or simulation based. While most simulation studies dealt with multi-evaporators, all experimental studies only used a limited number of evaporators (up to 5), with two being the most common number.

Although MEAC systems are being extensively used and related experimental and simulation research work has been carried out, current efforts have focused on controlling indoor air temperature only. No previous studies involving the control of indoor air humidity using MEAC systems can be identified. Furthermore, most simulation studies for MEAC systems basically focused on the operating characteristics

on the refrigerant side of MEAC systems, such as refrigerant flow distribution and evaporating pressures, without much attention paid to the detailed air side characteristics of the simultaneous air cooling and dehumidification in each IU of MEAC systems. This may appear understandable since most current research efforts focus on the control of indoor air dry-bulb temperature only.

Studies related to the operating performances of MEAC systems have been reviewed. The review results demonstrated that although there have been studies on the relationships among the coupled operating parameters in an MEAC system, most of them were simulation based. Experimental studies on the operating performances of MEAC systems were usually based on DEAC systems [Masuda et al. 1991, Choi and Kim 2003] or focused on the operating performances of MEAC systems in terms of energy efficiency.

Therefore, the literature review presented in this chapter has demonstrated that although there have been significant research interests and efforts to study MEAC systems, there still exist a number of areas where further in-depth research works are required. Given that most previous related studies for MEAC system were based on DEAC systems, any further research developments for MEAC systems should be based on an MEAC system having more than two evaporators. Therefore, these further in-depth research work can

be based on a TEAC system, and would include experimentally evaluating the operating characteristics of the TEAC system, establishing and experimentally validating a dynamic model for the TEAC system and developing a novel capacity control strategy for the TEAC system with an emphasis on improved indoor humidity control.

Chapter 3

Research plan

3.1 Background

From the literature review presented in Chapter 2, it becomes evident that MEAC systems are widely used in small- to medium-scale buildings due to their advantages of high energy efficiency, flexibility in design and installation and compactness in configuration. However, the review also reveals that there still exist a number of issues where further in-depth research works should be carried out. These issues include experimentally studying the operating characteristics, developing a dynamic model and developing an appropriate capacity control strategy over both air temperature and humidity for an MEAC system. These will be the focuses of the work reported in this thesis.

As it is concluded in Chapter 2, a large number of previous simulation and experimental studies on MEAC systems can be identified in the open literature. While most simulation studies dealt with multi-evaporators, all experimental studies only used a limited number of evaporators, with two being the most common number. Therefore, the further required research work for MEAC systems should be based on an MEAC system

having more than two evaporators. Hence, the further development work of MEAC system to be reported in this thesis will be based on a TEAC system, as using a TEAC system to represent an MEAC system could on one hand help reduce the cost for experimentation and simplify the developmental works of a mathematical model and control strategies, and on the other hand, will not lose the essential representation of an MEAC system.

3.2 Project title

This thesis focuses on three major pieces of work related to the modeling and control for an experimental TEAC system: (1) studying the influence of operating parameters on the operating characteristics of the experimental TEAC system; (2) developing a dynamic TEAC model for the experimental TEAC system taking into account both sensible and latent heat balances on the air side of all IUs and its experimental validation; (3) developing a novel capacity controller for the experimental TEAC system so that while indoor air temperature can be controlled within a preset range, improved indoor humidity control may also be achieved. The proposed research work to be reported in this thesis is therefore entitled “Modeling and control of a three evaporator air conditioning (TEAC) system with an emphasis on improved indoor humidity control”.

3.3 Aims and objectives

The objectives of the research work reported in this thesis are as follows:

To set up an experimental TEAC system, so that the intended operating characteristics study, model experimental validation and novel controller development for a TEAC system to improve the control over indoor air humidity, can be realized.

To experimentally study a TEAC system's operating characteristics and the coupling effects among the three IUs in the experimental TEAC system.

To develop a dynamic mathematical model for the experimental TEAC system. The TEAC model will be experimentally validated using the experimental TEAC system.

To develop the novel capacity controller for the experimental TEAC system, based on two previously developed control algorithms, one for temperature control for a DEAC system and the other for improved indoor humidity control for a SEAC system. The validated TEAC model will be used in assisting controller development. Extensive controllability tests will be carried out for the novel capacity controller developed using both the validated model and the experimental TEAC system.

3.4 Research methodologies

Experimental, numerical and analytical methods were employed throughout the research work.

Firstly, an experimental TEAC system with three ISs and one outdoor space will be purposely established. Inside each of the three ISs, a load generating unit (LGU) was placed to simulate both indoor sensible and latent cooling loads, that would include the space cooling load due to irradiative heat transfer. The experimental TEAC system will be fully instrumented and all of its operating parameters can be real time measured and recorded.

With the help of the experimental TEAC system, experimental work to obtain the operating characteristics of the TEAC system after being subjected to step changes in its major operating parameters will be carried out.

A dynamic mathematical model for the experimental TEAC system will be established, specially taking into consideration both the sensible and latent heat balances on the air side of all IUs. The model will be physical based and made of sub-models for both its refrigeration cycle and conditioned ISs. It is to be developed based on the principle of mass and energy conservation, and using the correlations describing the operating

performances of various components in the experimental TEAC system. In addition, the model developed for the experimental TEAC system will be experimentally validated using the experimental TEAC system.

The novel capacity controller development will be based on two previously developed control strategies, one for a DEAC system for temperature control [Xu et al. 2013b] and the other for a SEAC system for improved indoor humidity control [Xu et al. 2008]. Both the developed dynamic mathematical model and the experimental TEAC system will be used for carrying out simulative and experimental controllability tests for the novel controller developed.

Chapter 4

Development of an experimental TEAC system

4.1 Introduction

An experimental TEAC system has been set up in the HVAC Laboratory of Department of Building Services Engineering in The Hong Kong Polytechnic University. The primary purpose of establishing the experimental TEAC rig was to enable carrying out the research work proposed in Chapter 3, including studying the operating characteristics of the experimental TEAC system, establishing a dynamic mathematical model and its experimental validation for the TEAC system, and finally developing a novel capacity controller for the TEAC system, with a particular emphasis on improving indoor humidity using the TEAC system.

The experimental TEAC system reported in this chapter resembles a typical TEAC system, with three ISs and one outdoor space. Advanced technologies such as variable-speed compressor, EEVs, as well as a computerized data measuring, logging and control system have been incorporated into the experimental TEAC system.

This chapter reports on the details of the experimental TEAC system. Detailed

descriptions of the experimental system and its major components are firstly presented. This is followed by describing the computerized sensors/ measuring devices for temperatures, pressures and flow rates.

4.2 Detailed descriptions of the experimental TEAC system and its major components

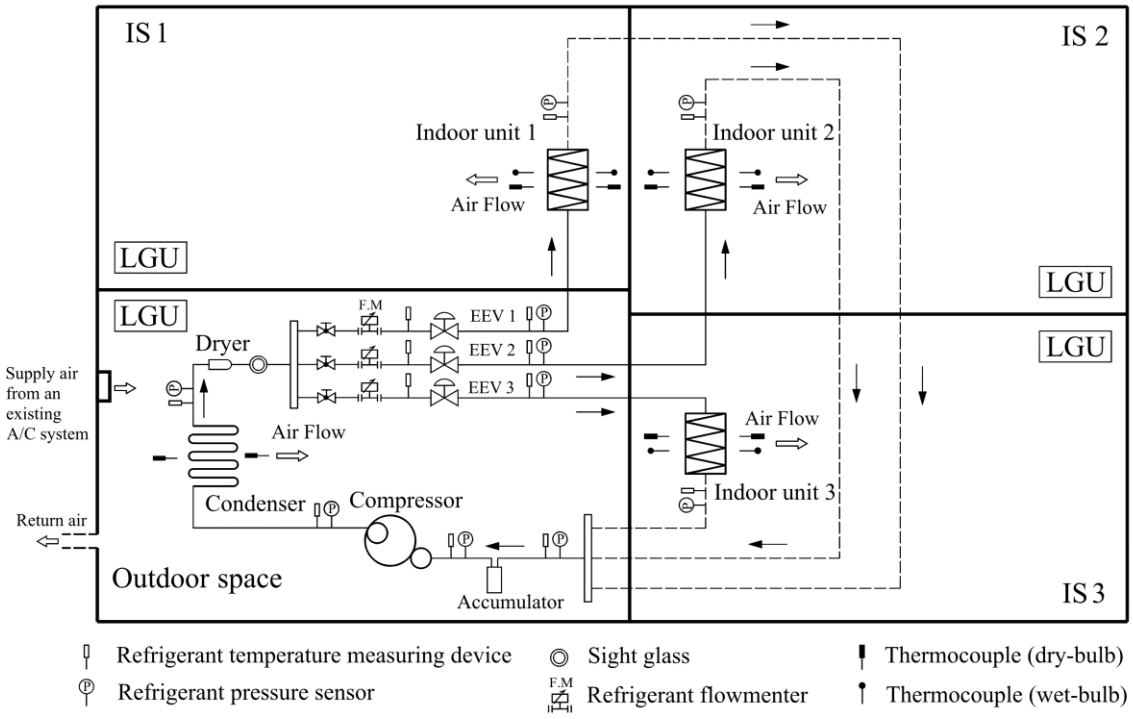

Fig. 4.1 Schematics of the experimental TEAC system

The experimental system, shown schematically in Fig. 4.1, was built in an existing testing chamber where there was an existing A/C system, so that appropriate experimental environments can be created and maintained, as and when required. Inside each of the three ISs, a LGU was used that is capable of simulating indoor loads, both sensible and latent. The imposed latent and sensible loads were achieved by a PI controlled water heater and an air heater inside the LGU. The indoor air temperatures and RH in each of the three ISs were jointly affected by the LGU and the IU of the experimental TEAC system. Since in each IS, the output from each LGU was the only source of heat gain, higher LGU outputs were required when the settings of indoor air temperature and RH level in the IS were raised for experimental purposes. Consequently, to maintain a steady experimental indoor air temperature and RH in each IS, the output cooling capacity of each IU would have to be correspondingly increased. Therefore, in the experiments in the current study, a higher indoor air temperature setting would imply a larger output cooling capacity for an IU. Furthermore, the air temperature and RH in the outdoor space were jointly maintained by the existing A/C system for the chamber and a LGU placed inside the outdoor space. The detailed specifications for the major components used in the experimental TEAC system are listed in Table 4.1.

Table 4.1 Specifications of the major components used in the experimental TEAC system

Components	Specifications	
Compressor	Number:	1
	Allowable frequency:	15-110 Hz
	Rated cooling capacity:	8.23 kW at 75 Hz
	Displacement:	30.4 mL/rev
EEV	Number:	3
	Pulse range:	0-480 Pulse
	Rated capacity:	5.3 kW
	Port diameter:	1.4 mm
Condenser	Number:	1
	Fin type	Plate fin
	Heat exchange external area	27.1 m^2
Evaporator (IU 1)	Number:	1
	Fin type	Plate fin
	Heat exchange external area	3.7 m^2
	Rated cooling capacity	2.2 kW
	Supply air volumetric flow rate	varied from 0.06 to 0.10 m^3/s
Evaporator (IU 2, 3)	Number:	2
	Fin type	Plate fin
	Heat exchange external area	3.78 m^2
	Rated cooling capacity	2.5 kW
	Supply air volumetric flow rate	varied from 0.07 to 0.12 m^3/s
Piping length connecting outdoor unit and each IU	IU 1	4.5m
	IU 2	6.2m
	IU 3	8.0m

R22 was used as the working fluid, with a total charge of 1.6 kg. It should be pointed out that the reason why R22 was used was that the experimental TEAC system was connected from a previous R22 DEAC system, where key system components such as compressor and refrigerant flow meters were only suitable for R22. Nonetheless, the current investigation aimed at study the operating characteristics of a TEAC system, but not the thermodynamic properties of a particular refrigerant. Although the use of different refrigerant may lead to slightly different absolute results, the general trends of variation should remain the same.

4.3 Sensors/ measuring devices for temperatures, pressures and flow rates

The experimental rig was fully instrumented for measuring all of its operational parameters, which may be classified into three types, i.e., temperature, pressure and flow rate. All sensors and measuring devices were able to output direct current signal of 4-20 mA or 1-5V with a 6-second sampling frequency, which were transferred to a data acquisition system for logging and recording. Details of measurements and sensors used in the experimental TEAC system are listed in Table 4.2.

Table 4.2 Details of measurements and sensors used in the experimental TEAC system

Sensor/ measurement	Full scale	Range of output signal	Range of measured value	Uncertainty (%)
Thermocouple (Type K)	-80-500 ºC	-	5-30 ºC	0.20-0.35
Air velocity (hot wire)	0-10 m/s	4-20 mA	0-3 m/s	0.20-0.50
High pressure transmitters	-1-20 Bar	4-20 mA	12-16 Bar	0.15-0.25
Low pressure transmitters	-1-12 Bar	1-5 V	5-7 Bar	0.17-0.30
Refrigerant volumetric flow rate	0-3.2L/min	4-20 mA	0-2 L/min	0.12-1.10

Pre-calibrated thermocouples (Type K) were used as temperature sensor for measuring both air dry-bulb and wet-bulb temperatures. For each IU (evaporator), a short air duct of 300 mm long was connected to its return grill, and four air dry-bulb temperature sensors and two air wet-bulb temperature sensors were fixed evenly inside the air duct to measure the return air temperature and RH for each IU. On the other hand, four air dry-bulb temperature sensors and two air wet-bulb temperature sensors were fixed evenly at air supply grille of each IU for measuring its supply air temperature and RH. Air dry-bulb temperature at the inlet and outlet of the outdoor unit were also monitored using the thermocouples.

To facilitate measuring the air mass flow rate through each of the three IUs, air velocities were measured at three evenly distributed measuring points inside the short air duct of 300 mm long using an air velocity transmitter (hot wire), and an average return air velocity can be calculated though averaging the three measured air velocities and the air flow rate obtained by multiplying the cross sectional area of the air duct by the average air velocity.

The measurements for refrigerant temperatures and pressures in the experimental TEAC system were performed using thermocouples and pressure transducers having a reported accuracy of ±0.13% of full scale reading, respectively. The refrigerant mass flow rate through each of the three IUs was measured using a refrigerant flow meter having an accuracy of ±1.6%. The power input to the experimental TEAC system was recorded using a power meter.

4.4 Summary

An experimental TEAC system has been set up. The system consisted of a variable speed compressor, an air-cooled condenser, three EEVs, three IUs and ISs. Three LGUs are placed inside the three conditioned ISs, one in each IS, for simulating both indoor sensible and latent cooling loads. The experimental system has been fully instrumented

using high quality sensors/ measuring devices and all of its operating parameters can be measured.

The availability of such an experimental TEAC system is expected to be extremely useful in carrying the research work proposed in Chapter 3.

Photos showing the experimental TEAC system are given in Appendix A.

Chapter 5

Operating characteristics of the experimental TEAC system

5.1 Introduction

An MEAC system originates from an SEAC system, and both operate based on vapor compression refrigeration cycle. The fundamental difference between the two is, however, the number of evaporators connected to a common condenser and compressor. Normally, in an MEAC system, a number of evaporators are joined together at compressor suction without pressure regulators. Hence, the evaporating temperatures or pressures in all the evaporators are close to one another [Winkler et al. 2008, Aynur 2010], and therefore, the operating parameters are inherently coupled. Consequently, changes in the operating condition in one of the evaporators due to the operational changes in the room it serves may cause changes in the operating conditions in all the other evaporators [Aynur 2010].

As pointed out in Chapter 2, due to the complexity of MEAC systems, in most reported studies, modeling approach was adopted [Park et al. 2001, Xia et al. 2003, Zhou et al. 2007, Zhu et al. 2013, Chen et al. 2005 and Pan et al. 2012]. Although limited experimentally based studies related to the operating performance of MEAC systems

may also be identified, they were either based on DEAC systems [Masuda et al. 1991, Choi and Kim 2003] or focused on the operating performance of MEAC systems in terms of energy efficiency [Xia et al. 2002, Hu and Yang 2005, Hai and Jun 2006, Aynur et al. 2006, Aynur et al. 2008a, Fujimoto et al. 2011a, Joo et al. 2011 and Kwon et al. 2014] and achieved level of thermal comfort [Aynur et al. 2006]. Furthermore, both reported simulation and experimental studies for DEAC systems focused primarily on the operating characteristics on the refrigerant side of a refrigeration system, including refrigerant flow distribution and evaporating temperatures, without much attention paid to the detailed characteristics on the air side for the simultaneous air cooling and dehumidification in each IU of the MEAC systems.

This chapter presents the results of two Sets of specially designed experiments on the operating characteristics on both its refrigerant side and air side of the experimental TEAC system. The schematic diagram of the experimental TEAC systems is shown in Figure 4.1, and is described in details in Chapter 4. In this chapter, firstly, the experimental conditions for the two specially designed test Sets are specified. Secondly, the experimental results of the two test Sets are reported. Finally, a conclusion is given.

5.2 Experimental conditions

All the experiments were performed with reference to ASHRAE Standard 116 [ASHRAE 1983] and ANSI Standard 210/240 [ANSI 1985] that specified test conditions for an SEAC unit. Using the experimental TEAC system, two Sets of experiments were specifically designed and carried out, against a baseline case. Table 5.1 shows the experimental conditions for the baseline case, and Table 5.2 that for the two experimental Sets. In the first Set, while the experimental conditions in both IS 2/ IU 2 and IS 3/ IU 3 were the same as those in the baseline case, one of the following two operating parameters, indoor air temperature in IS 1 and EEV opening of IU 1, was altered each time for the two tests in Set One, as detailed in Table 5.2. For example, in Test 1-2 in Table 5.2, while five different openings of EEV 1, 20%, 30%, 40%, 50% and 60% of the full opening of the EEV, were used, the other three parameters were the same as those in the baseline case in IS 1/ IU 1, i.e., indoor air temperature at 25 ºC, RH at 50% and supply air volumetric flow rate at 0.10 m^3/s. Furthermore, in the second Set, while the experimental conditions in IS 3/ IU 3 were the same as those in the baseline case during the tests, indoor air temperatures or EEV openings in the other two ISs/ IUs were changed each time. For example, in Test 2-1 in Table 5.2, while all other operating parameters in the three ISs/ IUs were the same as those in the baseline case, the following five testing indoor air temperatures in IS 1 and IS 2, 25/ 25 ºC, 24/ 26 ºC, 23/

27 ºC, 22/ 28 ºC, 21/ 29 ºC, were used as the five testing pairs.

Table 5.1 Baseline case experimental conditions

Operating parameter	Baseline case		
	IS 1/ IU 1	IS 2/ IU 2	IS 3/ IU 3
Indoor air temperature (ºC)	25	27	25
Indoor air RH (%)	50	50	50
EEV opening (%)	40	40	40
Supply air volumetric flow (m^3/s)	0.10	0.12	0.12

During all the tests, compressor speed was constant at 3960 rpm and the outdoor space temperature maintained at 32 ºC. On the other hand, at a testing point, once the experimental TEAC system was operated at a steady state, experimental data were recorded continuously for 30 minutes with a 6-second interval and the recorded data were then averaged, as the experimental values for the operating parameters in the tests. The performances of the experimental TEAC system were analyzed, based on the obtained experimental data under the assumption that when operated at a steady state, the output cooling capacity from each IU was the same as the cooling load in the IS it served. The power input to the LGU in an IS was automatically adjusted to maintain the

settings of both air temperature and RH there.

Table 5.2 Experimental conditions for two experimental Sets

Test	Operating parameters						
Set One							
1-1	Indoor air temperature (ºC)	IS 1/ IU 1	21	23	25	27	29
1-2	EEV opening (%)		20	30	40	50	60
Set Two							
2-1	Indoor air temperature (ºC)	IS 1	25	24	23	22	21
		IS 2	25	26	27	28	29
2-2	EEV opening (%)	IU 1	40	35	30	25	20
		IU 2	40	45	50	55	60

5.3 Results and discussions

Using the experimental TEAC system, two Sets of experiments to exam the operating characteristics on both the refrigerant and air side, and the coupling effects among the operating parameters of the TEAC system, were carried out and the experimental results

are presented in this section.

In this section, the following operating parameters of both the air side and refrigerant side in the experimental TEAC system were used to describe its operating characteristics:

Air side: supply air temperature (ºC) and equipment sensible heat ratio (E SHR), i.e., the ratio of the output sensible cooling load to the total output cooling capacity of an IU [Xu et al. 2010].

Refrigerant side: cooling capacity (kW); evaporating pressure (Bar) and DS (ºC).

5.3.1 Results of test Set One

In this test Set, two tests, whose experimental conditions are shown in Table 5.2, were carried out and the measured results are presented in Figs. 5.1 to 5.7.

5.3.1.1 Results of Test 1-1

Figs. 5.1 to 5.3 show the measured variation of cooling capacity, evaporating pressure and E SHR of each IU in the experimental TEAC system at the following five different air temperature settings in IS 1, i.e., 21, 23, 25, 27 and 29 ºC. During the test, indoor air

temperature settings in IS 2 and IS 3 were maintained at 27 ºC and 25 ºC, respectively.

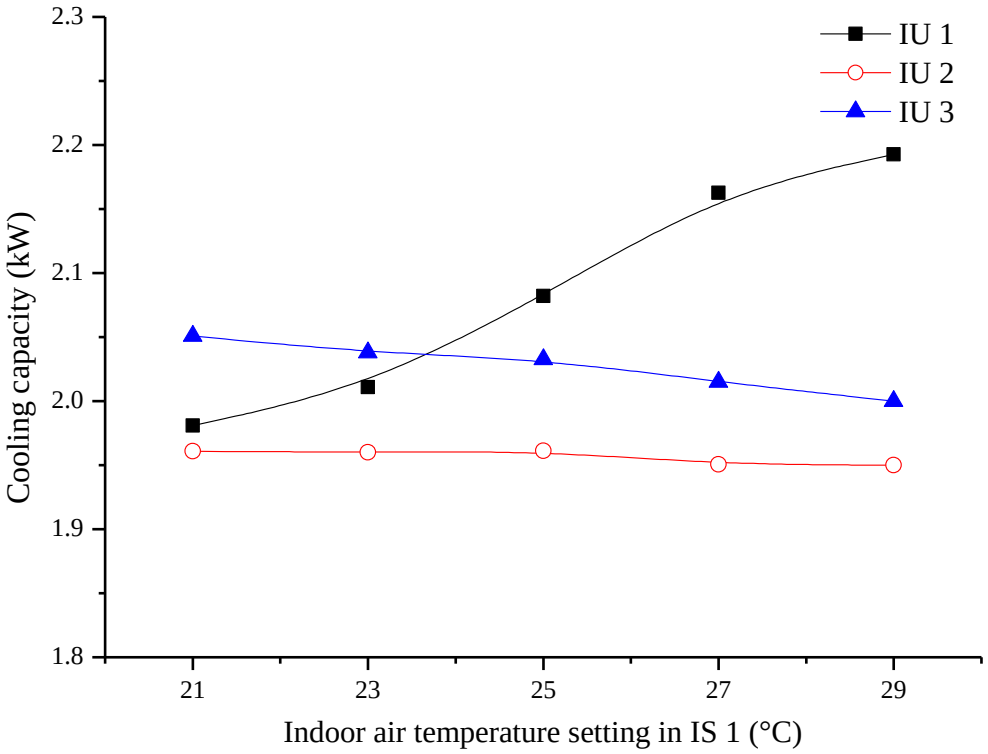

Fig. 5.1 Influences of the changes in indoor air temperature setting in IS 1 on the output cooling capacity from the three IUs

As explained in Chapter 4, Fig. 5.1 shows that a higher output cooling capacity from IU 1 was required at a higher testing indoor air temperature in IS 1. Since the compressor speed remained unchanged, small variations in the total output cooling capacity from the TEAC system may be observed, because of varying condensing and evaporating temperatures [Li and Deng 2007b]. Therefore, the output cooling capacities from the other two IUs were correspondingly reduced. As seen from Fig. 5.1, when indoor air

temperature in IS 1 was varied from 21 ºC to 29 ºC, the output cooling capacity from IU 1 was increased by 10.6%, while those in IU 2 and IU 3 were reduced by 0.5% and 2.5%, respectively. These trends were consistent with the measured results reported by Choi and Kim [2003] where a DEAC system was studied. On the other hand, during the test, to maintain a constant testing indoor air temperature and RH in IS 2 and IS 3, the outputs of the LGUs in IS 2 and IS 3 were correspondingly reduced.

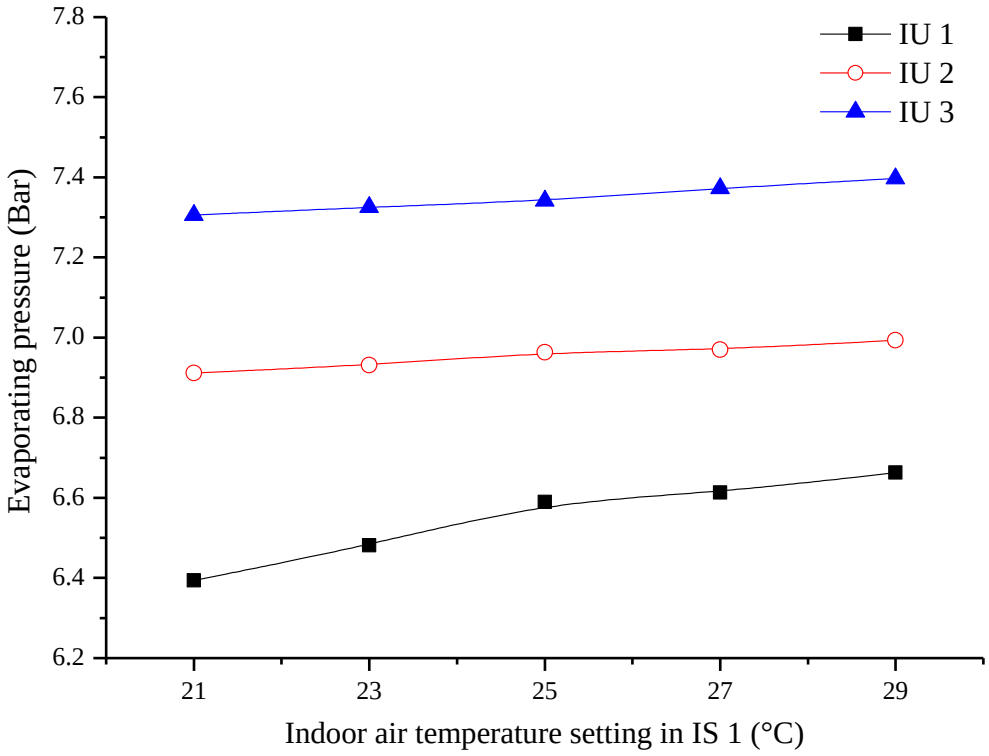

Fig. 5.2 Influences of the changes in indoor air temperature setting in IS 1 on the evaporating pressure of the three IUs

Fig. 5.2 shows the evaporating pressures in the three IUs at different indoor air

temperatures in IS 1. As seen, in IU 1, a higher indoor air temperature in IS 1 would imply a higher supply air temperature, thus a higher evaporating temperature. However, the evaporating temperatures in the other two IUs were also subjected to a moderate increase, as the three IUs in the experimental TEAC system were all directly connected to the suction of the compressor.

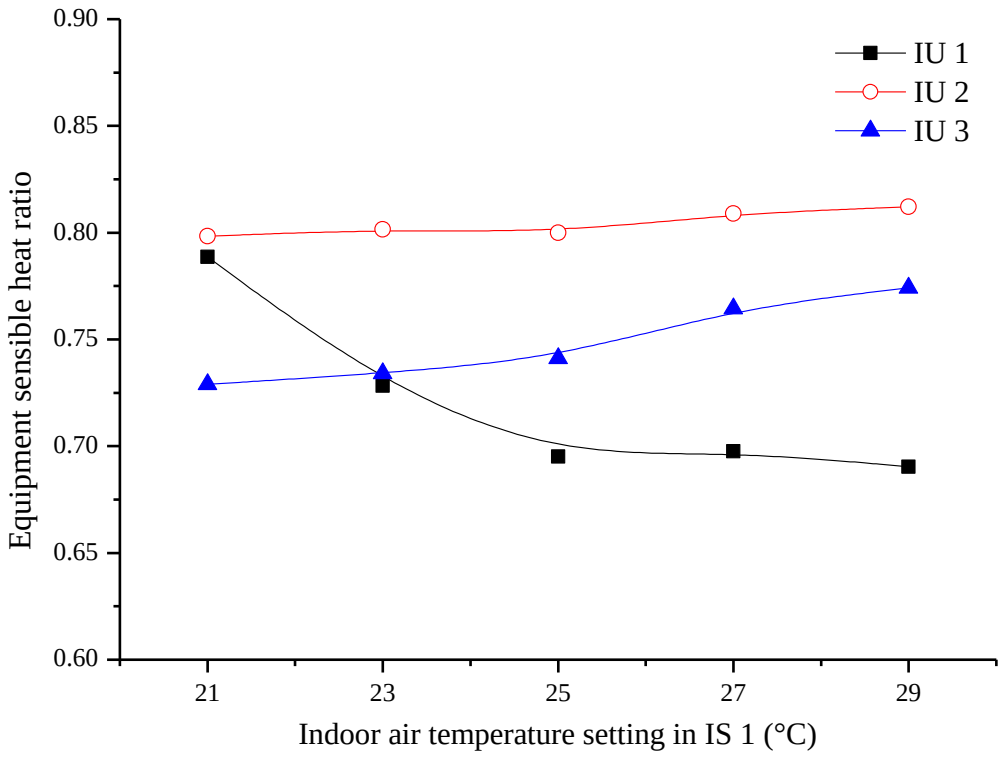

Fig. 5.3 Influences of the changes in indoor air temperature setting in IS 1 on the E SHR of the three IUs

In Fig. 5.3, the measured E SHRs of each IU in the experimental TEAC system under different indoor air temperatures in IS 1 are presented. It can be seen that an increase in

inlet air temperature to IU 1 but at a constant RH level would lead to a reduced E SHR for IU 1, which was consistent with the results reported by Li et al. [2014]. At a higher indoor air temperature setting but a constant RH level of 50% in IS 1, indoor moisture content would be higher, leading to an increase in space latent cooling load. However, the overall effect was that the increase in latent cooling load in IS 1 was more than that in sensible load, and consequently the increase in the output latent cooling capacity from IU 1 was more than that in the output sensible cooling capacity, leading to a reduced E SHR value for IS 1. On the other hand, at fixed indoor settings in IS 2 and IS 3, since the evaporating pressures in IU 2 and IU 3 were slightly increased as shown in Fig. 5.2, the E SHR values for IU 2 and IU 3 were also slightly increased.

The experimental results in Test 1-1 suggested that due to the change in the indoor air temperature setting in IS 1, the operational conditions in the other two IUs would be accordingly affected, due to the coupling effects of the three IUs in the experimental TEAC system.

5.3.1.2 Results of Test 1-2

In this sub-section, the steady-state responses of the operating parameters in the experimental TEAC system to the varying degrees of the opening of EEV 1 are

presented. During the test, the opening of EEV 1 was set at 20%, 30%, 40%, 50% and 60% of its full opening, but the openings of EEV 2 and EEV 3 were fixed at the baseline case values of 40%. The indoor air temperatures in the three ISs were maintained at 25 ºC, 27 ºC and 25 ºC, respectively.

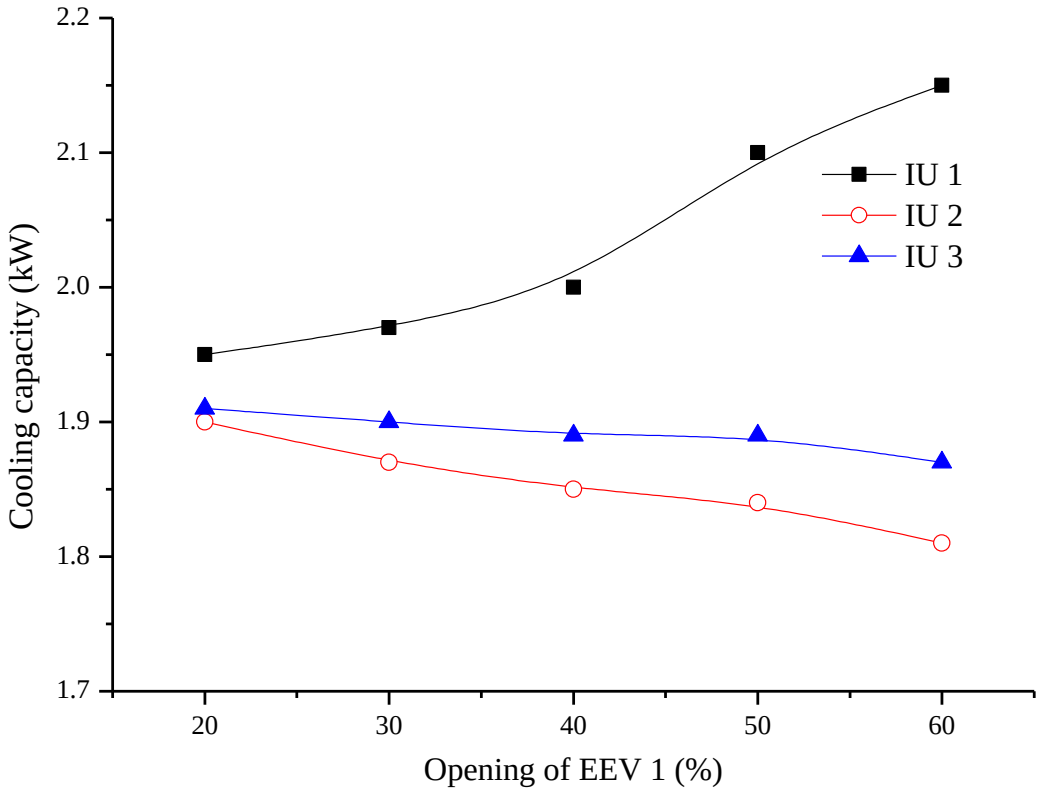

Fig. 5.4 Influences of the changes in the opening of EEV 1 on the output cooling capacity from the three IUs

As shown in Fig. 5.4, at a constant compressor speed, as the opening of EEV 1 was increased, refrigerant mass flow rate to, and hence the output cooling capacity from IU 1 were increased. It can also be observed that the cooling capacity from the other two IUs

were reduced, similar to that in Test 1-1. When the opening of EEV 1 was increased from 20% to 60%, the cooling capacity from IU 1 was increased by 10.3%, but those from IU 2 and IU 3 were decreased by 4.7% and 2.1%, respectively.

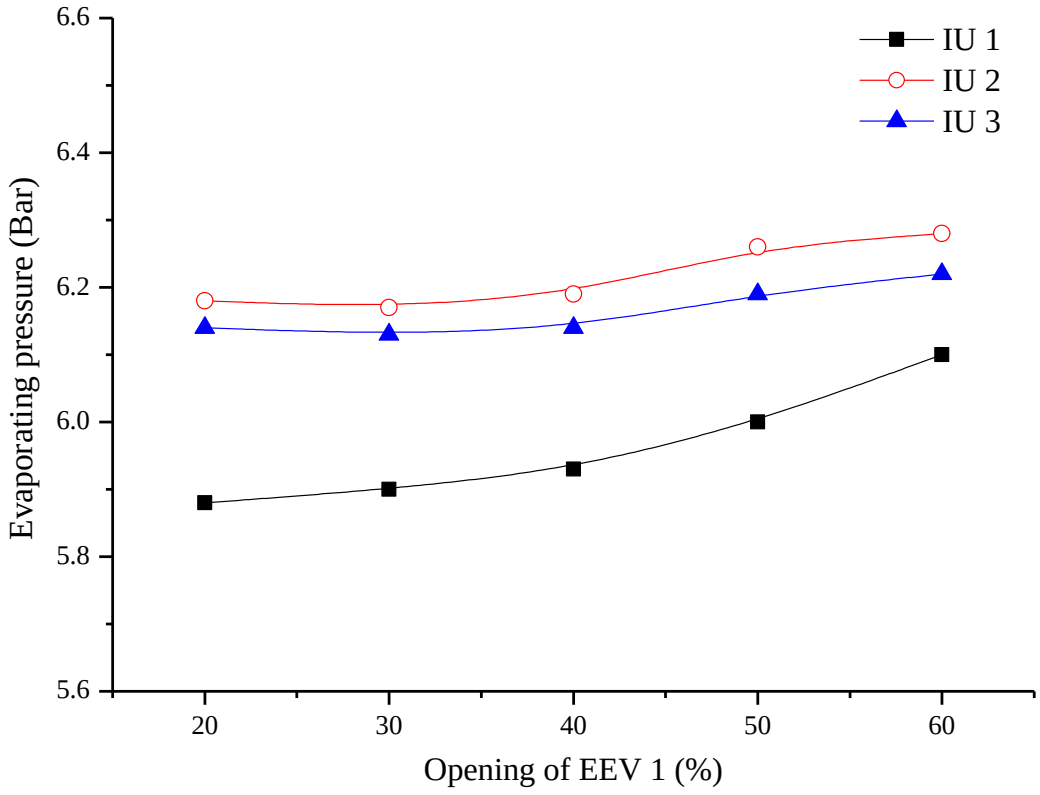

Fig. 5.5 Influences of the changes in the opening of EEV 1 on the evaporating pressure of the three IUs

In a refrigeration system, an EEV acts as a throttling device to control the refrigerant mass flow rate to an evaporator. On the other hand, the total refrigerant mass flow being circulated in a refrigerant system is determined by the compressor speed. In Fig. 5.5, it can be seen that as the opening of EEV 1 was increased, the evaporating pressure in IU

1 was also increased. This was also similar to the results reported by Choi and Kim [2003]. Such a variation trend was largely due to the fact that with a larger EEV opening, although more refrigerant flowed in, the rate of increase in EEV opening was greater than that of the refrigerant mass flow, under the constraint of constant compressor speed, so that a small pressure drop across the EEV was resulted in, leading to an increased evaporating pressure. This was more obvious at a larger EEV opening, e.g., 50% or 60%, as the increase in evaporating pressure was more remarkable. Furthermore, as the three IUs were connected to the compressor, the increase in the evaporating pressure in IU 1 also led to relatively moderate increases in evaporating pressure in IU 2 and IU 3.

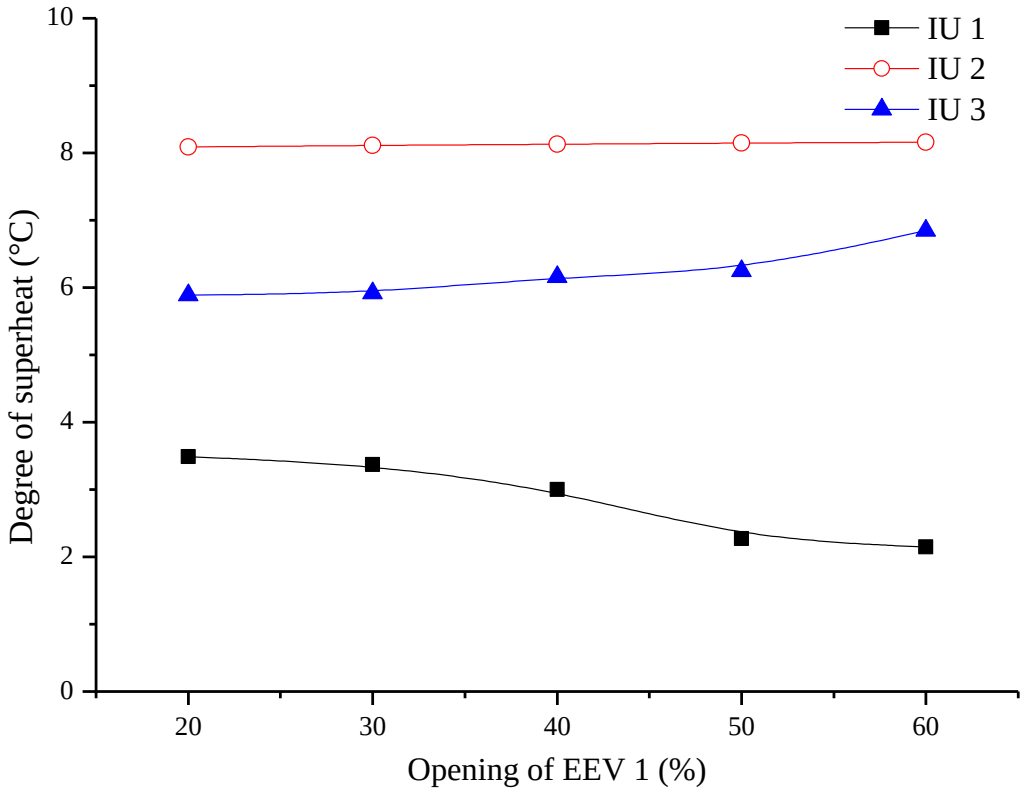

Fig. 5.6 Influences of the changes in the opening of EEV 1 on the DS of the three IUs

A higher evaporating pressure and a higher output cooling capacity due to a higher refrigerant mass flow rate through IU 1, led to a small DS at the outlet of IU 1 as shown in Fig. 5.6.

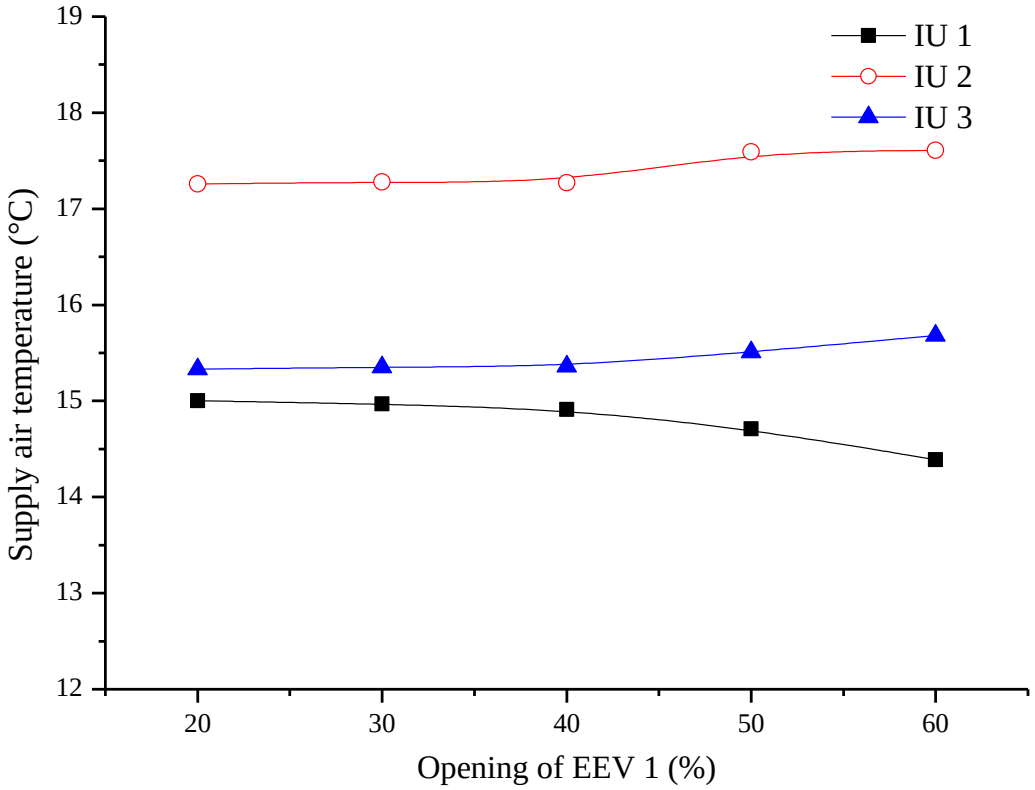

Fig. 5.7 Influences of the changes in the opening of EEV 1 on the supply air temperature from the three IUs

Fig. 5.7 shows the variation of the supply air temperature from each IU in the experimental TEAC system, at different EEV 1 openings. The supply air temperature from IU 1 was reduced from 15 ºC at 20% opening to 14.4 ºC at 60% EEV 1 opening, although the evaporating pressure in IU 1 was increased from 5.88 to 6.10 Bar. This was because the indoor air temperature in IU 1, or the return air temperature to IU 1 remained at 25 ºC, a higher output cooling capacity could cause a lower supply air temperature. On the contrary, due to the reduced output cooling capacity from IU 2 and

IU 3, their supply air temperatures were slightly increased.

The experimental results in Test 1-2 clearly also suggested that varying the opening of EEV 1 would alter the operating characteristics of not only IU 1 but also IU 2 and IU 3.

5.3.2 Results of test Set Two

To further explore the coupling effects among the three IUs in the experimental TEAC system, the performances of the TEAC system were studied when changing the following operating parameters in two of the three ISs/ IUs of the TEAC system, indoor air temperature in IS 1 and IS 2 and the EEV openings of IU 2 and IU 3, respectively. These experimental results are the first of their kinds reported in the open literature.

5.3.2.1 Results of Test 2-1

Figs. 5.8-5.10 show the measured variations of cooling capacity, evaporating pressures and E SHR of the three IUs in the experimental TEAC system as different indoor air temperatures in both IS 1 (decreased from 25 to 21 ºC) and IS 2 (increased from 25 to 29 ºC), but at a fixed air temperature in IS 3.

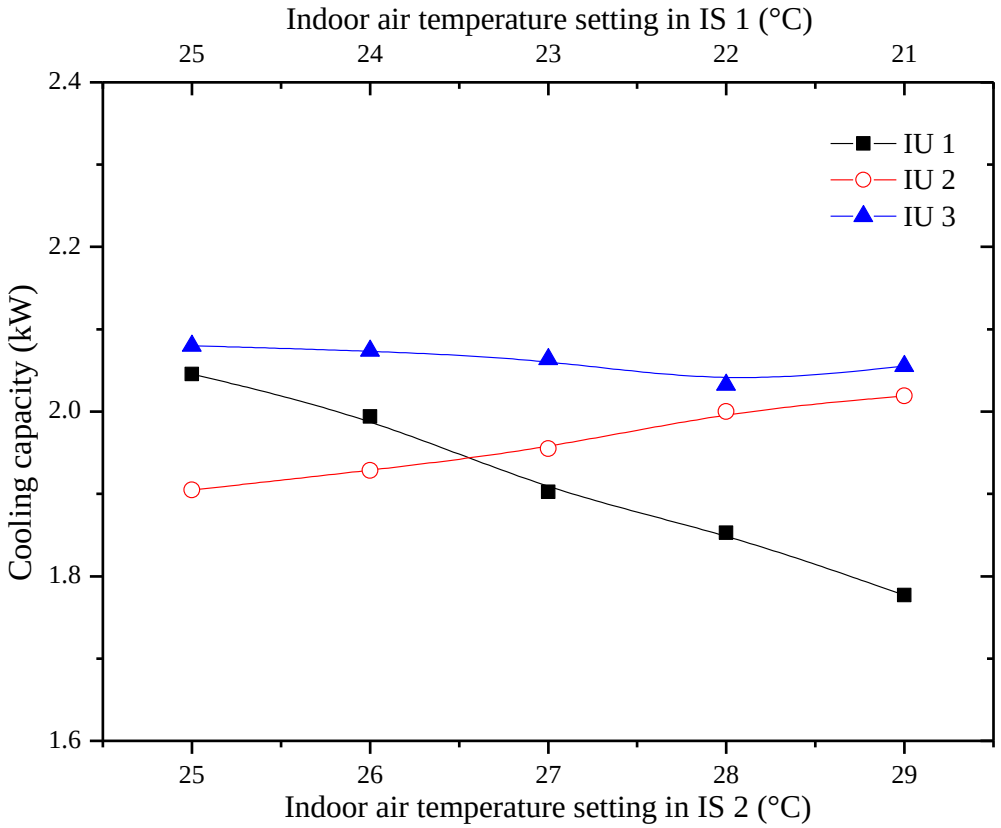

Fig. 5.8 Influences of the simultaneous changes in indoor air temperature settings in both IS 1 and IS 2 on the output cooling capacity from the three IUs

As seen in Fig. 5.8, similar to that in Test 1-1, the output cooling capacity from IS 1 was reduced but that from IU 2 was increased, while that from IU 3 was not significantly varied. A 4 ºC reduction in indoor air temperature setting in IS 1 resulted in a 13.1% reduction in the output cooling capacity from IU 1. However, a 4 ºC increase in indoor air temperature in IS 2, led to a 6.3% increase in the output cooling capacity from IU 2. It should be noted that, however, the change rate of the output cooling capacity from IU 1 in Test 2-1 was greater than that in Test 1-1, even with a smaller variation of 4 ºC in

indoor air temperature setting in Test 2-1 than that of 8 ºC in Test 1-1. This suggested that varying the operating parameters in two IUs/ ISs simultaneously would lead to a greater disturbance than only varying that in one IU/ IS in a TEAC system.

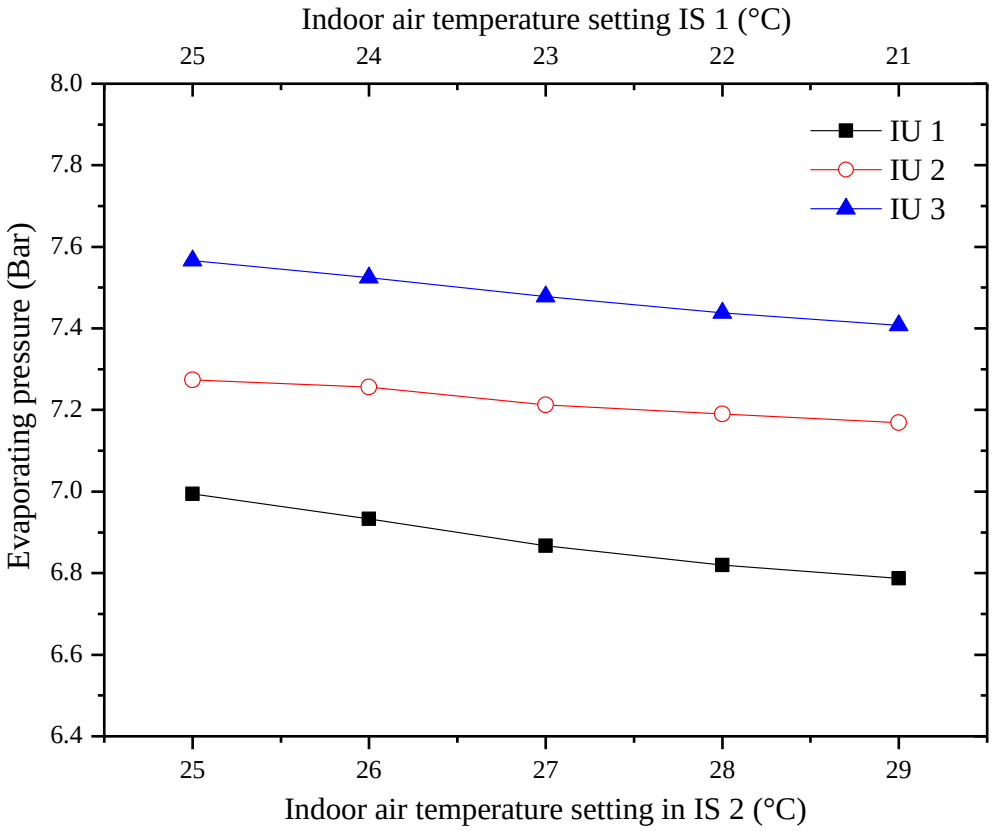

Fig. 5.9 Influences of the simultaneous changes in indoor air temperature settings in both IS 1 and IS 2 on the evaporating pressure of the three IUs

As already demonstrated by the experimental results in Test 1-1, evaporating pressures in all IUs would increase when the indoor air temperature setting in IU 1 was increased but at different rates of increase. In Test 2-1, air temperature setting in IS 1 was

decreased but that in IS 2 was increased. The former led to a reduction of evaporating pressure in IU 1, but the latter would increase evaporating pressure. However, it appeared that the changes in IU 1 dominated the evaporating pressure variation in the TEAC system. This was perhaps due to the fact that to maintain a suitable difference between evaporating temperature and supply air temperature in IU 1, at a lower indoor air temperature, and also a smaller air flow rate, the evaporating pressure in IU 1 had to be reduced. Consequently, since the three IUs were connected at evaporators' outlet, a reduced evaporating pressure in IU 1 affected the evaporating pressure in the other two IUs. Therefore, the evaporating pressure in IU 2 was not increased but instead, slightly decreased. It can be thus seen that the mutual influences of operation in a TEAC system can be much more complicated than that in a DEAC system.

Fig. 5.10 shows that E SHR values in IU 1 were higher at a lower indoor air temperature setting in IS 1, and that E SHR values in IU 2 were lower at a higher indoor air temperature setting in IS 2. These were also consistent with the results by Li et al. [2014]. Furthermore, when indoor air temperature in IS 3 remained unchanged, E SHR values in IU 3 only experienced a very small drop due to the change in its evaporating pressure.

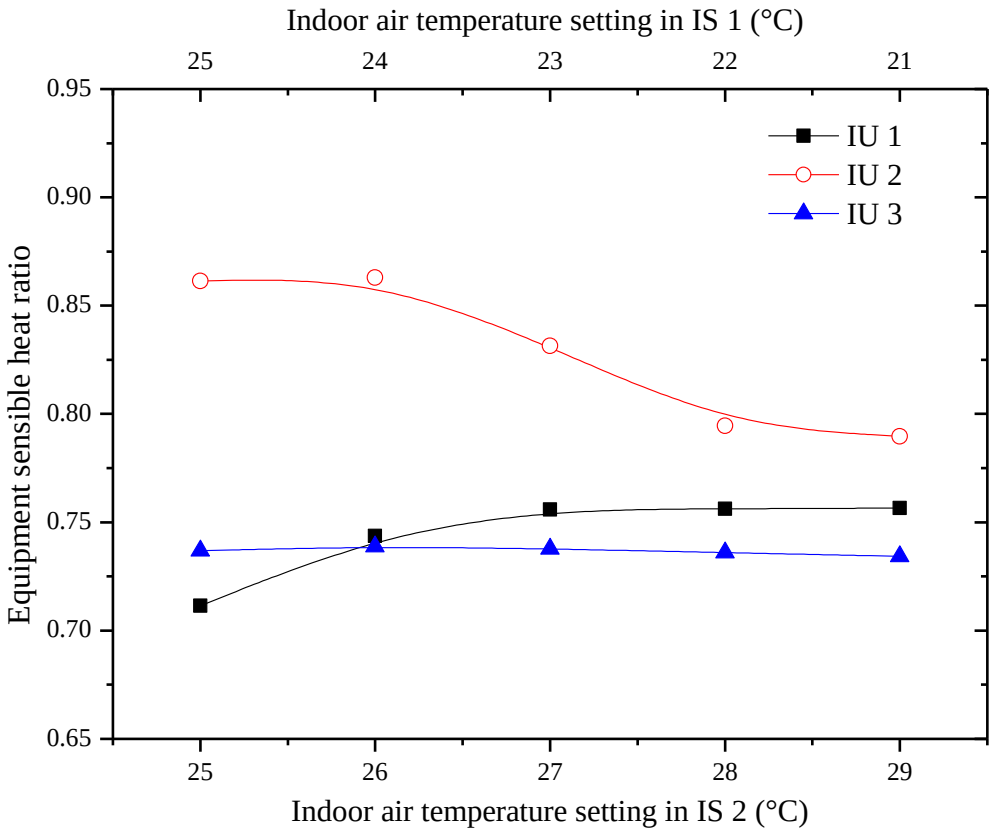

Fig. 5.10 Influences of the simultaneous changes in indoor air temperature settings in both IS 1 and IS 2 on the E SHR of the three IUs

5.3.2.2 Results of Test 2-2

Figs. 5.11 to 5.14 show the variations of cooling capacity, evaporating pressures, DS and supply air temperature of each IU in the experimental TEAC system as the openings of EEV 1 and EEV 2 varied. During the test, EEV 1 opening was reduced from 40% to 20% of its full opening, and that of EEV 2 increased from 40% to 60% of its full opening, while that of EEV 3 remained unchanged.

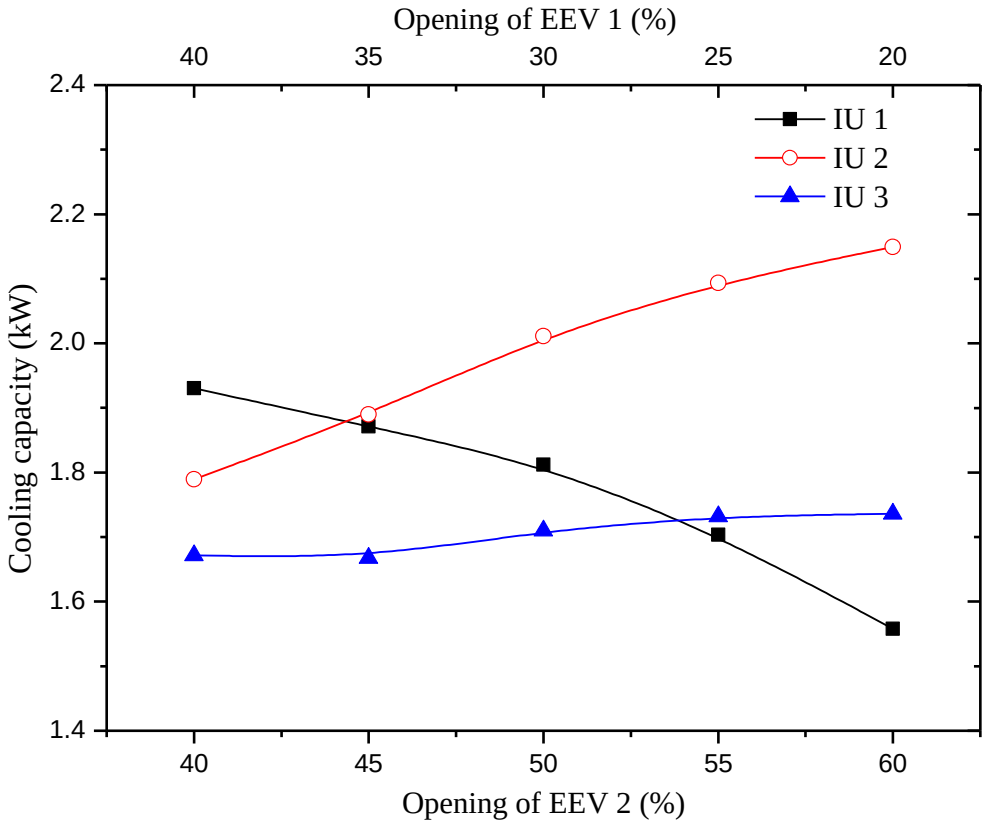

Fig. 5.11 Influences of the changes in the openings of EEV 1 and EEV 2 on the output cooling capacity from the three IUs

As shown in Fig. 5.11, the output cooling capacity from IU 2 was increased with increased opening of EEV 2. On the contrary, the output cooling capacity from IU 1 was decreased because the opening of EEV 1 was decreased. These results were consistent with those obtained in Test 1-2. Reducing the opening of EEV 1 from 40% to 20%, the output cooling capacity from IU 1 was decreased by 19.3%. On the contrary, increasing the opening of EEV 2 from 40% to 60%, the cooling capacity from IU 2 was increased by 20.1%. However, the cooling capacity from IU 3 was only slightly increased. Again,

it can be seen, that, as compared to the results shown in Fig. 5.4, in a TEAC system, the rate of change for key operating parameters, such as cooling capacity, would be more remarkable than that in a DEAC system.

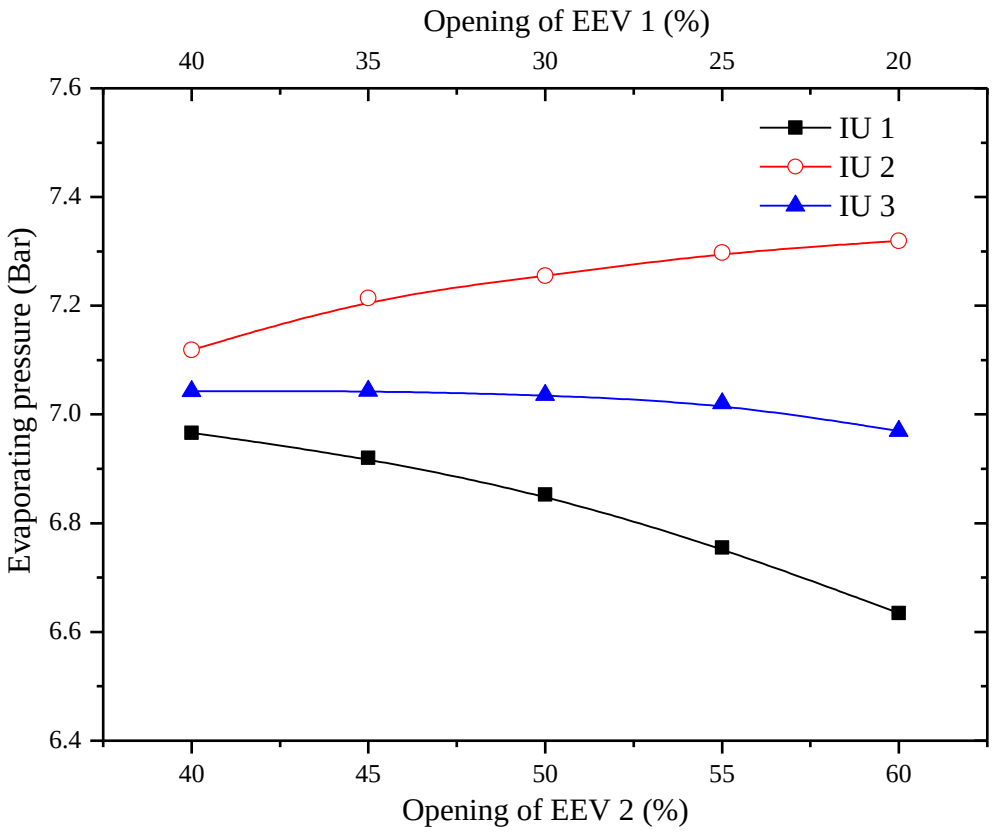

Fig. 5.12 Influences of the changes in the openings of EEV 1 and EEV 2 on the evaporating pressure of the three IUs

Furthermore, as shown in Fig. 5.12, the evaporating pressure in IU 1 was reduced with decreased opening of EEV 1, and that in IU 2 increased with increased opening of EEV 2, which were consistent with the results obtained in Test 1-2. However, the evaporating

pressure in IU 3 was only slightly reduced.

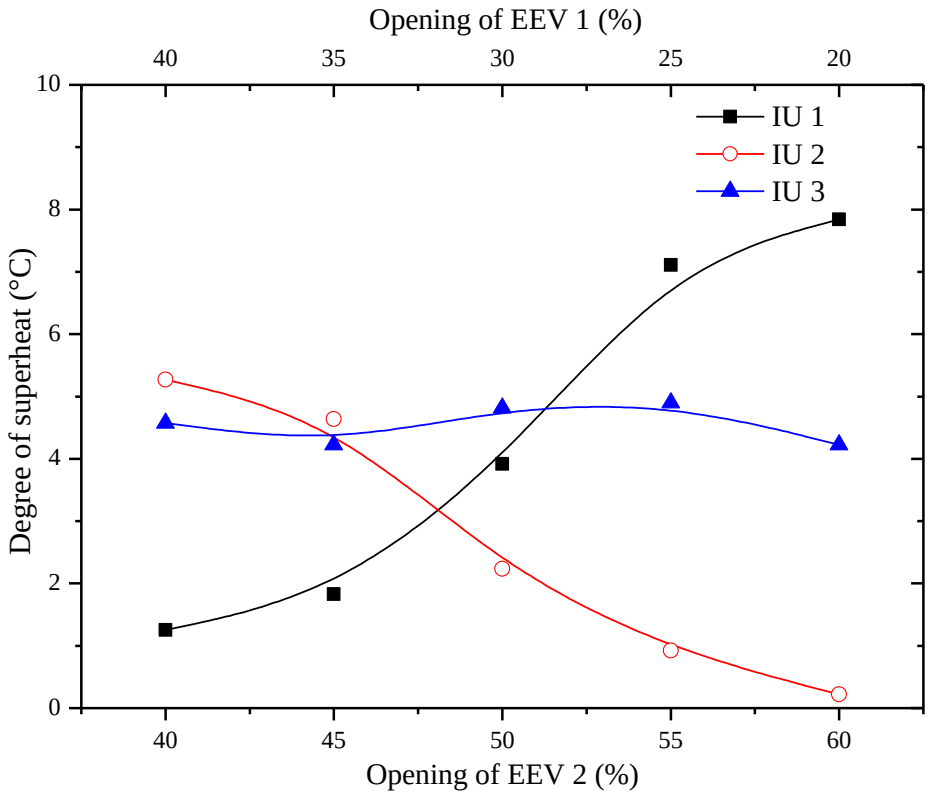

Fig. 5.13 Influences of the changes in the openings of EEV 1 and EEV 2 on the DS of the three IUs

Fig. 5.13 presents the DS at the exit of the three IUs in the experimental TEAC system at different openings of both EEV 1 and EEV 2. The DS in IU 1 was increased with reduced opening of EEV 1, because the refrigerant flow rate passing through IU 1 was reduced. On the contrary, the DS of IU 2 was reduced with increased opening of EEV 2. The DS of IU 3 did not change much.

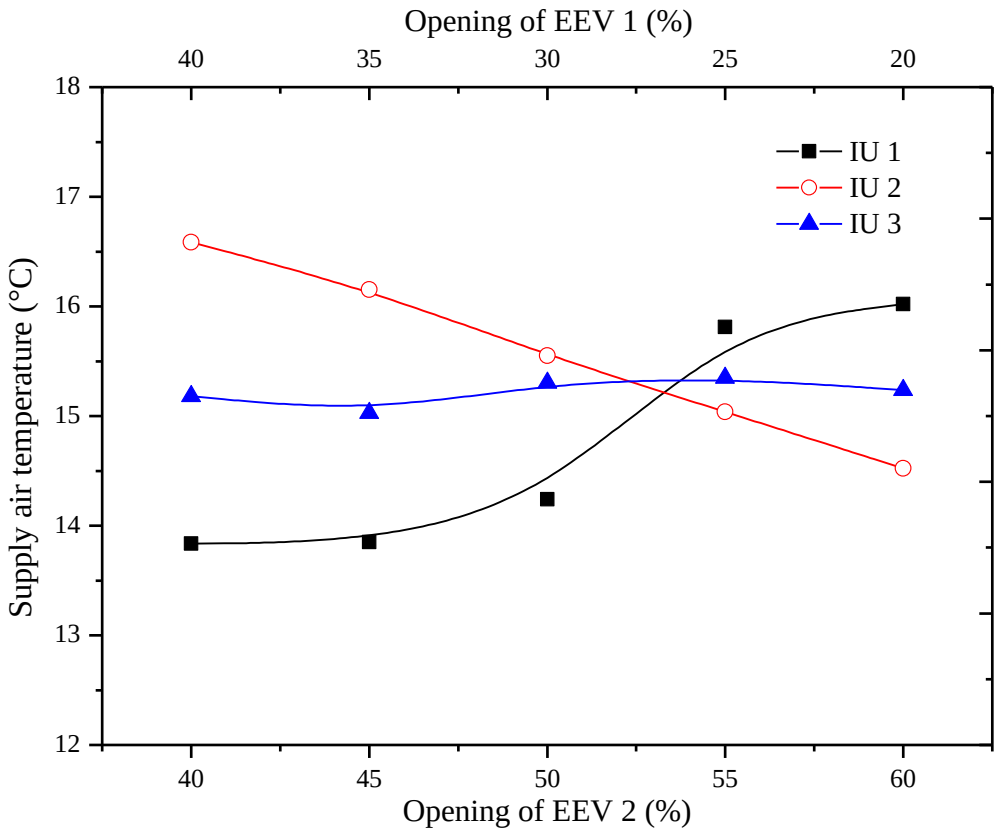

Fig. 5.14 Influences of the changes in the openings of EEV 1 and EEV 2 on the supply air temperature of the three IUs

Fig. 5.14 shows the supply air temperatures of the three IUs at different openings of EEV 1 and EEV 2. The supply air temperature from IU1 was increased due to a reduction in its output cooling capacity, and that from IU 2 reduced due to an increase in its cooling capacity. However, the supply air temperature form IU did not significantly vary, since its output cooling capacity only slightly varied.

5.4 Conclusions

An experimental study on the operating characteristics of the experimental TEAC system was carried out and the study results are reported in this chapter. Two Sets of experiments were specifically designed and carried out, with changes in the operating parameters in one of the three IUs/ ISs in the first Set but that in two of the three IUs/ ISs in the second. Unlike previous reported studies for DEAC systems, in the current study, the operating parameters on both refrigerant side and air side of each IU/ IS in the experimental TEAC system were studied. The experimental results reported in this chapter are the first of their kinds in the open literature.

The study results reported show that when the operating parameters in only one of the IUs/ ISs varied, similar coupling effects of mutual influences reported for previous DEAC systems may also be observed. However, when the operating parameters in two of the IUs/ ISs varied, the coupling effects became more complicated, with mutual influences being more remarkable than that in the experimental TEAC system when the operating parameters in only one of the IUs/ ISs were varied with even less variation magnitude. This would consequently imply that the coupling effects in an MEAC system should be very complex, when the operating parameters in each of its multi-evaporators or the ISs can randomly vary. Furthermore, in the current study, the changes

on both refrigerant side and air side were studied, as the air side operating conditions, such as the temperature difference between supply air and indoor air setting could certainly constrain the changes of operating parameters on the refrigerant side.

The experimental study reported in this chapter clearly demonstrated that the coupling effects in an MEAC system can be very complex when the operating parameters in each of its multi-evaporators or ISs can randomly vary, thus deserving more in-depth investigation. While both experimental and modeling approaches may be employed in further studying the operating characteristics and coupling effects in an MEAC system, using modeling approach is more cost effective. A dynamic mathematical model for the experimental TEAC system has been developed to better understand the complex coupled operating characteristics. The model can also assist to develop suitable capacity controllers for a TEAC system. In the next Chapter, the model development and its experimental validation are presented.

Chapter 6

Developing and validating a dynamic mathematical model of the experimental TEAC system

6.1 Introduction

As shown in Chapter 2, most existing studies related to modeling MEAC systems are based on DEAC systems, with experimental validation [Pan et al. 2012, Shah et al. 2004, Zhu et al. 2013, Elliott and Rasmussen 2013, Shao et al. 2008]. Although limited TEAC system models have also been developed, they were either simulation based without experimental validation [He and Asada 2003, Chen et al. 2005], or based on system identification [Lin and Yeh 2007b, Lee et al. 2011], which is not physical based. In addition, in most previous MEAC models reported, only the refrigerant side in each IU was detailed, without much attention paid to both sensible and latent heat balances on the air side in an IU.

This chapter reports on the development of a dynamic mathematical model for the experimental TEAC system as described in Chapter 4. The model developed is expected to be greatly helpful for better understanding the complex coupled operating characteristics and developing advanced control strategies for the experimental TEAC

systems. It is to be component-based, and takes into consideration the operating characteristics of both the refrigerant side and air side in each IU of the TEAC system. In this chapter, firstly, the model development for the experimental TEAC system is presented by detailing the sub-models for both its refrigeration cycle and conditioned ISs. Secondly, details of the experimental validations of the TEAC model developed are presented.

6.2 Dynamic Modeling of the TEAC System

A dynamic mathematical model for the experimental TEAC system, specially taking into consideration both the sensible and latent heat balances on the air side of all IUs, has developed. The model was built on sub-models for both its refrigeration cycle and conditioned ISs in the TEAC system and was implemented using MATLAB programming environment. The dynamic model was developed based on the principle of mass and energy conservation, and using the correlations describing the operational performances of various components in the experimental TEAC system. Refrigerant R22 was used as the working fluid in the TEAC system.

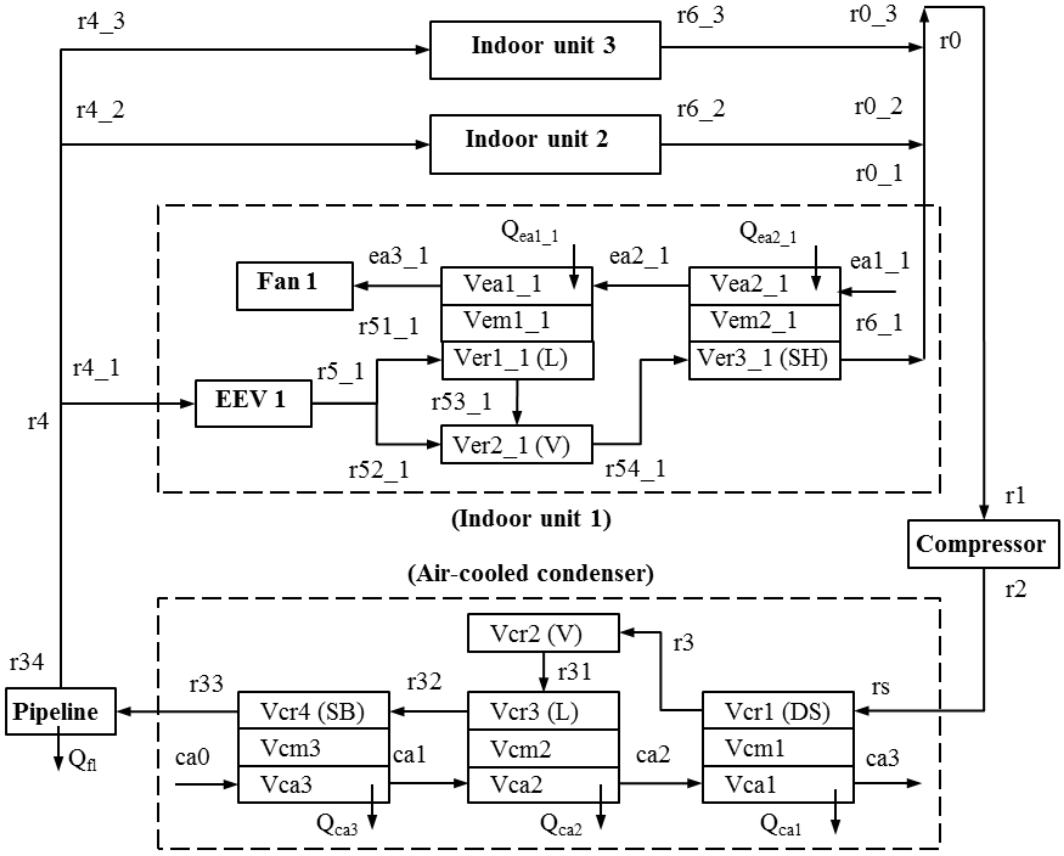

Fig. 6.1 The conceptual model of the experimental TEAC system

When modeling, the DX evaporator was divided into two regions, i.e., a two-phase and a superheated region (SH); and the air-cooled condenser into three regions, i.e., a desuperheating region (DS), a two-phase region and a sub-cooled region (SB). Since a good representation of heat exchangers was required, the two-phase region was further divided into a liquid (L) and a vapor zone (V). The schematic diagram of the experimental TEAC system modeled is shown in Figure 4.1, and is described in detail in Chapter 4. The major components of the refrigeration cycle included a variable speed

compressor, an air-cooled condenser, and three IUs each having an EEV and an evaporator. The model was established by zoning the TEAC system, and the complete conceptual model which depicts the zoning of the experimental TEAC system is shown in Figure 6.1. Each zone was treated as a stirred tank; and the dynamic model so developed was of partial-lumped-parameter type. In this chapter, when presenting the sub-models, reference is made to Fig. 6.1 for symbols representing the zones and subscripts indicating the actual locations in the experimental TEAC system. For the nomenclatures used in Fig. 2, V indicates the space volume and Q the heat transfer of each region/ zone, respectively. For the sub-scripts following V or Q, e indicates an evaporator and c an air-cooled condenser, respectively; r indicates refrigerant side, a air side and m metal of each region, respectively; and $\_i (i = 1, 2, 3)$ represents the i^{th} evaporator. For example, the refrigerant side of the two phase region of Evaporator 1 is separated into two zones, i.e., a liquid zone which is represented by $V_{er1\_1}(\text{L})$ and a vapor zone, which is represented by $V_{er2\_1}(\text{V})$. The zone representing the metal tube wall of the two-phase region of Evaporator 1 is denoted by V_{em1_1}, and the amount of heat released by the air in the airside zone V_{ea1_1} by Q_{ea1_1}.

The commonly used Cleland Correlations [Cleland 1986], and the air state correlations recommended by ASHRAE [2001] to describe the thermal and physical properties of refrigerant R22 and air, respectively, were used.

6.2.1 Sub-model for the variable-speed compressor

In the dynamic simulation of a vapor compression system, a compression process was often treated as a steady-state process. Therefore, the outputs of the compressor sub-model were instantaneously updated based on the current refrigerant states at its suction and discharge pressures, as follows:

$$m_{r2} = m_{r1} \tag{6.1}$$

$$m_{r1} = \lambda \rho_{r1} \dot{V}_d n / 60 \tag{6.2}$$

$$w_{com} = \frac{1}{\eta_i} \frac{\beta}{\beta - 1} \frac{P_{r1}}{\rho_{r1}} \left\{ \left(\frac{P_{r2}}{P_{r1}} \right)^{\beta/\beta - 1} - 1 \right\} \tag{6.3}$$

$$h_{r2} = h_{r1} + w_{com} \tag{6.4}$$

6.2.2 Sub-models for the EEVs

After leaving the air-cooled condenser, the sub-cooled liquid refrigerant flowed to the three IUs via its matching EEV, yielding:

$$m_{r4} = m_{r4\_1} + m_{r4\_2} + m_{r4\_3} \tag{6.5}$$

In IU 1, IU 2 and IU 3, the mass flow rates through the EEVs were represented by the same orifice equation:

$$m_{r5\_i} = m_{r4\_i} \ (i = 1,2,3) \tag{6.6}$$

$$m_{r5\_i} = C_{d\_i} A_{\_i} \sqrt{\rho_{r5\_i}\left(P_{r4} - P_{r5\_i}\right)} \quad (i = 1, 2, 3) \tag{6.7}$$

$$h_{r5\_i} = h_{r4\_i} \quad (i = 1, 2, 3) \tag{6.8}$$

Generally, an EEV can be assumed to have a linear inherent flow characteristic. Its opening is assumed to be linear with the actual pulse output of the EEV 's PI controller, i.e.,

$$A_i = K_{EEV} \times Pulse \ (i = 1, 2, 3) \tag{6.9}$$

where K_{EEV} is the valve opening per unit of pulse output and obtainable from the performance data of the EEV. PI control algorithm is usually adopted and the pulse output is modulated in response to the degree of refrigerant superheat at the evaporator exit.

6.2.3 Sub-models for heat exchangers

Both the air-cooled condenser and evaporators were approximated to be ideal counter-flow heat exchangers. According to the state of refrigerant, a heat exchanger was divided, when modeling, into several regions. In each region, the heat and mass transfer on both the refrigerant side and air side were separately modeled. Furthermore, on the air side, both sensible and latent heat transfers were considered. The log mean temperature difference (LMTD) method was applied to each region of the heat exchangers to determine their heat transfer rates. The zoning of heat exchangers is depicted in Fig. 6.1.

Since a good representation of heat exchangers was required, a two-phase region was further divided into liquid and vapor zones. Evaporator 1 was chosen as an example for illustrating the modeling process. The modeling approaches for the air-cooled condenser and the other two evaporators were similar to that for Evaporator 1, so this is not repeated here.

6.2.3.1 Refrigerant side of the two-phase region of Evaporator 1

Mass and energy balances in the two-phase region were represented by the following equations:

$$m_{r51\_1} - m_{r53\_1} = \frac{\rho_{le} d(V_{er1\_1})}{dt} \tag{6.10}$$

$$m_{r52\_1} + m_{r53\_1} = m_{r54\_1} \tag{6.11}$$

$$m_{r5\_1} h_{r5\_1} - m_{r54\_1} h_{r54\_1} + Q_{e1\_1} = \frac{\rho_{le\_1} d(V_{er1\_1} h_{r51\_1})}{dt} \tag{6.12}$$

$$Q_{e1\_1} = \alpha_{ie,tp\_1} A_{ie,tp\_1} \left(T_{em1\_1} - \frac{T_{r5\_1} + T_{r54\_1}}{2} \right) \tag{6.13}$$

The internal heat transfer area in the two-phase region was:

$$A_{ie,tp\_1} = \frac{V_{ie,tp\_1}}{V_{ie\_1}} A_{ie\_1} \tag{6.14}$$

The volume of the two-phase region was:

$$V_{ie,tp\_1} = \frac{1}{1 - Z_e} V_{er1\_1} \tag{6.15}$$

where Z_e is the void fraction and was calculated using the Zivi Equation [Zivi 1964].

The convective heat transfer coefficient, α_{ie,tp_1}, on the refrigerant side in the two-phase region of Evaporator 1 was determined using the Kandlikar Equation [Kandlikar 1990].

The refrigerant pressure drop in the two-phase region was evaluated by:

$$\Delta P_{e\_1} = 5.986\times10^{-5}\left(q_{e1\_1}g_{r\_1}\right)^{0.91}\frac{l_{e\_1}}{D_{ie}} \tag{6.16}$$

$$P_{r54\_1} = P_{r5\_1} - \Delta P_{e\_1} \tag{6.17}$$

6.2.3.2 Refrigerant side of the superheated (single-phase) region of Evaporator 1

Neglecting both mass storage and thermal capacitance of the vapor refrigerant inside the superheated region, the mass and energy balances in zone V_{er3_1} yielded:

$$m_{r6\_1} = m_{r54\_1} \tag{6.18}$$

$$Q_{e2\_1} = m_{r6\_1}h_{r6\_1} - m_{r54\_1}h_{r54\_1} \tag{6.19}$$

$$Q_{e2\_1} = \alpha_{ie,sh}A_{ie,sh\_1}LMTD_{ie,sh\_1} \tag{6.20}$$

where the log mean temperature difference is:

$$LMTD_{ie,sh\_1} = \frac{\left(T_{em2\_1} - T_{r54\_1}\right) - \left(T_{em2\_1} - T_{r6\_1}\right)}{\ln\left(\frac{T_{em2\_1} - T_{r54\_1}}{T_{em2\_1} - T_{r6\_1}}\right)} \tag{6.21}$$

The heat transfer area is:

$$A_{ie,sh\_1} = A_{ie\_1} - A_{ie,tp\_1} \tag{6.22}$$

The convective heat transfer coefficient for the single-phase refrigerant in the superheated region was evaluated also using the Dittus-Boelter Equation [Winterton 1998].

The pressure drop of vapor refrigerant in the superheated region was negligible, i.e.,

$$P_{r6\_1} = P_{r54\_1} \tag{6.23}$$

Finally, the DS at Evaporator 1 exit was evaluated by:

$$T_{sh\_1} = T_{r6\_1} - T_{r54\_1} \tag{6.24}$$

6.2.3.3 Air side of Evaporator 1

When modeling the air side of a heat exchanger, both the thermal capacitance and mass storage of air were considered negligible and hence the energy and mass transfer between air and tube-fin was assumed to be steady-state. On the air side of each region, wet-cooling of air occurs when the tube-fin surface temperature of the exchanger is

below the dew-point temperature of the air entering the respective regions; otherwise, dry-cooling of air occurs. Dry-cooling and wet-cooling of air were separately modeled in the two-phase region of Evaporator 1 here, since the modeling in other regions might be similarly treated.

6.2.3.3.1 dry-cooling of air

The metal temperature was used to link the heat transfer between refrigerant and air.

$$Q_{ea1\_1} - Q_{e1\_1} = M_{em1\_1} CP_{em} \frac{dT_{em1\_1}}{dt} \tag{6.25}$$

$$g_{ea3\_1} = g_{ea2\_1} \tag{6.26}$$

$$Q_{ea1\_1} = m_{ea\_1}(h_{ea2\_1} - h_{ea3\_1}) \tag{6.27}$$

$$Q_{ea1\_1} = \alpha_{oe,dry} A_{oe,tp\_1} LMTD_{oe,tp\_1} \tag{6.28}$$

The correlations developed by Wang et al. [1999 and 2000] for a louver-finned evaporator under dry-cooling conditions were adopted to calculate the air side theoretical heat transfer coefficient:

$$\alpha_{oe,dry} = j_{dry}\rho_{ea}v_{ea,\max}\frac{CP_{ea}}{\Pr_{ea}^{\frac{2}{3}}} \tag{6.29}$$

where j_{dry} is the Coburn factor, which could be obtained through geometric parameters of the evaporator [Hong and Webb 1996, Chen 2005].

By solving these correlations and using air state equations, the temperature and moisture content of the air leaving the evaporator, i.e., g_{ea3_1} and T_{ea3_1} could be obtained.

6.2.3.3.2 wet-cooling of air

The heat and mass transfer equations of air in the wet-cooling condition are similar to that in dry-cooling condition, except for the calculation of the air side theoretical heat transfer coefficient. It is known that the existence of condensate in a dehumidifying process would enhance the total heat transfer in an evaporator. By adopting a dehumidifying augmentation factor, ξ, the effect of dehumidification on the total heat transfer can be taken into account.

$$\alpha_{oe,wet} = \alpha_{oe,dry} \times \xi \tag{6.30}$$

where the dehumidifying augmentation factor was calculated by:

$$\xi = 1 + 2.46 \times \frac{0.5 \times \left(g_{ea2\_1} + g_{ea3\_1}\right) - g_{em1\_1}}{0.5 \times \left(T_{ea2\_1} + T_{ea3\_1}\right) - T_{em1\_1}} \tag{6.31}$$

Where g_{em1_1} is the moisture content of saturated air under temperature T_{em1_1}.

6.2.4 Sub-models of the connection between the three evaporators and the compressor in the TEAC system

In a TEAC system, three IUs are connected in parallel without any pressure regulators. The refrigerant pressure at the meeting point of three IUs before entering the compressor should be the same, i.e.,

$$P_{r0\_1} = P_{r0\_2} = P_{r0\_3} = P_{r0} \tag{6.32}$$

The refrigerant mass flow rate was instantaneous and the sum of the three mass flow rates leaving each evaporator should be equal to the mass flow rate to be sucked in by the compressor, which was computed by the compressor sub-model. It was also assumed that the mixing of refrigerant leaving the three evaporators was perfect without energy loss.

$$m_{r0\_1} + m_{r0\_2} + m_{r0\_3} = m_{r1} \tag{6.33}$$

$$m_{r0\_1}h_{r0\_1} + m_{r0\_2}h_{r0\_2} + m_{r0\_3}h_{r0\_3} = m_{r1}h_{r1} \tag{6.34}$$

The challenge in modeling MEAC systems often came from the coupling of evaporators operated at a similar pressure but different refrigerant mass flow rates [Pan et al. 2012]. In an SEAC system, the refrigerant mass flow rate leaving its evaporator can be obtained directly from a compressor model. However, in an MEAC system, a mass distribution strategy is required at the compressor suction to determine the mass flow rate leaving each evaporator.

At a specific pipe flow condition, the mass flow rate can be related to the pipe loss through the flow [Moody 1944] if the pipe friction factors are known. Thus, in this study, the pressure drops in the refrigerant suction lines from each evaporator to the compressor could be evaluated by using the Darcy-Weisbach equation [Moody 1944]:

$$\Delta P_{\_i} = P_{r6\_i} - P_{r0\_i} = f_{\_i}\frac{8l1_{\_i}}{\pi^2 D_{ie\_i}{}^5}\frac{m_{r6\_i}^2}{\rho_{re}} \quad (i = 1, 2, 3) \tag{6.35}$$

where $f_{\_i}\ (i = 1, 2, 3)$ is the friction factor coefficient for refrigerant pipe and is given by the general Colebrook function [Moody 1944], which is also known as the interpolation formula for the Moody Chart.

Using Equations (6.32-6.35) and sub-models for evaporators and the compressor, refrigerant mass flow rates leaving all evaporators and the compressor suction pressure can be evaluated on a transient basis.

6.2.5 Sub-models for indoor spaces

It was assumed that throughout an IS, both indoor air temperature and moisture content were the same as those at the inlet of the IU serving the IS, T_{ea1} and g_{ea1}. The space sensible cooling load and latent cooling load in an IS are represented by Q_{s_i} and Q_{l_i}, respectively. For an IS i ($i = 1, 2, 3$), its energy and mass balances yielded:

$$\rho_a V_{\_i} Cp_{ea} \frac{dT_{ea1\_i}}{dt} = Q_{s\_i} - \rho_{ea} V_{ea\_i} Cp_{ea} \left(T_{ea1\_i} - T_{ea3\_i}\right) \quad (i = 1, 2, 3) \tag{6.36}$$

$$\rho_a V_{\_i} \frac{dg_{ea1\_i}}{dt} = \rho_{ea} V_{ea\_i} \left(g_{ea1\_i} - g_{ea3\_i}\right) + Q_{l\_i} \quad (i = 1, 2, 3) \tag{6.37}$$

6.2.6 Numerical solution procedure

Totally, the TEAC model developed consisted of eighty-six equations, with twenty-three being first-order ordinary differential equations. In addition, there were seventeen equations for the thermal properties of R22 and air. The differential equations were solved using the Euler integration approach.

When numerically solving the model, firstly, geometrical parameters of various system components such as compressor and heat exchangers were input to the model. Initial values were also required as a starting point for a transient simulation. These included the evaporating and condensing pressures, space volumes of heat exchangers' two-phase region, inlet air conditions of evaporators and the condenser, etc.

The numerical solution of the dynamic TEAC model started from the inlet of the evaporator, where the mass flow rate and enthalpy of the refrigerant were updated by the sub-model for the EEV at the next simulation time step. The boundaries between different regions in heat exchangers, for example, the two-phase and superheated regions in an evaporator, were on the move during simulation because of the changes of space volumes in different regions. On the refrigerant side of the TEAC system, constraint conditions were that the refrigerant mass flow rates leaving all evaporators must be equal to that given by the compressor's sub-model and the refrigerant pressure drops across the three IUs should be the same. Split-half iteration was used to calculate the refrigerant mass flow rate leaving each evaporator. Once the above conditions were satisfied, the degree of refrigerant superheat and the heat transfer in the superheated region can be obtained. With the availability of refrigerant mass flow rate leaving an evaporator, the refrigerant mass flow rates at different locations in the evaporator, except for the evaporator's inlet, were reversely calculated. Knowing the state of the

refrigerant entering the compressor would allow the state of the refrigerant at compressor discharge to be determined by using the compressor's sub-model. The state parameters of the refrigerant at the compressor discharge were then passed on to the sub-model of the condenser. With the states of the refrigerant entering the condenser updated for the current time step, various parameters in the condenser such as condensing pressure were then given their new current values by solving the related energy and mass balance equations. The updated pressure drop across an EEV was utilized in the sub-model for the EEV to provide a new mass flow rate of the refrigerant entering its matching evaporator at next time step.

Moreover, the sum of refrigerant flow rates of the three EEVs was equal to the refrigerant mass flow rate leaving the condenser. Therefore, mathematical correlations for different components in the TEAC system modeled were linked together following the flow direction of refrigerant being circulated. The integration time step Δt for the numerical solution was 0.1 second. The flow chart illustrating the numerical solution procedure for the complete model of the TEAC system is shown in Fig. 6.2.

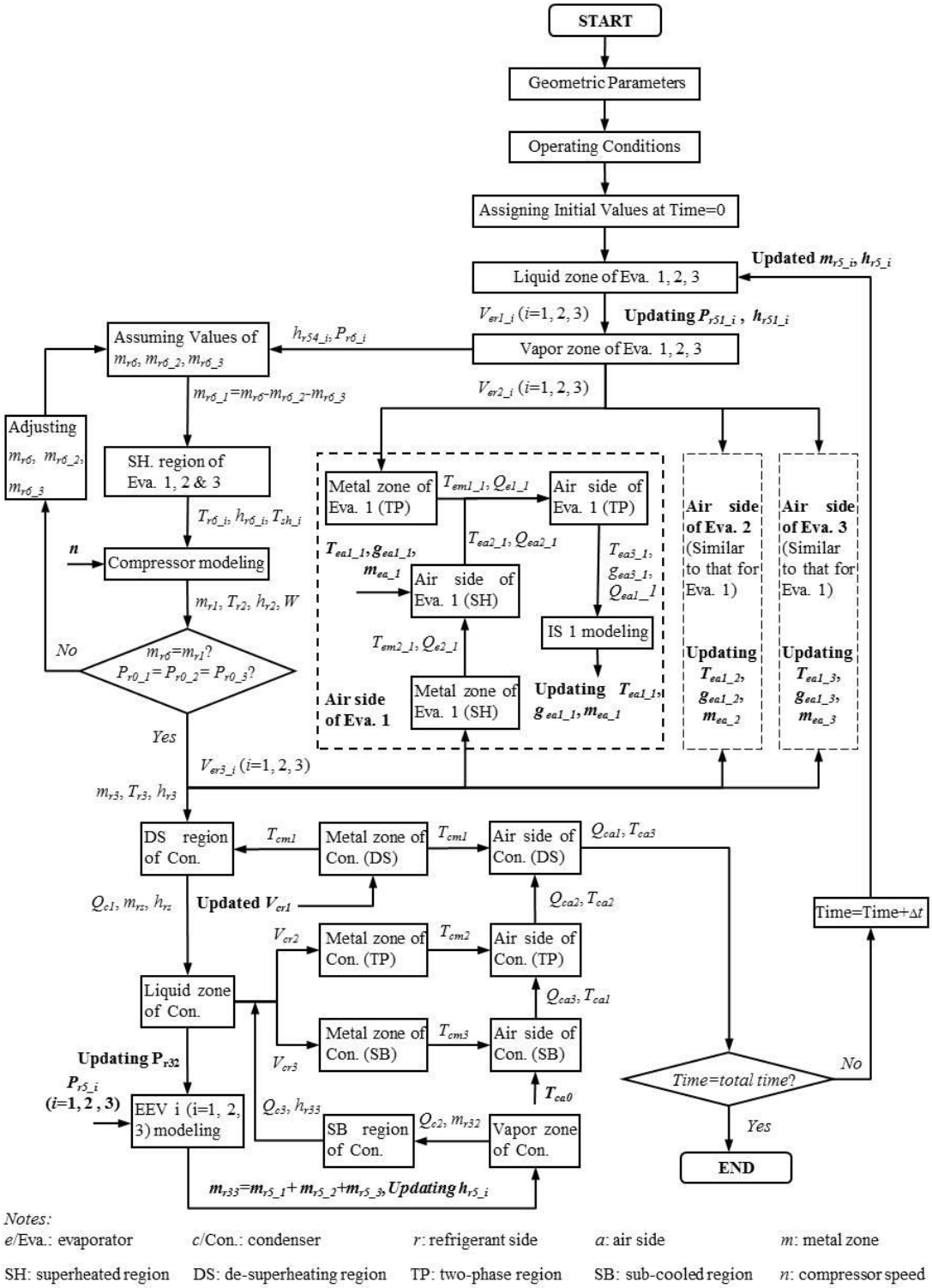

Fig. 6.2 Flow chart for the numerical solution procedure of the TEAC model

Both the steady-state and dynamic behaviors from the experimental TEAC system can be simulated by the model. The complete TEAC model had a flexible structure, which would therefore enable the extension of modeling a TEAC system to an MEAC system having any number of evaporators by adding and removing IUs and ISs.

6.3 Experimental validation of the TEAC system model

Using the dynamic TEAC mathematical model developed, many transient and steady state system responses, in response to changes in system operating parameters or ambient conditions can be predicted. On the other hand, using the experimental TEAC system, the same responses can also be obtained. Model validation was carried out by comparing the predicted model responses with the measured results obtained from the experimental TEAC system, and the examples of the comparison are shown in Figs. 6.3 to 6.7.

Figs. 6.3 to 6.5 show the measured and predicted results of supply air temperature, RH and evaporating pressures in the three evaporators following a fan speed change in IU 3 at 600s. As seen in the three figures, prior to the change at 600s, the TEAC system was operated at a steady state condition, at a constant air mass flow rate for all IUs at 0.10 m^3/s. The indoor air environment in the three ISs were all maintained at 26 ºC and 55%

RH, respectively. At 600 s, the air mass flow rate in IU 3 was altered from 0.10 m^3/s to 0.08 m^3/s. As seen from the figures, all evaporating pressures and supply air temperatures from the IUs started to decrease at that time point and reached new steady state conditions 150 seconds after the fan speed change. The supply air temperature and evaporating pressure in IU 3 were subjected to a more significant drop due to the reduction in supply fan speed, while these in IU 1 and IU 2 were also reduced, but much less significantly. The supply air RH of IU 3 was increased, while those of the other two IUs remained virtually unchanged for both the measured and predicted results.

The relative errors in the predicted supply air temperature for the three IUs prior to the step decrease in IU 3 fan speed were 0.5%, 1.28% and 1.42%, respectively. A maximum relative error of 1.5% existed in the predicted supply air temperature for all the three IUs after the step change in IU 3's fan speed at 600s. Furthermore, as seen in Fig. 6.4, the predicted and the measured supply air RH also agreed well. In Fig. 6.5, the predicted and the measured evaporating pressures are compared, and the relative errors between the two for all the three IUs were all less than 2.5%, during the entire experimental period of 1800s.

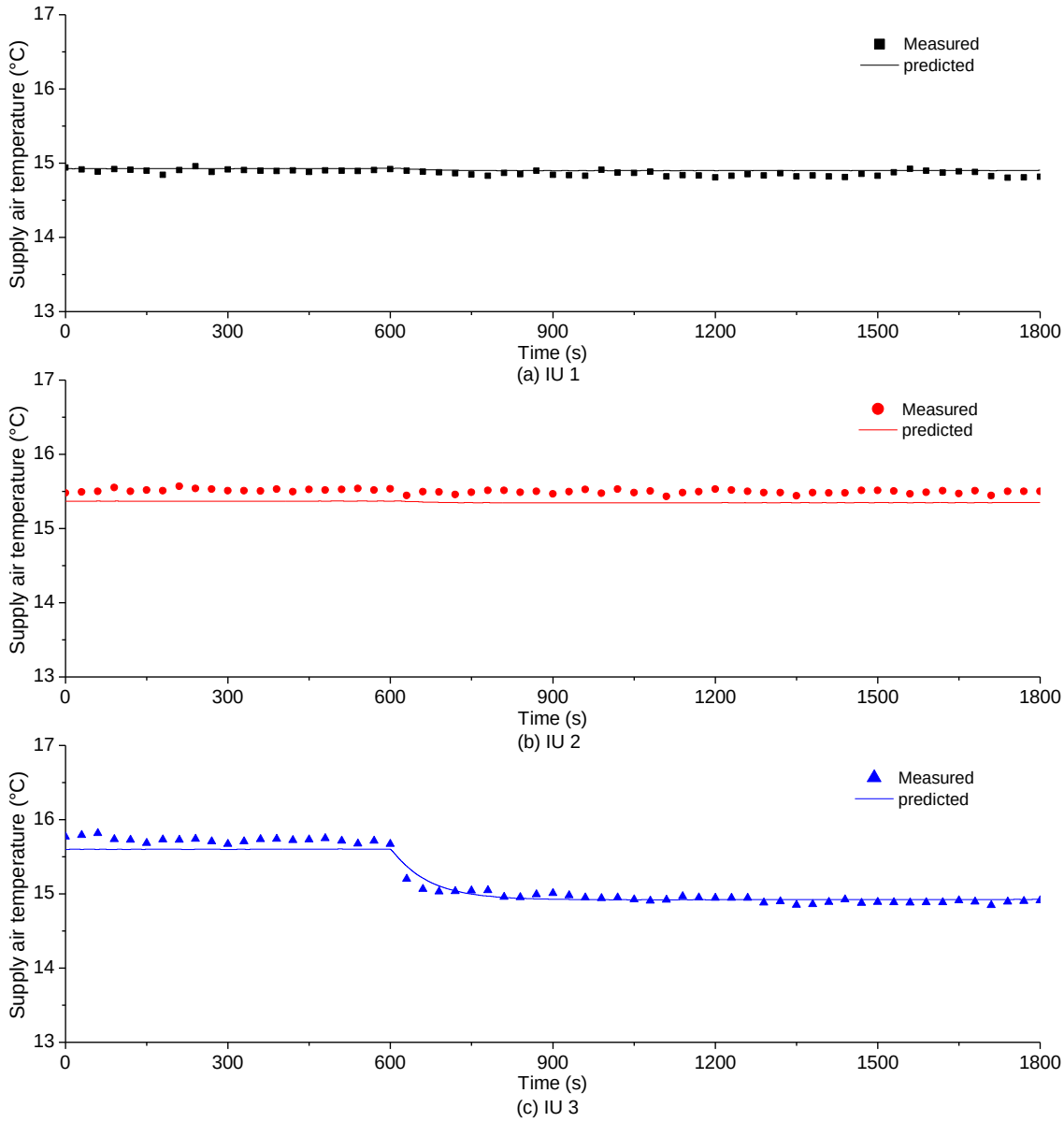

Fig. 6.3 Comparison between predicted and measured supply air temperatures following a fan speed change in IU 3 at 600s

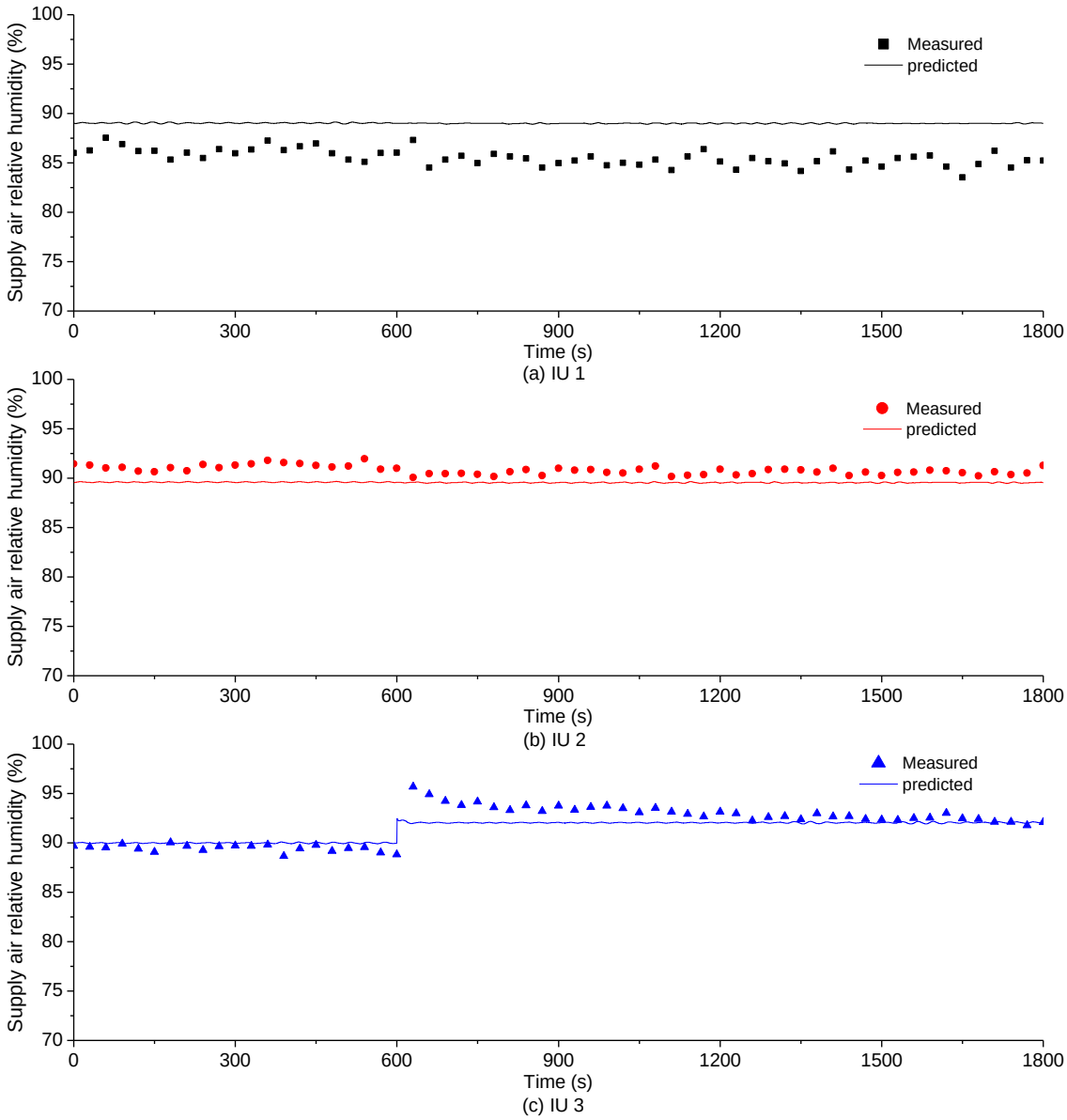

Fig. 6.4 Comparison between predicted and measured supply air RH following a fan speed change in IU 3 at 600s

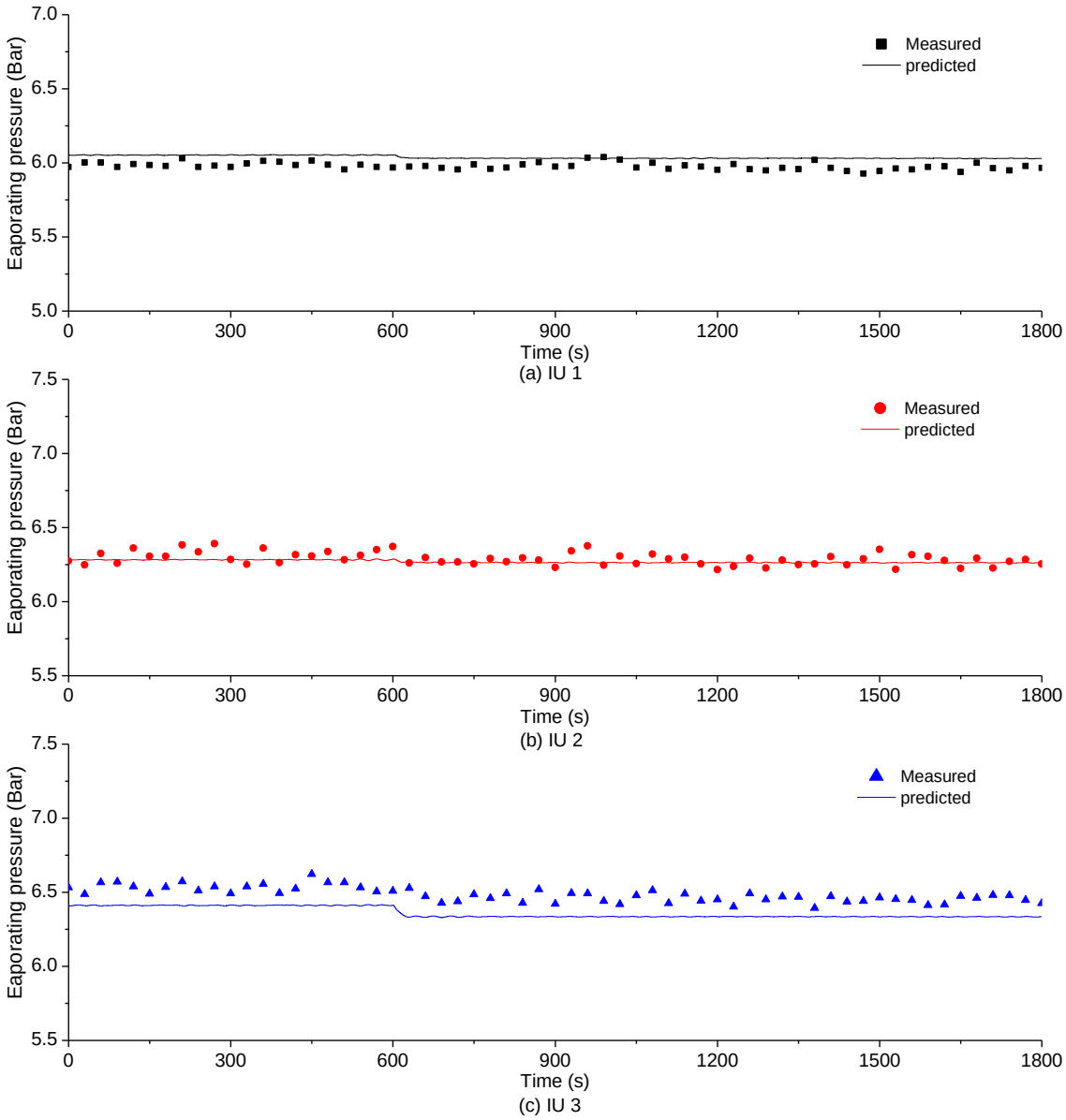

Fig. 6.5 Comparison between predicted and measured evaporating pressure following a fan speed change in IU 3 at 600s

Figs. 6.6 and 6.7 present the predicted and measured evaporating pressures and cooling capacities of the TEAC system following a step change in compressor speed from 3960 rpm to 3000 rpm at 600s. As seen, the step change in the compressor speed caused a

sudden rise in the evaporating pressures in the three IUs. The predicted evaporating pressures in the three IUs agreed reasonably well with measured values, during and after the step change, within ±5.8%, ±5.2% and ±5.4%, respectively. As shown in Fig. 6.6, the fluctuations in evaporating pressure can be observed in both the predicted and measured evaporating pressures between 700 and 800 seconds. This was because the three EEVs were used to control the degree of superheat at the outlet of each evaporator. At steady-state operation, before and after the compressor speed change, a maximum relative error of 3.7% existed in the predicted and measured evaporating pressures in the three evaporators.

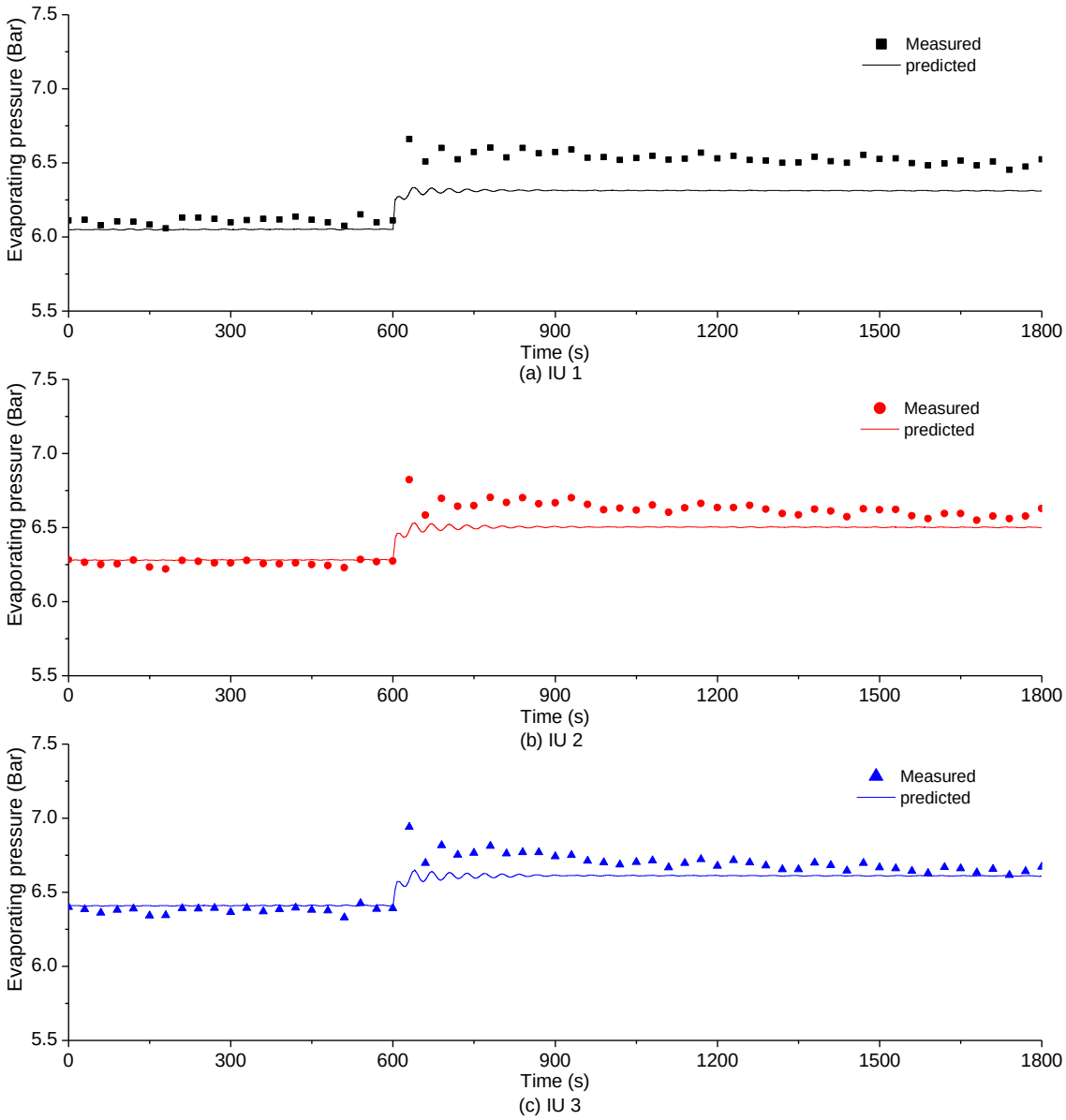

Fig. 6.6 Comparison between predicted and measured evaporating pressures following a compressor speed change at 600s

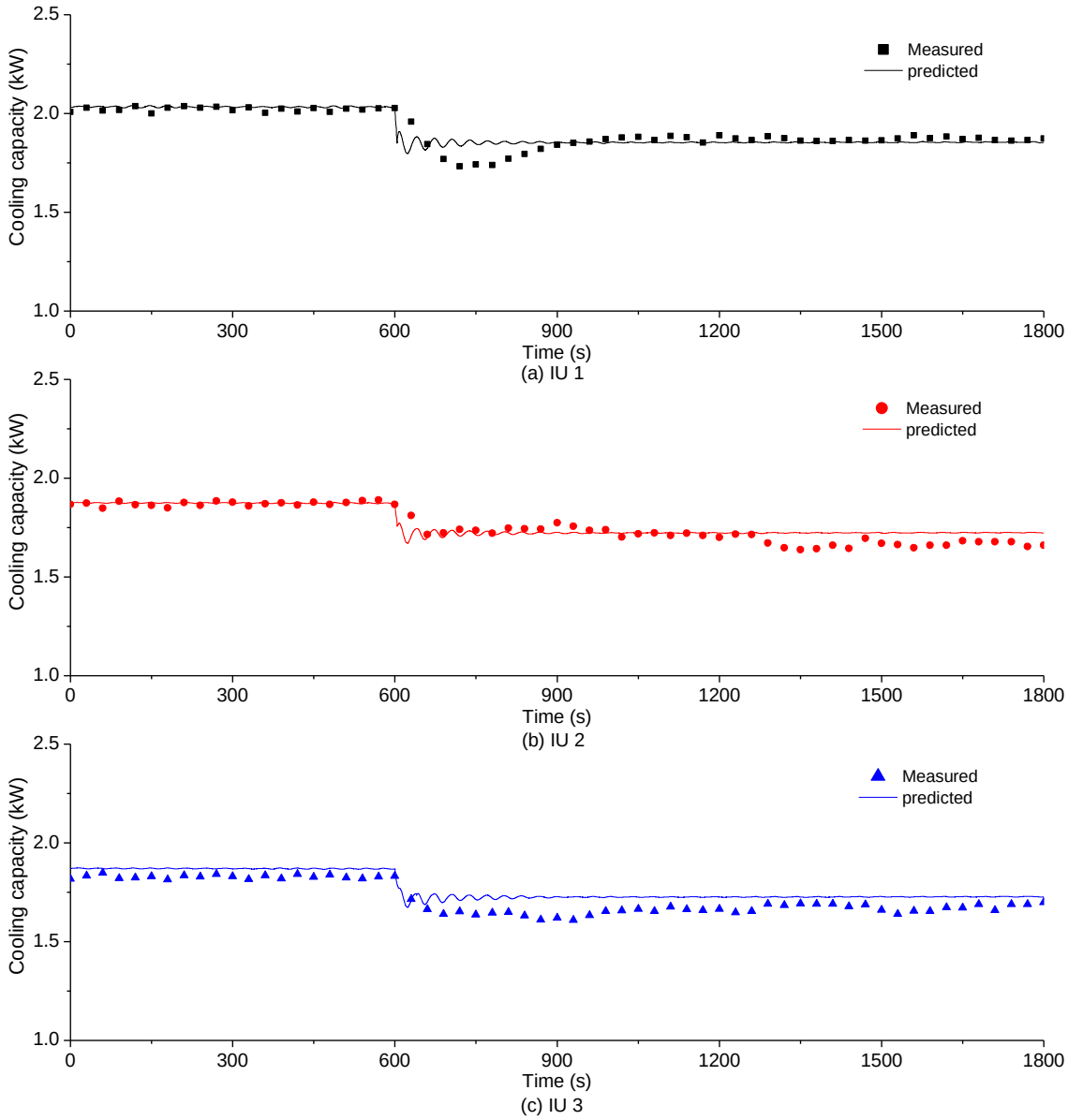

Fig. 6.7 Comparison between predicted and measured cooling capacities following a compressor speed change at 600s

In Fig. 6.7, following the step change in compressor speed at 600s, the predicted and the measured cooling capacities for the three IUs of the TEAC system are compared. As a result of the step change in compressor speed at 600s, less refrigerant was circulated,

leading to a decrease in the output cooling capacities for all the IUs as illustrated in Fig. 6.7.

As seen in Fig. 6.7a, before the step change in compressor speed at 600s, the measured and predicted cooling capacities of IU 1 were 2.01 kW and 2.06 kW, respectively, but dropped to 1.87 kW and 1.85 kW at time 800s after the change. In IU 2, the measured and predicted cooling capacities were both at 1.88 kW. After the change, at 800s when a new steady state arrived, the two were 1.66 kW and 1.72 kW, respectively, representing a 3.6% steady state error, as shown in Fig. 6.7b. Finally, in IU 3, there were steady state relative errors of 1.2% and 2.3%, respectively, between the measured and the predicted cooling capacity before and after the compressor speed change, as shown in Fig. 6.8c.

From the validation results shown in Figs. 6.3-6.7, it can be seen that the physics-based dynamic mathematical model for a TEAC system developed can represent an actual TEAC system in both steady-state and transient condition, within an acceptable modeling accuracy of not greater than ±6%. Therefore, the model developed can be regarded as being experimentally validated.

6.4 Conclusions

In this chapter, the development and experimental validation of a dynamic mathematical

model for the experimental TEAC system detailed in Chapter 4 are presented. The system components modeled included a variable-speed compressor, an air-cooled condenser, three EEVs, three IUs and ISs. Unlike all other reported MEAC models, both sensible and latent heat balances on the air side of all IUs were specifically taken into account in the TEAC model developed. The complete dynamic mathematical model for the experimental TEAC system has been implemented using MATLAB programming environment.

The model was experimentally validated by comparing the predicted results using the model with the measured results obtained from the experimental TEAC system, with the difference between the predicted and the measured being less than ±6%. The TEAC model developed and reported in this chapter was first of its kind because, firstly, it was physics-based with full experimental validation, and secondly it specifically took into account both the sensible and latent heat balances on the air side of its IUs. It is therefore expected that the model can be used as an effective platform in studying the operating performance, and developing advanced control strategies of a TEAC system. Given that both sensible and latent heat balances on the air side in each IU were considered during modeling, the model developed is also expected to be particularly useful in developing a control strategy for improved indoor humidity control using a TEAC system.

The validated model for the experimental TEAC system will be used to assist the development of a novel capacity controller for not only controlling indoor air temperature but also improving indoor humidity control for the TEAC system, which will be reported in Chapter 7.

Chapter 7

A novel capacity controller for the experimental TEAC system for improved indoor humidity control

7.1 Introduction

In buildings located in hot and humid climates such as Hong Kong, controlling indoor air humidity at an appropriate level is very important since this directly affects building occupants' thermal comfort, IAQ and the operating efficiency of the building A/C installations [Toftum and Fanger 1999, Berglund 1998].

Using an MEAC system to correctly control indoor air temperatures only in a multi-room application is already a challenging and difficult task, let alone the control of both indoor air temperature and humidity. This is because in an MEAC system, a number of IUs, possibly of different cooling capacities, are connected to a common condensing unit. Hence, changes in the operating condition of one particular IU are very much likely to influence the operating conditions of the other IUs [Shah et al. 2004], and therefore the appropriate control action required should ensure that each IU receives the exact amount of refrigerant flow for the space cooling needs. On the other hand, the complex dynamic characteristics of heat and mass transfer taking place on the air side of

each IU make it extremely difficult to achieve simultaneous control of indoor air temperature and humidity.

Although MEAC systems are being extensively used and related experimental and simulation research work has been carried out, current efforts have focused on controlling indoor air temperature only [Gordon et al. 1999, Chen et al. 2005, Elliott and Rasmussen 2009, Lin and Yeh 2009a, Lin and Yeh 2009b] without paying much attention to indoor humidity control. However, with the previous related work on both temperature control for a DEAC system [Xu et al. 2013b] and improved indoor humidity control for an SEAC system using the H-L controller [Xu et al. 2008], it was considered possible to integrate these two control algorithms to develop a novel controller for MEAC systems for not only indoor air temperature control but also improved indoor humidity control.

In this chapter, therefore, the development of such a novel capacity controller for the experimental TEAC system, which is a typical example of MEAC systems, for improved indoor humidity control, is report. Firstly, the control algorithm is detailed. This is followed by reporting the results of simulative controllability tests for the controller using the dynamic model for the experimental TEAC system as described in Chapter 6. Thirdly, following the successful simulative controllability tests, the results

of experimental controllability tests using the experimental TEAC system presented in Chapter 4 are presented. Finally, conclusions are given.

7.2 Control algorithm for improved indoor humidity control

As mentioned, the novel controller development was built on the two previous developed controllers [Xu et al. 2008 and Xu et al. 2013b]. Similar to the H-L controller previously developed [Xu et al. 2008], the novel capacity controller reported in this chapter was not directly to control indoor air humidity, but to address two issues causing possible high indoor air humidity for an On-Off temperature only controlled TEAC system. These were the absence of dehumidification and the re-evaporation of condensate on the surface of an IU while its matching fan may still operate during an Off-period when the indoor air temperature setting was satisfied and the refrigerant supply to the IU was completely stopped. This was done by supplying less refrigerant, instead of completely stopping its supply, and at the same time, running the supply fan at a lower speed. Consequently, improved humidity control, as compared to that under On-Off temperature only control, can be achieved.

In a TEAC system, for the $i^{th}\left(i=1,2,3\right)$ IU serving the i^{th} IS, with its indoor air temperature setting, T_{set_i}, a control signal at a time point t, $E_i(t)$, can be defined as:,

$$
\begin{aligned}
&\text{If } T_i(t) \geq T_{set\_i} + \Delta T_i && E_i(t) = 1 \\
&\text{If } T_{set\_i} - \Delta T_i < T_i(t) < T_{set\_i} + \Delta T_i && E_i(t) = E_i(t-1) \\
&\text{If } T_i(t) \leq T_{set\_i} - \Delta T_i && E_i(t) = 0
\end{aligned} \tag{7.1}
$$

where $T_i(t)$ is the actual space air temperature at t time point, $t-1$the last time point and ΔT_i the temperature control dead-band.

The period when $E_i(t) = 1$ was referred to as an H (high)-period when the compressor and fan are operated at higher speeds and that when $E_i(t) = 0$, L (low)-period at lower speeds. At an H-period, the supply refrigerant mass flow rate to the i^{th} IU was m_{ri}, or the design refrigerant mass flow rate. At a L-period, instead of stopping supplying refrigerant to the IU, less refrigerant was supplied at $x_i \times m_{ri} \left(0 < x_i < 1\right)$, where $x_i (i = 1, 2, 3)$ is the ratio of refrigerant mass flow rate at a L-period to that at an H-period.

The refrigerant mass flow rate entering an evaporator or an IU was controlled by its matching EEV. When $E_i(t) = 1$, the EEV functioned to control the refrigerant DS and the supply fan operated at its full speed. On the other hand, when $E_i(t) = 0$, the EEV functioned as a modulating valve to reduce the refrigerant mass flow rate to supply less refrigerant to an IU. At the same time, the supply fan speed was also reduced, resulting in a smaller supply air flow rate passing through the IU. When the indoor air

temperature was within the dead-band, as represented by Equation (7.1), the operational status of both EEV and the supply fan at time t were the same as they were at time $t-1$. Consequently, totally there were eight different operating IU combinations for a TEAC system at any time, evaluated by: $\sum_{i=0}^{3} C_3^i = 8$, as shown in Table 7.1.

Table 7.1 Control logics for determining compressor speed at different combinations of operating IUs for a TEAC system

Serial number	H/ L period of each IU			Total required refrigerant mass flow rate to be provided by compressor	Compressor speed
	IU 1	IU 2	IU 3		
1	H	H	H	$m_{r1}+m_{r2}+m_{r3}$	$n_1 = f(m_{r1}+m_{r2}+m_{r3})$
2	H	H	L	$m_{r1}+m_{r2}+x_3m_{r3}$	$n_2 = f(m_{r1}+m_{r2}+x_3m_{r3})$
3	H	L	H	$m_{r1+}x_2m_{r2}+m_{r3}$	$n_3 = f(m_{r1+}x_2m_{r2}+m_{r3})$
4	L	H	H	$x_1m_{r1}+m_{r2}+m_{r3}$	$n_4 = f(x_1m_{r1}+m_{r2}+m_{r3})$
5	H	L	L	$m_{r1}+x_2m_{r2}+x_3m_{r3}$	$n_5 = f(m_{r1}+x_2m_{r2}+x_3m_{r3})$
6	L	H	L	$x_1m_{r1}+m_{r2}+ x_3m_{r3}$	$n_6 = f(x_1m_{r1}+m_{r2}+ x_3m_{r3})$
7	L	L	H	$x_1m_{r1}+x_2m_{r2}+m_{r3}$	$n_7 = f(x_1m_{r1}+x_2m_{r2}+m_{r3})$
8	L	L	L	$x_1m_{r1}+x_2m_{r2}+x_3m_{r3}$	$n_8 = f(x_1m_{r1}+x_2m_{r2}+ x_3m_{r3})$

The compressor speed, *n*, could then be determined by the relationship between compressor speed and the required total refrigerant mass flow rate to be delivered by the compressor, which can be either provided by the compressor manufacturer or obtained

experimentally, as follows:

$$n = f(m_r) \tag{7.2}$$

Where m_r is the required total refrigerant flow rate to be delivered by the compressor, which was the sum of the refrigerant mass flow rates to all the operating IUs at a time point. For example, in Table 7.1, if IU 1 and IU 2 were operated at H-periods and IU 3 at a L-period, then EEV 1 and EEV 2 functioned to control the DS, and the refrigerant mass flow rates to IU1 and IU1 were m_{r1} and m_{r2}. EEV 3, however, functioned as a modulation valve to reduce m_{r3} to $x_3 \times m_{r3}\,(0 < x_3 < 1)$, and the compressor speed was determined by $n = f\left(m_{r1} + m_{r2} + x_3 \times m_{r3}\right)$ (the Serial number 2 in Table 7.1). It should be noted, if an IU, for example IU 2, in the TEAC system was not turned on because the 2nd IS was not used, m_{r2} should be set to 0 by completely closing EEV 2, and a TEAC system actually becomes a DEAC system.

In practice, indoor fan speed cannot be set too low to adversely affect the indoor air flow pattern. Since (1) the impact of varying fan speed on the total output cooling capacity of an IU was much less significant than that of varying compressor speed [Xu et al. 2010], (2) the heat transfer coefficient on the refrigerant side was much higher than that on the air side; and (3) the fan power consumption was much low than the compressor power

consumption, only a 60% fan speed reduction was utilized in this study, i.e., at a L-period, an indoor fan was operated at 60% of the fan speed at an H-period.

On the other hand, to determine the exact extent of refrigerant flow reduction at a L-period, or the exact value of x_i $(i = 1, 2, 3)$, there were two points of consideration, avoiding space overcooling, and providing a non-stop dehumidification ability without requiring a precise control over indoor air humidity. During an H-period, the output cooling capacity from the IU should be greater than the yearly design cooling load [ASHRAE 2004] to provide adequate cooling, but during a L-period, smaller than the yearly minimum cooling load [ASHARE 2007] to avoid overcooling. In the current study, values of $x_i = 0.5$ $(i = 1, 2, 3)$ were adopted. Under the proposed novel controller, the matching of output cooling capacity for an IU in the TEAC system to the actual cooling load in an IS was not realized by accurately controlling the refrigerant mass flow rate at a specific value, but rather by the different operating durations at H and L periods. The deviation between the actually required refrigerant mass flow rate and the operating refrigerant flow rate as determined by the novel controller was expected to be restrained within a narrow range, but to be compensated by the adjustment in time duration through the switching between H and L periods.

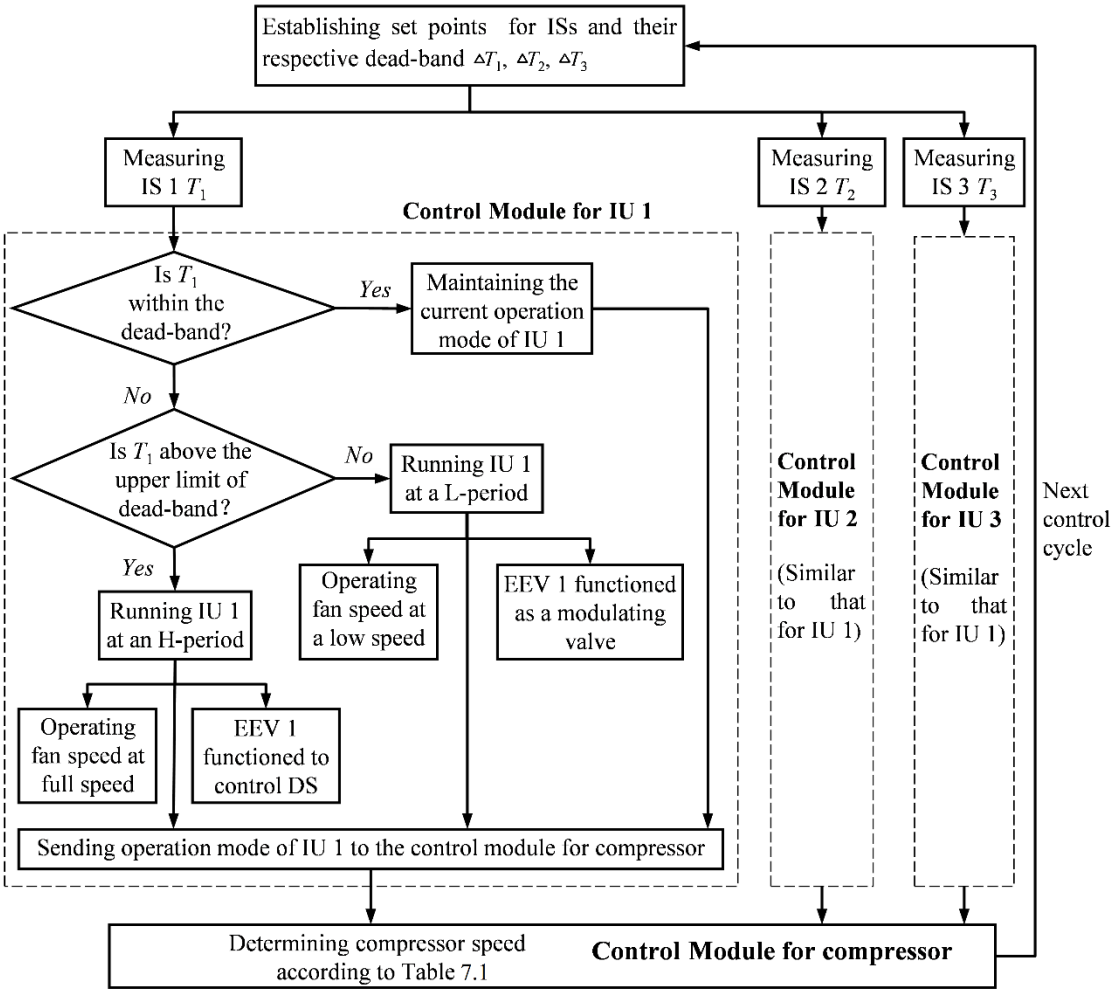

Fig. 7.1 Flow chart of the novel control algorithm for a TEAC system for improved humidity control

The flow chart of the above novel control algorithm for the experimental TEAC system for improved humidity control is shown in Fig. 7.1. As seen, the controller had a flexible structure, with a specific control module for each IU. Therefore, it can be easily extended to controlling an MEAC system, even though the controller development was

based on a TEAC system.

Controllability tests for the novel controller were carried out using both simulation and experimental approaches. Simulative tests using the experimentally validated dynamic mathematical TEAC model presented in Chapter 6 were carried out to ascertain the controller's correctness and robustness prior to its experimental validation. The results of simulation and experimental controllability tests are reported in Sections 7.3 and 7.4, respectively.

7.3 Controllability tests - simulation

A dynamic mathematical model for the experimental TEAC was developed and experimentally validated as described in Chapter 6. The model was made of sub-models for major system components, such as compressor and evaporators, etc. The experimental validation suggested that the model could simulate a real TEAC system in both transient and steady-state operations, with a prediction error of not greater than 6%.

Using the validated TEAC model, extensive simulation-based controllability tests were carried out and two examples of test results are given in this section. The testing conditions for the two tests are shown in Table 7.2. In order to prevent frequent speed change of the compressor, a dead-band of ±0.35 ºC was utilized for indoor air

temperature control in all the ISs. The air dry-bulb temperature in the outdoor space was maintained at 35 °C. In all the tests, indoor air RH was not controlled directly but allowed to fluctuate, depending on the actual latent output cooling capacity from each IU.

Table 7.2 Details of the two simulation-based controllability tests

Test	IS	Dimension of each IS (m)	Indoor air T_{set} (°C)	sensible load (W)	latent load (W)
S1	1	1.5×3.7×3.3	26	1150	450
	2	1.85×3.7×3.3	26	1250	650
	3	1.85×3.7×3.3	26	1350	550
S2	1	1.5×3.7×3.3	27	step change from 1300 to 1400 W at t = 2400 s	step change from 500 to 700 W at t = 2400 s
	2	1.85×3.7×3.3	26	1300	500
	3	1.85×3.7×3.3	25	1300	500

Fig. 7.2 shows the simulation results of controllability Test S1. As seen in Fig. 7.2a, indoor air temperatures in all ISs fluctuated around the same temperature setting point (26°C) in a repeatable pattern. However, the variation patterns for indoor air

temperature in the three ISs were different, because of the different indoor sensible and latent cooling loads. For example, indoor air temperature in IS 1, T_1, reached its low boundary of the ±0.35°C dead-band earlier than that in IS 2 and IS 3. When T_1 reached its low boundary of the dead-band, i.e., $T_1 < T_{set\_1} - \Delta T_1$, the speed of the supply fan in IU 1 was reduced to run at a L-period and compressor speed was also reduced to supply less refrigerant to IU 1.

Fig. 7.2b shows the simulated results of indoor air RH in the three ISs when the TEAC system was controlled by the novel controller. It can be seen that the RH fluctuation ranges in all the three ISs were small, at around 1.6%, 1.3% and 0.9%, respectively. The indoor air RH level in all ISs was increased at their respective H-periods but reduced at their respective L-periods, suggesting that the dehumidifying ability of the TEAC system during the L-periods was better than that during the H-periods.

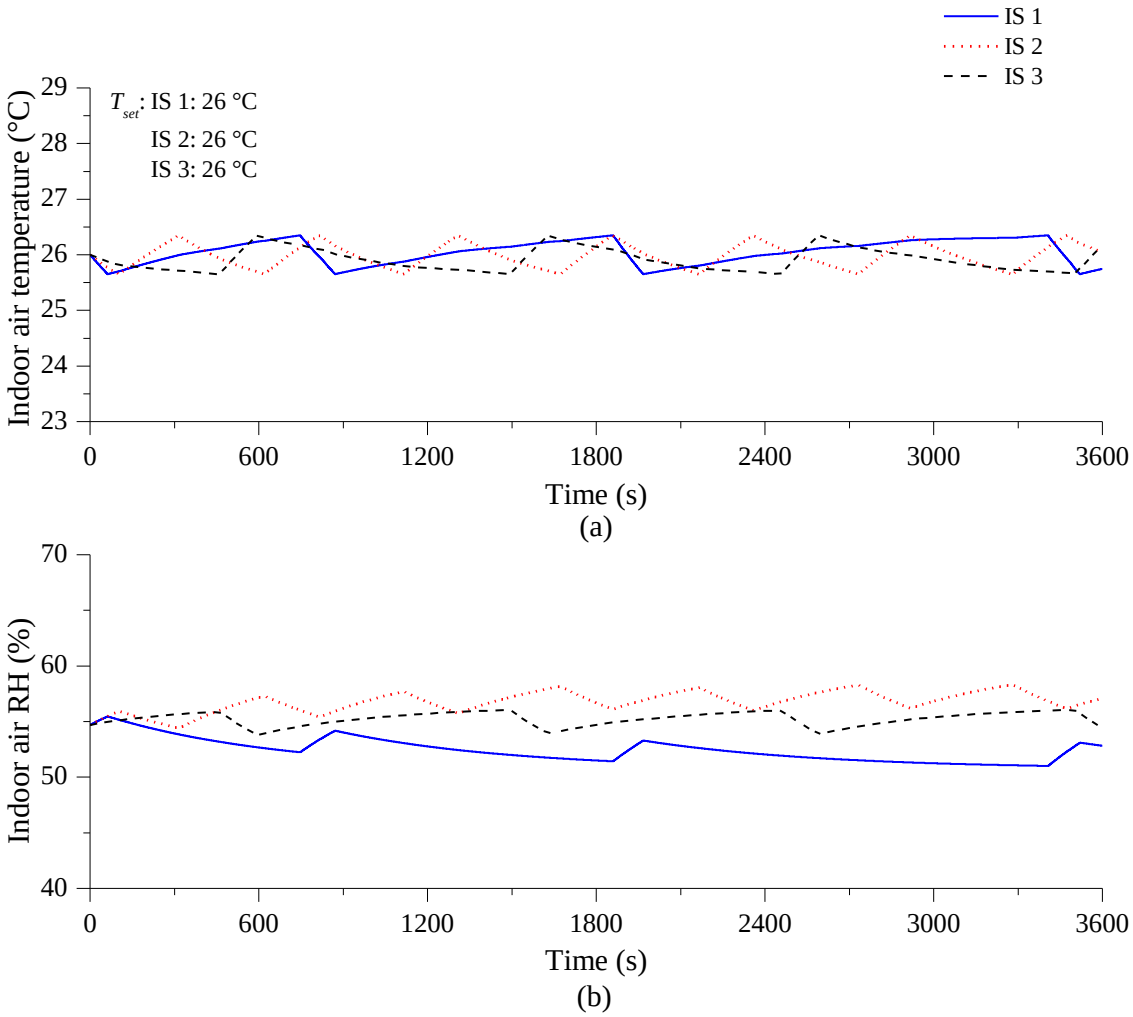

Fig. 7.2 Variations of the simulated indoor air temperature and RH in all ISs under the novel controller (Test S1)

It should be mentioned that with the novel controller, the matching of the output cooling capacity of an IU in a TEAC system to the cooling load in an IS was not realized by accurately controlling the refrigerant mass flow rate at a specific value, but rather by the different operating durations at H and L periods. While indoor air dry-bulb temperature was controlled within a dead-band, indoor air humidity was indirectly controlled

without a specific setting point. Therefore, with the enhanced dehumidification ability due to low speed operation, in general, a lower indoor RH can be resulted in. For instance, the latent load in IS 2 was much higher than that in other ISs, its RH was only slightly higher than those in the other two ISs.

Fig. 7.3 shows the simulation results of controllability Test S2 where there were step increases in space sensible and latent loads at t = 2400 s in IS 1, as detailed in Table 7.2. As seen in Fig. 7.3, air temperatures in all spaces were stabilized at their respective set points, within ±0.35 °C before the change introduced at t = 2400 s. In IS 1, where the step increases in thermal loads were introduced at t = 2400 s, the controller responded by operating the IU 1 at a longer H-period. This, together with an increase in the latent load in IS 1, led to an increase in the indoor air RH in IS 1. However, the RH levels in the other two ISs were slightly reduced.

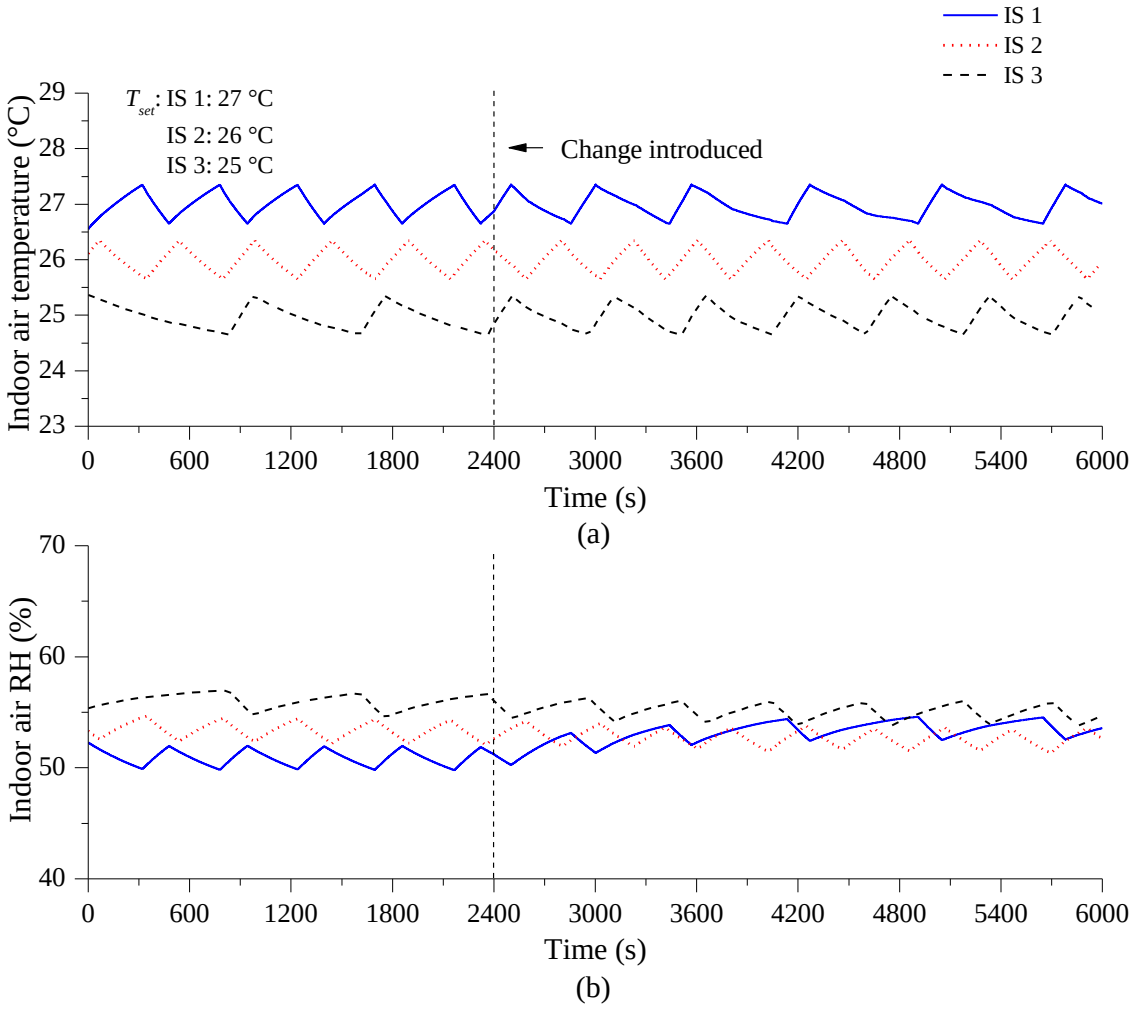

Fig. 7.3 Variations of the simulated indoor air temperature and RH in all ISs under the novel controller (Test S2)

The examples of simulative controllability test results shown in Figs. 7.2 and 7.3 clearly demonstrated that the novel controller for the experimental TEAC system for improved indoor humidity control appeared operational, being able to maintain the required indoor air temperature and stable indoor RH. However, further experimental evidences were desired, and the experimental controllability test results are reported in Section 7.4.

7.4 Controllability tests - experiments

7.4.1 Experimental controllability test conditions

Using the experimental TEAC system described in Chapter 4, three sets of experimental controllability tests were carried out as detailed in Table 7.3. In the first set, where there were three tests, indoor air dry-bulb temperatures in the three ISs remained unchanged at their respective settings during the tests, but the space cooling load in one or two ISs were altered at a time. In the second set containing also three tests, while space sensible and latent cooling loads in the three ISs remained unchanged during the tests, indoor air temperature set-points in one or more ISs were changed to new values at a time. In the last set, there were two tests where the performance of the novel controller and that of a tradition On-Off controller, in terms of the control of indoor air temperature and RH level and energy consumption, were compared.

Table 7.3 Experimental controllability test conditions

		Fixed settings		Changed Setting	
				Before	After
Set One					
Test	IS	Fixed IS air T_{set} (ºC)		Sensible/ Latent load (W)	
E1	1	27.5		1300/ 400	1350/ 550
	2	26.5		1100/ 200	1200/ 400
	3	25.5		1300/ 300	1300/ 300
E2	1	27		1250/ 750	1250/ 350
	2	25		1400/ 250	1400/ 250
	3	27		1300/ 400	1300/ 650
E3	1	26.5		1100/ 750	1100/ 750
	2	26.5		1250/ 300	0/ 0
	3	25.5		1400/ 300	1400/ 300
Set Two					
Test	IS	Sensible/ Latent load (W)		IS air setting T_{set} (ºC)	
E4	1	1100/ 750		26.5	27.5
	2	950/ 500		26.5	26.5
	3	1200/ 650		26.5	26.5
E5	1	1200/ 600		26.5	27.5
	2	1100/ 400		26.5	26.5
	3	1200/ 600		26.5	25.5
E6	1	1000/ 800		27.5±0.5	27.5±0.35
	2	1100/ 500		26.5±0.5	26.5±0.35
	3	1200/ 600		25.5±0.5	25.5±0.35
Set Three					
Test	IS	T_{set} (ºC)	Sensible/ Latent load (W)	Control strategy	
E7	1	25.5	1300/ 450	novel controller	On-Off controller
	2	26.5	1200/ 250		
	3	27.5	1300/ 450		
E8	1	25.5	1000/ 800	novel controller	On-Off controller
	2	26.5	1000/ 600		
	3	27.5	1200/ 450		

For each of the tests listed in Table 7.3, the test duration was 9600 s. In the first half of test, i.e., 4800 s, all experimental conditions and settings remained unchanged, and the experimental TEAC system was operated at a steady condition. The changes as specified in Table 7.3 were then introduced at 4800 s and each test went on for a further 4800 s (second half).

During all tests when the experimental TEAC system was under the novel controller and indoor air temperatures reached their respective settings, the corresponding EEV would function as a modulating valve to supply less refrigerant to its matching IU. At the same time, the supply fan speed was also reduced. However, in Test E3 when both sensible and latent cooling load in IS 2 were reduced to zero, IU 2 was completely shut off by closing its matching EEV and switching off its supply fan. The settings of DS for the three IUs were the same at 6 °C. Furthermore, in the simulated outdoor space, air dry-bulb temperature was maintained at 32 °C ± 0.15 °C, using the existing separate A/C system and the LGU placed there.

On the other hand, according to the detailed technical specification of the compressor used in the experimental system, the relationship between its output cooling capacity and input electrical supply frequency was linear. As seen in Table 4.1, the three IUs in the experimental TEAC system had a similar cooling capacity. For the sake of clarity,

the same refrigerant mass flow rates at an H-period, $m_{ri}\,(i=1,2,3)$ for the three IUs were assumed. In the current study, when the three IUs were operated at H-periods at the same time, the electric supply frequency to the compressor, i.e., n_1 in Table 7.1, was set at 75 Hz.

Given that the temperature sensors used in the experimental TEAC system were highly sensitive, in order to prevent frequent speed change of the compressor, a dead-band was introduced to the temperature control. A ±0.5 ºC dead-band was applied to most experimental tests except for the second half of Test E6, when all the dead-bands were reduced to ±0.35 ºC. While a control dead-band of ±0.5 ºC has been commonly used in On-Off controlled A/C systems, a smaller temperature dead-band setting was further used to demonstrate the robustness of the novel controller that indoor air temperature can be controlled closer to its settings.

7.4.2 Experimental controllability test results and discussions

Using the experimental TEAC system and following the experimental conditions presented in Section 7.4.1 and Table 7.3, eight tests to examine the controllability of the novel controller developed were carried out and the test results are presented in Figs. 7.4 to 7.11.

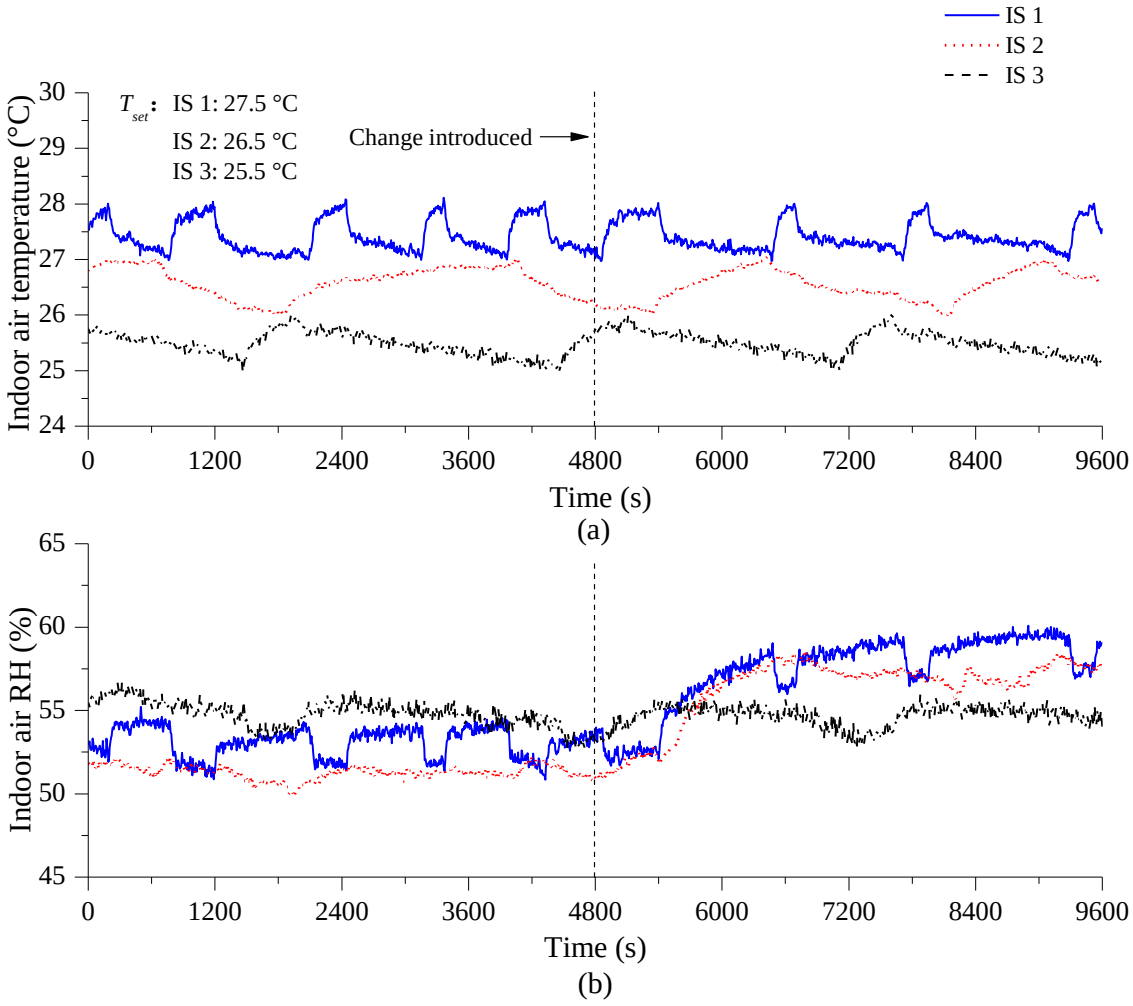

Fig. 7.4 Variations of indoor air temperature and RH in all ISs under the novel controller (Test E1)

Fig. 7.4 shows the experimental results of indoor air dry-bulb temperatures and RH in the three ISs in Test E1. As seen, before the changes at 4800 s, indoor air temperatures in the three ISs were oscillated around their respective set points within the dead-band, but having different variation patterns because of different cooling loads and IUs' capacities. Indoor RH levels in the three ISs were lowered at their respective L-periods

and raised at their respective H-periods, suggesting that the dehumidifying ability of the TEAC system during L-periods was even better than that during H-periods. This resulted in indoor RH in the three ISs in Test E1 being below 60%. In addition, the fluctuation in indoor air RH level in the three ISs mainly took place following a switch between an H-period and a L-period and lasted for only a short while, leading to relative small fluctuations in RH in the three ISs.

After the cooling loads in IS 1 and IS 2 were increased at 4800 s, the H-periods for IU 1 and IU 2 were further prolonged and their L-periods shortened. The increase in latent loads in the two ISs led to an increased indoor air RH level, from 53.1% to 57.4% in IS 1and 51.3% to 56.3% in IS 2, respectively, reflecting the nature of indirect control of indoor air humidity by the novel controller. However, after the changes in cooling loads in the two ISs, the variations of air temperatures in the three ISs were still within the expected control range.

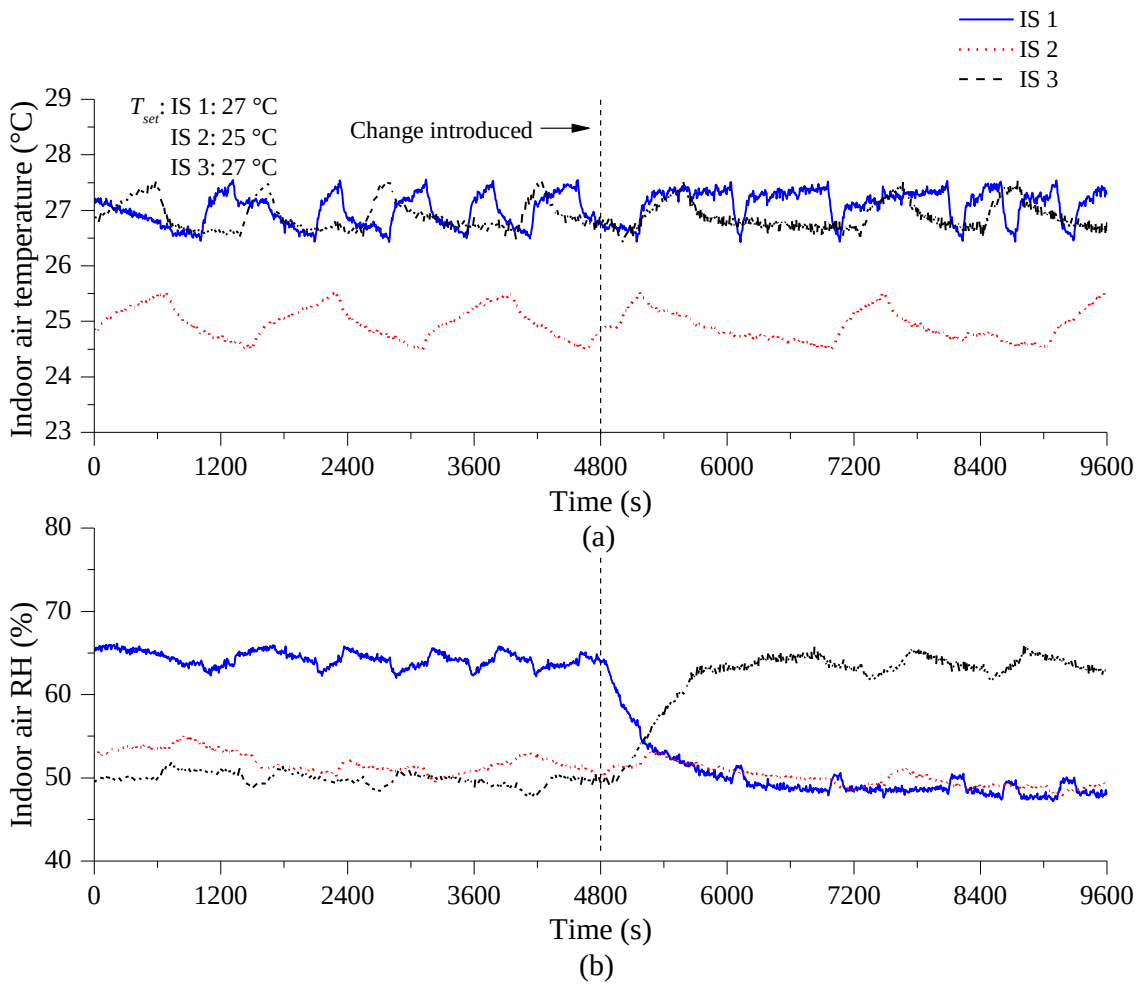

Fig. 7.5 Variations of indoor air temperature and RH in all ISs under the novel controller (Test E2)

Fig. 7.5 shows the variations of indoor air dry-bulb temperatures and RH in the three ISs in Test E2 under the novel controller. In the first half, while indoor temperature in the three ISs were controlled around their respective setting points, indoor air RH in IS 1 was much higher than that in the other two ISs, due to its very high latent load. At t = 4800 s, the latent load in IS 1 was reduced but that in IS 3 increased. Consequently,

between 4800 s and 9600 s, IU 1 was operated with shortened H-periods, leading to a significant reduction in RH level in IS 1. On the contrary, IU 3 was operated with prolonged H-periods, leading to an increased indoor RH level in IS 3. It should be further noted that even the operating conditions of IU 2 remained unchanged, the variation patterns of indoor air temperature and RH in IS 2 would also vary if there were changes to the other two IUs' operation.

Fig. 7.6 shows the experimental results of indoor air temperatures and RH in the three ISs in Test E3. During the second half of the Test, the LGU and IU in IS 2 were shut off. Since the electrical heater inside the LGU was still at a high temperature even after the shutdown, the air temperature in IS 2 kept rising after the shutdown of IU 2. In this case, there were only two IUs operated. As seen, while the air temperature and RH in IS 2 where its IU was stopped were freely varied, the air temperature and RH in the other rooms where IUs were on, remained under control.

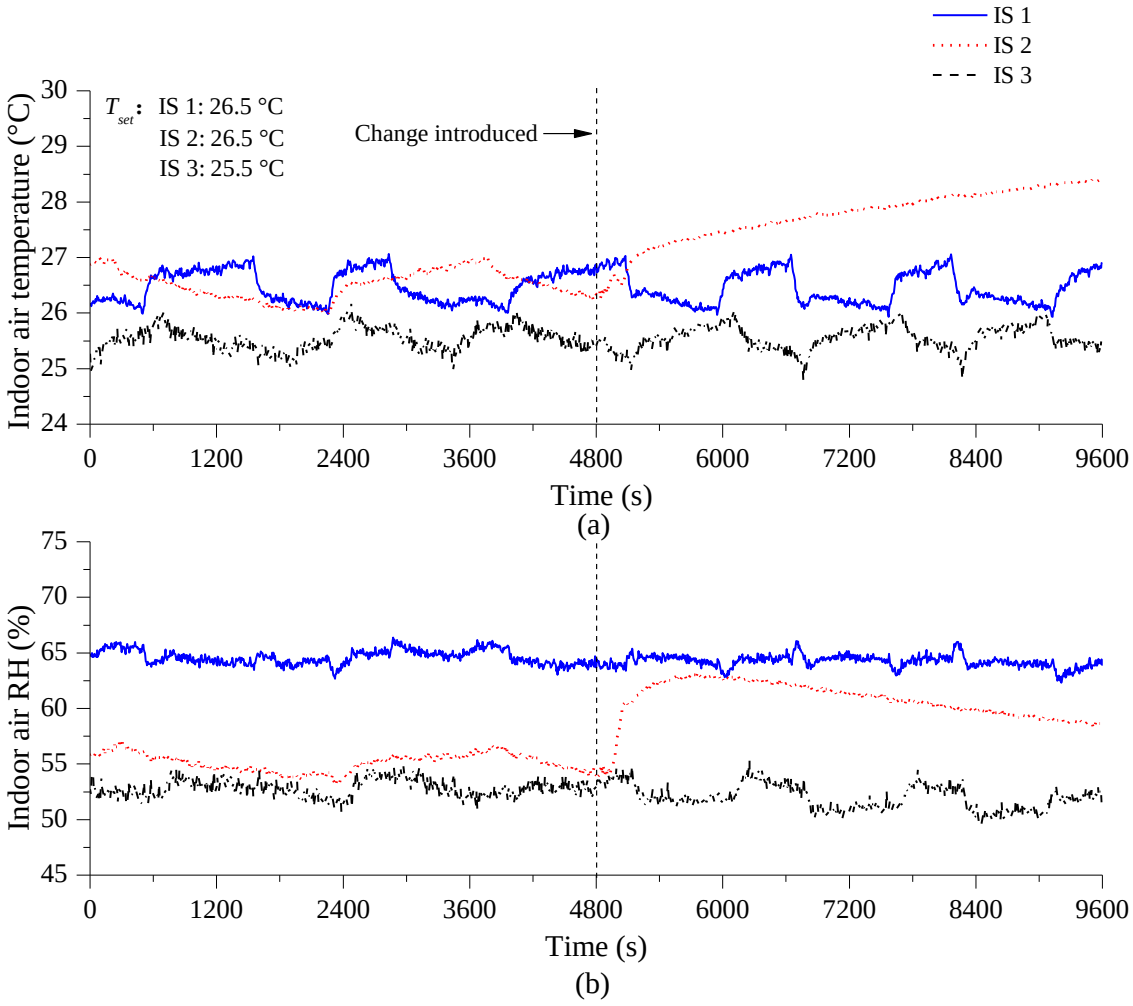

Fig. 7.6 Variations of indoor air temperature and RH in all ISs under the novel controller (Test E3)

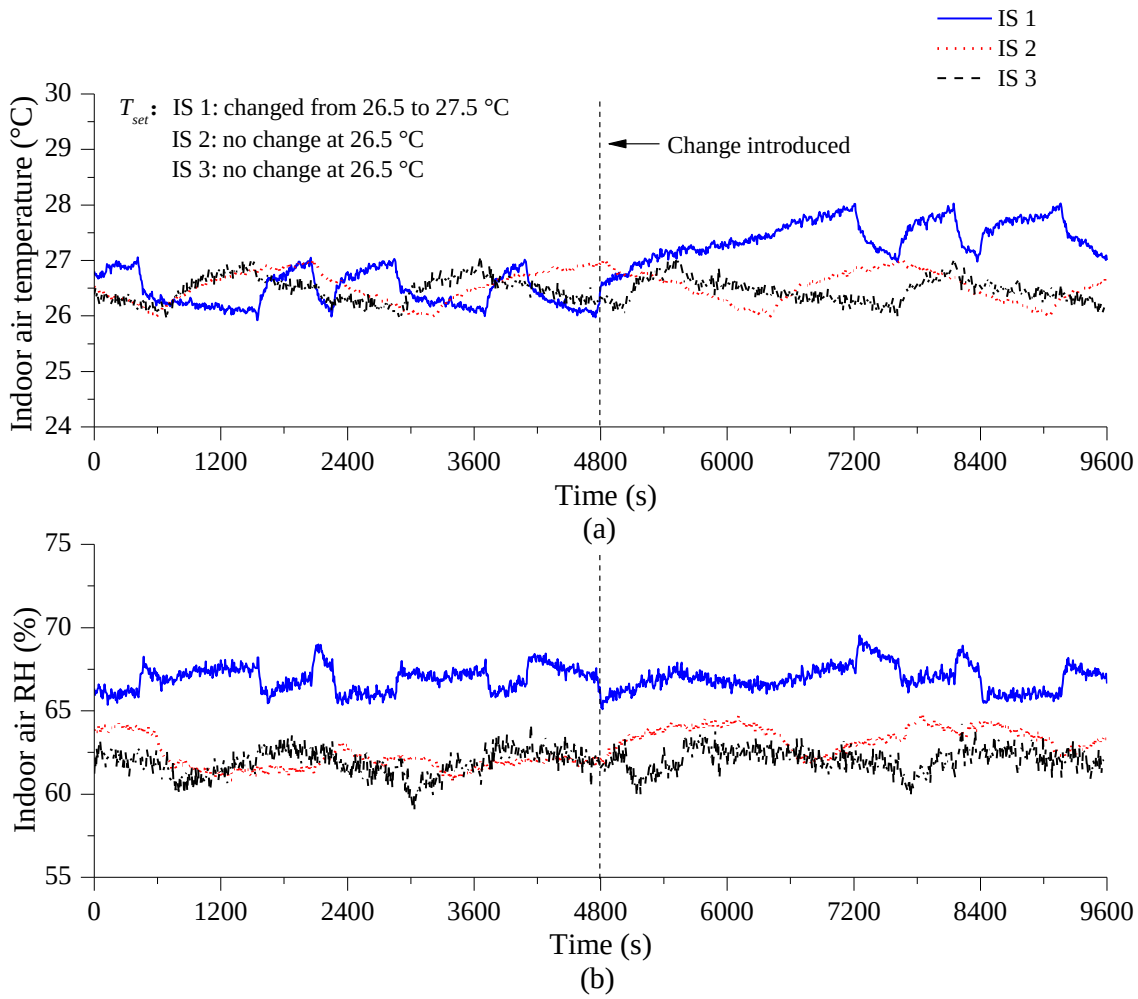

Fig. 7.7 Variations of indoor air temperature and RH in all ISs under the novel controller (Test E4)

Figs. 7.7 to 7.9 show the variations of indoor air dry-bulb temperatures and RH level in the three ISs in Tests E4 to E6 under the novel controller, when the cooling loads in the three ISs were fixed but indoor air temperature settings were varied. As seen in Fig. 7.7, as the indoor air temperature setting in IS 1 was increased by 1 ºC, its RH level was slightly reduced. It can be seen from Fig. 7.7 and 7.8 that, altering air temperature

settings would definitely affect the variation patterns of indoor air temperature, shortening its H-period when increasing the temperature setting and shortening its L-period when reducing the temperature setting. However, the variation patterns of indoor RH levels were not disturbed. In Test E6, when indoor air temperature dead-band was reduced from ±0.5 ºC to ±0.35 ºC, the variation ranges of air temperature and RH became correspondingly smaller but with more variation cycles. Hence, the use of the novel controller showed good control robustness in the three tests, i.e., the changes in air temperature settings in one or more ISs did not significantly disturb the indoor air temperature and RH levels in the other ISs.

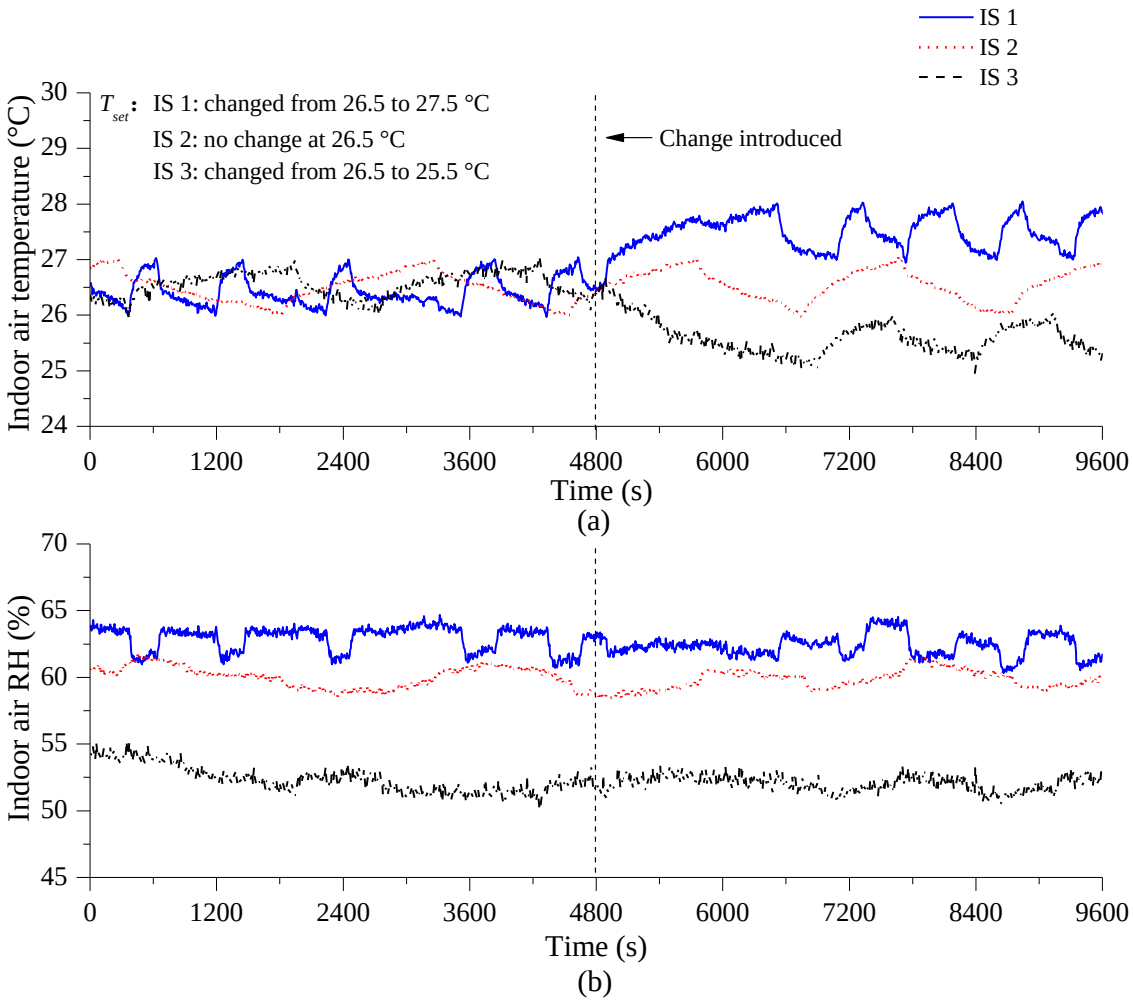

Fig. 7.8 Variations of indoor air temperature and RH in all ISs under the novel controller (Test E5)

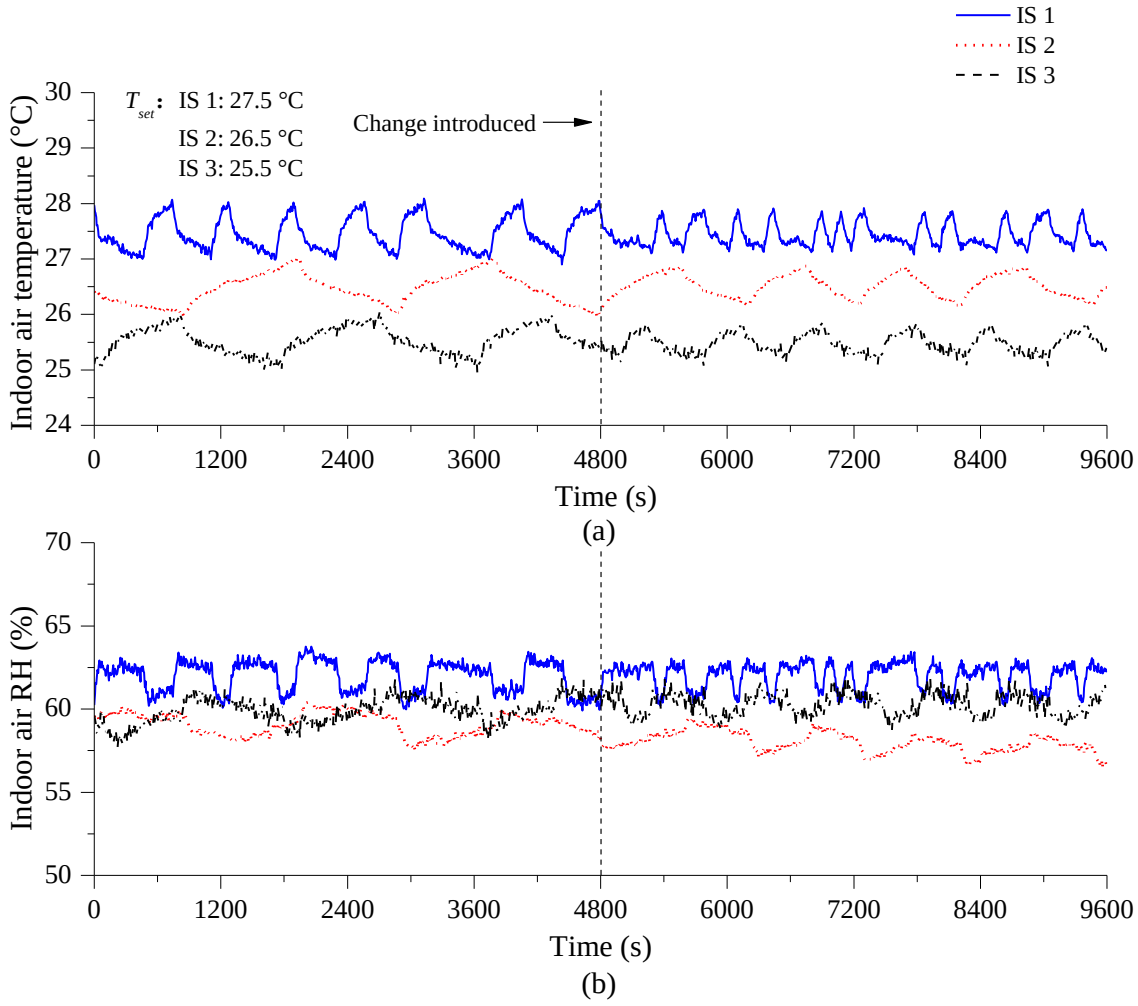

Fig. 7.9 Variations of indoor air temperature and RH in all ISs under the novel controller (Test E6)

In Test E7 and E8, the experimental TEAC system were controlled by the novel controller in the first half but by a traditional On-Off temperature controller in the second half. Control signals described in Equation (7.1) were also adopted when under On-Off controller, but with different control actions. In this case, the period when $E_i(t)=1$ was referred to as an On-period when an EEV functioned to control the

refrigerant DS, and that when $E_i(t) = 0$ as an Off-period when EEV was closed. While an IU in the TEAC systems was On-Off controlled, its supply fan would be operated at a lower speed when the EEV in the IU was closed. The compressor speeds were also determined as described in Table 7.1, but with $x_i = 0\ (i = 1, 2, 3)$. When the three IUs were operated, the electric supply frequency to the compressor was set equal to that when the three IUs were operated at H-periods under the novel controller, at 75 Hz.

As seen in Fig. 7.10a, in the second half of Test E7, i.e., under On-Off controller, while indoor air temperatures in the three ISs were controlled to their respective set points, their variation magnitudes and cycles were greater than those under the novel controller in the first half. In fact, what were demonstrated in the second half were typical system responses under On-Off control. These were further complicated by a delay of 30 seconds for restarting compressor after shutdown due to safety protection. This meant that once the compressor was shut down, it had to wait for at least 30 seconds before returning operation even though air temperature in one or more ISs were over its respective upper limit. This would effectively prolong the off-durations for these IUs. In Test E7, during the second 4800 s operation, compressor start-up delay occurred for three times at around 6050 s, 7400 s and 8520 s, resulting in that indoor air temperatures were actually 0.35-0.45 ºC higher than its respective upper limit. However, under the novel controller, when an indoor setting was satisfied, instead of completely stopping

refrigerant supply to an IU as under On-Off controller, less refrigerant was supplied. Therefore, as compared to the situation under On-Off controller, the rate of increase in indoor air temperature was smaller, leading to a smaller variation magnitudes and frequencies in temperature control, as seen in the first half of Test E7.

Fig. 7.10b shows the experimental results of air RH level in the three ISs in Test E7. It can be seen that, corresponding to the variations in air temperature, fluctuations of the RH in the three ISs in the first half were around 0.91%, 0.93% and 1.36%, which were smaller when compared to those under On-Off controller in the second half. Also under the novel controller, improved averaged RH level in the three ISs were achieved, for example, in IS 3, 53.8% under the novel controller compared to 56.9% under On-Off controller, reflecting improved dehumidifying ability of the TEAC system under the novel controller.

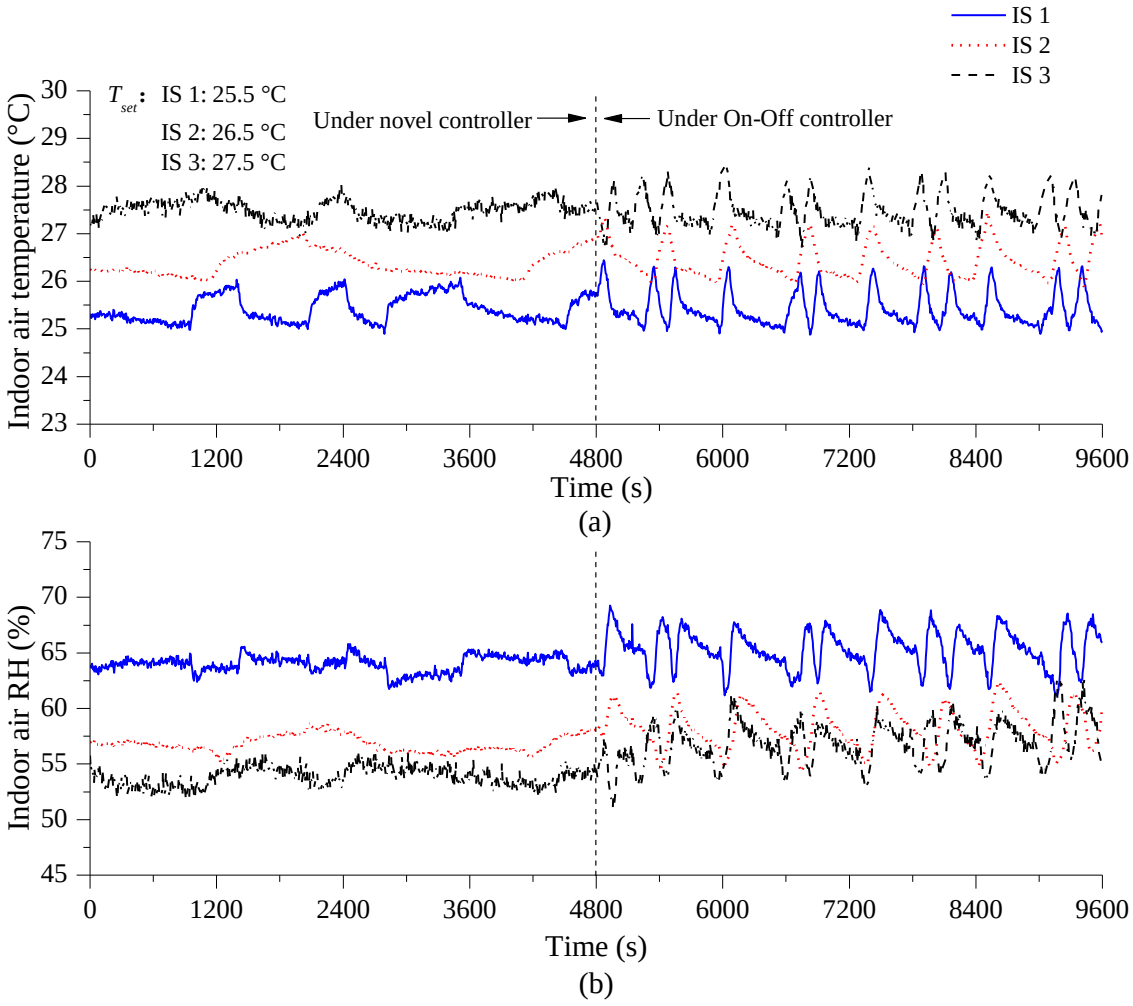

Fig. 7.10 Comparison of indoor air temperature and RH in all ISs between using the novel controller and a traditional On-Off controller (Test E7)

The power input to the compressor was in proportion to compressor speed, which was determined by the operation status of the three IUs. To compare the energy efficiency of the TEAC system under two different control strategies, the total power input to the experimental TEAC system was also recorded. The power input to compressor, under the novel controller in the first half of Test E7 was 2.39 kWh, which was 12.5% less

than that in the second half of Test E7 under the On-Off controller.

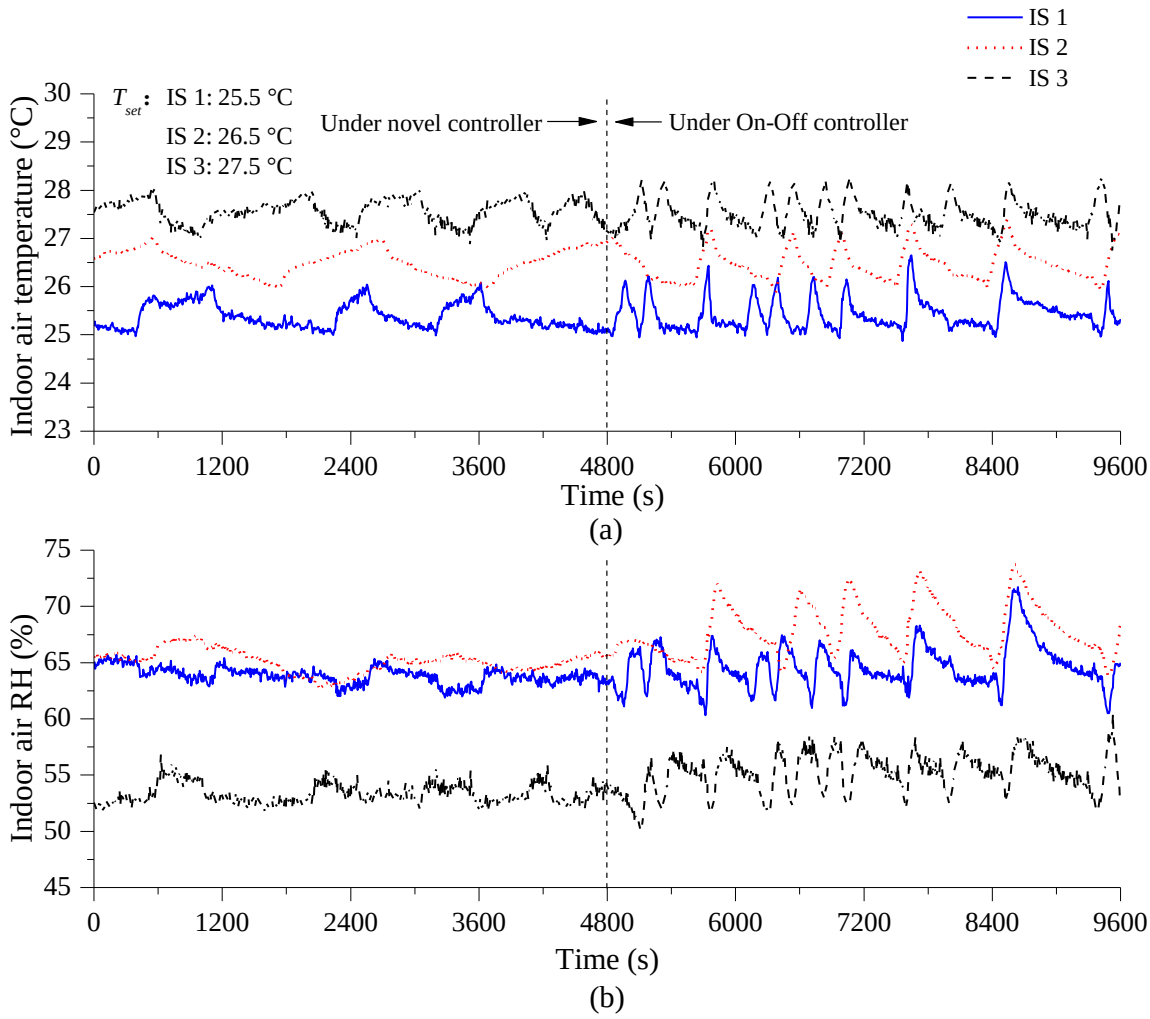

Fig. 7.11 Comparison of indoor air temperature and RH in all ISs between using the novel controller and a traditional On-Off controller (Test E8)

Fig. 7.11 shows the experimental results in Test E7. As seen, in the first half of the test when the novel controller was enabled, while indoor temperatures in the three ISs were controlled at around their respective setting points, indoor air RH levels varied with

small fluctuations, at around 0.90%, 1.57% and 1.47%, respectively. However, in the second half of the test, when the TEAC system was On-Off controlled, where the fluctuation ranges of indoor air temperatures in the three ISs were slightly greater than those under the novel controller, the fluctuations of indoor RH levels in the three ISs were around 2.27%, 2.78% and 2.58%, higher than those under the novel controller in the first half of the test.

Furthermore, in Test E8, at the same thermal loads in the three ISs throughout the entire test, the power input to compressor under the novel controller in the first half of the test was 2.42 kWh, which was 15.4% less than that under On-Off controller in the second half.

Therefore, the experiment results presented in this section demonstrated the successful development of the novel controller for a TEAC system by integrating previously developed temperature control algorithms for a DEAC system [Xu et al. 2013b] and a previously developed improved indoor humidity control algorithm for an SEAC system [Xu et al. 2008]. With the novel controller, improved control over indoor air temperature and RH, and better energy efficiency for a TEAC system can be obtained.

7.5. Conclusions

The development of a novel capacity controller for the experimental TEAC system for improved indoor humidity control is reported in this chapter. The novel controller was developed by integrating two previously developed control algorithms, one for temperature only control in an MEAC system, and the other for improved humidity control in an SEAC system. Both simulative and experimental controllability tests, using the validated TEAC model and the experimental TEAC system, respectively, were carried out and tests results are presented. Using the novel controller, not only indoor air dry-bulb temperatures in the three ISs can be directly controlled around their respective settings under a wide range of operation conditions, but also an improved control over indoor air humidity and energy saving of about 12.5% -15.4% could be achieved, as compared to the use of traditional On-Off controllers extensively used in MEAC systems. With a flexible structure, the novel controller, which was developed based on a TEAC system, can be extended to controlling MEAC systems with any number of IUs.

Chapter 8

Conclusions and future Work

8.1 Conclusions

A programmed research work on firstly investigating the coupled operating characteristics of the experimental TEAC system, secondly developing and validating a dynamic mathematical model for the TEAC system and finally developing a novel capacity controller for the TEAC system for improved indoor humidity control, has been successfully carried out and is reported in this thesis. The conclusions of the thesis are:

An experimental study on the operating characteristics of the experimental TEAC system has been carried out and the study results are reported in Chapter 5. The results demonstrated that when the operating parameters in only one of the IUs/ ISs varied, similar coupling effects of mutual influences to those reported in previous studies for DEAC systems may also be observed. However, when the operating parameters in two of the IUs/ ISs varied, the coupling effects became more complicated, with the mutual influences being more remarkable than that in the TEAC system when the operating parameters in only one of the IUs/ ISs were varied with even less variation magnitude. This would consequently imply that the coupling effects in an MEAC system can be

very complex, when the operating parameters in each of its multi-evaporators or the ISs can randomly vary. It is true that the dynamics and complexity of an MEAC system would increase with the increased number of IUs. Daikin [2015] reported that 128 IUs may be connected to a single outdoor unit. However, for better controllability, it may become necessary to have a maximum number of IUs, since coupling effects can be very complex. To solve this, a large MEAC system may be broken into a few smaller systems. Furthermore, in the current study, the changes on both refrigerant side and air side were studied, as the air side operating conditions, such as the temperature difference between supply air and indoor air setting could certainly constrain the changes of operating parameters on the refrigerant side.

The development and experimental validation of a physics-based dynamic mathematical model for the experimental TEAC system is presented in Chapter 6. Unlike all other reported MEAC models, the TEAC model developed specifically took into account both sensible and latent heat balances on the air side of all IUs. The model was experimentally validated by comparing the predicted and measured results, with an acceptable predicting error of not greater than ±6%.

A novel capacity controller for the experimental TEAC system has been developed by integrating two previously developed control algorithms, one for temperature only

control for an MEAC system, and the other for improved humidity control for an SEAC system. Both simulative and experimental controllability tests were carried out and tests results are presented in Chapter 7. Using the novel controller, not only indoor air dry-bulb temperatures in the three ISs can be directly controlled around their respective settings under a wide range of operating conditions, but also an improved control over indoor air humidity levels and energy saving of about 12.5% -15.4% could be achieved, as compared to the use of traditional On-Off controllers extensively used in MEAC systems.

The outcomes of the programmed research work reported in this thesis have made significant impacts to the advancement of MEAC technologies, contributing to better indoor thermal control and energy saving using MEAC systems. The coupled operating characteristics of the TEAC system reported in this thesis can be used as an important reference for the optimization of system design and developments of appropriate capacity controllers for MEAC systems. The mathematical model developed for the TEAC system and reported in this thesis is first of its kind, because, firstly, it was physics-based with full experimental validation, and secondly it specifically took into account both the sensible and latent heat balances on the air side of its IUs. It is therefore expected that the model can be used as an effective platform in studying the operating characteristics and developing advanced control strategies for a TEAC system,

in particular for achieving an improved indoor humidity control using a TEAC system. The successful development of the proposed novel capacity controller will help achieve better thermal comfort for occupants, improved IAQ and reduced energy use, through improved indoor air humidity. With a flexible structure, the novel controller, which was developed based on a TEAC system, can be extended to controlling MEAC systems with any number of IUs. While the outcomes of the programmed research work are expected to be globally applicable, they will be particularly useful in subtropical Hong Kong where dehumidification using A/C systems has always been a challenge.

8.2 Proposed further work

Following the successful completion of the research work reported in this thesis, a number of future possible studies are proposed as follows:

The experimental study reported in Chapter 5 illustrated the influences of indoor air temperature setting and EEV opening on the operating characteristics of the TEAC system. Other operating parameters, such as indoor air humidity and supply fan speed might also affect the operating characteristics of a TEAC system. Therefore, it is suggested that the influences of other operating parameters in an MEAC system on its operating characteristics should be further studied.

The dynamic mathematical model for the experimental TEAC system has been experimentally validated and used in assisting the development of the novel capacity controller for improved indoor humidity control using the TEAC system. Given its modular structure, modules for additional IUs/ ISs may be easily added to the current TEAC system model to obtain a mathematical model for an MEAC system having more than three IUs/ ISs. Further modeling study on the operating characteristics of an MEAC system having more than three IUs/ ISs shall therefore be carried out, as more complex coupling effects for the operating parameters in the MEAC system will be expected and shall therefore be investigated.

The development of a novel capacity controller for the experimental TEAC system for improved indoor humidity control is reported in Chapter 7. This has provided one practical way of using MEAC systems for controlling not only indoor air temperature but also air humidity. Nonetheless, with the current novel controller, while dry-bulb temperature in the three ISs can be directly controlled around their respective settings directly, indoor air RH are indirectly controlled. Therefore, further research on directly controlling indoor air humidity using MEAC systems should be carried out. Advanced control algorithms such as fuzzy logics, ANN can be applied.

Appendix A

Photos of the experimental TEAC system

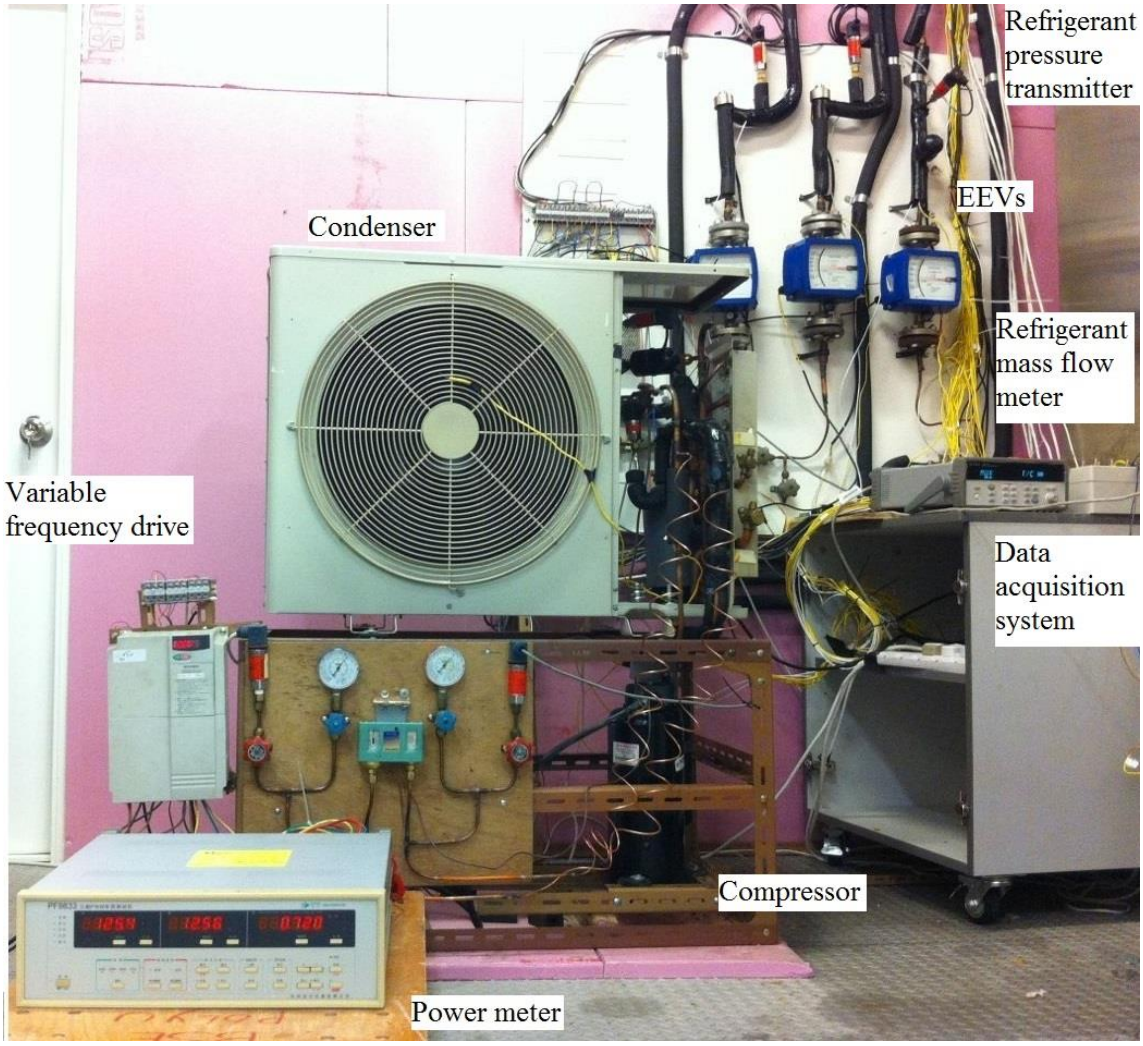

Photo 1 Overview of the experimental TEAC system

Photo 2 Overview of the indoor unit

Photo 3 Load generation unit inside each indoor space

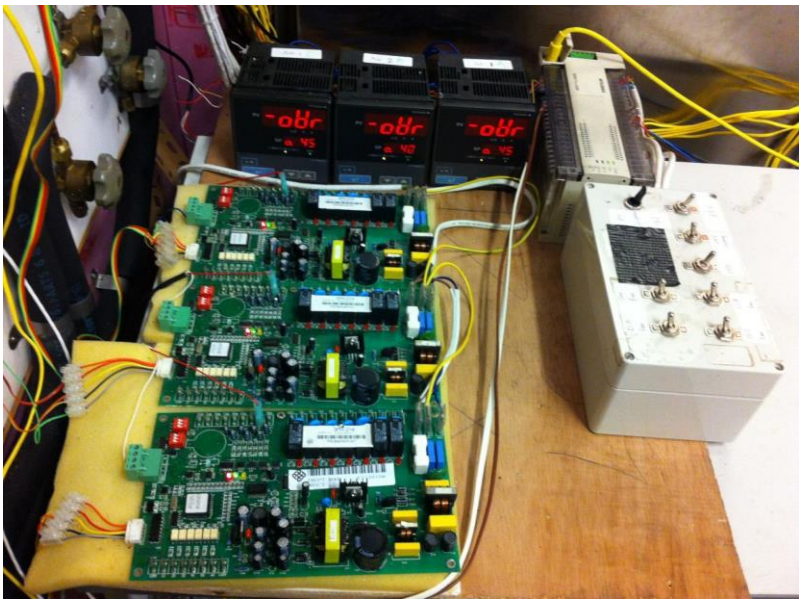

Photo 4 Control console

Appendix B

Publications arising from the thesis

Journal papers

Yan Huaxia, Deng Shiming, Chan Mingyin, Operating characteristics of a Three-evaporator air conditioning (TEAC) system. Applied Thermal Engineering, 103 (2016) 883-891. (Based on Chapter 5).

Yan Huaxia, Deng Shiming, Chan Mingyin, Developing and validating a dynamic mathematical model of a Three-evaporator air conditioning (TEAC) system. Applied Thermal Engineering, 100 (2016) 880-892. (Based on Chapter 6).

Yan Huaxia, Deng Shiming, Chan Mingyin, A novel capacity controller for a three-evaporator air conditioning (TEAC) system for improved indoor humidity control. Applied Thermal Engineering, 98 (2016): 1251–1262 (Based on Chapter 7).

Conference paper

Yan Huaxia and Shiming Deng. Transient simulation of a dual-evaporator air conditioning system for developing an improved humidity control strategy. Energy Procedia, 75 (2015): 1832-1837.

References

1. Afify 2008

   Afify R.

   Designing VRF systems. ASHRAE Journal, 50.6 (2008): 52-55.

2. Alpuche et al. 2005

   Alpuche M. G., Heard C., Best R. and Rojas J.

   Exergy analysis of air cooling systems in buildings in hot humid climates. Applied Thermal Engineering, 25.4 (2005): 507-517.

3. Amrane et al. 2003

   Amrane K., Hourahan G. and Potts G.

   Latent performance of unitary equipment. ASHRAE Journal, 45.1 (2003): 28-31.

4. Amarnath and Blatt 2008

   Amarnath A., and Blatt M.

   Variable refrigerant flow: where, why, and how. Engineered systems, 25.2 (2008): 54.

5. Andrade and Bullard 1999

   Andrade M. A. and Bullard C. W.

   Controlling indoor humidity using variable-speed compressors and blowers. Air Conditioning and Refrigeration Center. College of Engineering, University of

Illinois at Urbana-Champaign, 1999.

6. Andrade and Bullard 2002

Andrade M. A. and Bullard C. W.

Modulating blower and compressor capacities for efficient comfort control. ASHRAE Transactions, 108.1 (2002): 631-637.

7. Angrisani et al. 2012

Angrisani G., Minichiello F., Roselli C. and Sasso M.

Experimental analysis on the dehumidification and thermal performance of a desiccant wheel. Applied Energy, 92 (2012): 563-572.

8. ANSI 1985

ANSI/AMCA Standard 210.

Laboratory methods of testing fans for rating. ANSI, Arlington, VA (1985).

9. Aprea and Mastrullo 2002

Aprea C. and Mastrullo R.

Experimental evaluation of electronic and thermostatic expansion valves performances using R22 and R407C. Applied Thermal Engineering, 22.2 (2002): 205-218.

10. Aprea et al. 2004

Aprea C., Mastrullo R. and Renno C.

Fuzzy control of the compressor speed in a refrigeration plant. International

Journal of Refrigeration, 27.6 (2004): 639-648.

11. ASHRAE 1983

ASHRAE Standard 116.

Methods of Testing for Seasonal Efficiency of Unitary Air Conditioners and Heat Pumps. American Society of Heating, Refrigerating and Air-Conditioning Engineers, (1983).

12. ASHRAE 2001

ASHRAE Standard 62-2001.

Ventilation for acceptable indoor air quality. American Society of Heating, Refrigeration and Air-conditioning Engineers, Atlanta GA: (2001).

13. ASHRAE 2004

ASHRAE Standard 55-2004.

Thermal environmental conditions for human occupancy. American Society of Heating, Refrigeration and Air-conditioning Engineers, (2004).

14. ASHRAE 2007

ANSI/ASHRAE Standard 90.1-2007.

Energy Standard for buildings except low-rise residential buildings. American Society of Heating, Refrigeration and Air-conditioning Engineers, (2007).

15. Aynur et al. 2006

Aynur T. N., Hwang Y. and Radermacher R.

Field performance measurements of a VRV AC/ HP system. International Refrigeration and Air Conditioning Conference, (2006): Paper 756.

16. Aynur et al. 2008a

Aynur T. N., Hwang Y. and Radermacher R.

Experimental evaluation of the ventilation effect on the performance of a VRV system in cooling mode-Part I: Experimental evaluation. HVAC&R Research, 14.4 (2008): 615-630.

17. Aynur et al. 2008b

Aynur T. N., Hwang Y. and Radermacher R.

Field performance measurements of a heat pump desiccant unit in dehumidification mode. Energy and Buildings, 40.12 (2008): 2141-2147.

18. Aynur et al. 2008c

Aynur T. N., Hwang Y. and Radermacher R.

Simulation evaluation of the ventilation effect on the performance of a VRV system in cooling mode-Part II, simulation evaluation. HVAC&R Research, 14.5 (2008): 783-795.

19. Aynur 2010

Aynur T. N.

Variable refrigerant flow systems: A review. Energy and Buildings, 42.7 (2010): 1106-1112.

20. Berglund 1998

Berglund L. G.

Comfort and humidity. ASHRAE Journal, 40.8 (1998): 35.

21. Changenet et al. 2008

Changenet C., Charvet J. N., Géhin D., Sicard F. and Charmel B.

Study on predictive functional control of an expansion valve for controlling the evaporator superheat. Proceedings of the Institution of Mechanical Engineers, Part I: Journal of Systems and Control Engineering, 222.6 (2008): 571-582.

22. Chen et al. 2005

Chen W., Zhou X. X. and Deng S. M.

Development of control for multi-evaporator air conditioners (MEAC) method and dynamic model. Energy Conversion and Management, 46 (2005): 451-465.

23. Chen 2005

Chen W.

Modeling and control of a direct expansion (DX) variable-air-volume (VAV) air conditioning (A/C) system. PhD Thesis, The Hong Kong Polytechnic University, 2005.

24. Cheung and Braun 2014

Cheung H. and Braun J. E.

Component-based, gray-box modeling of ductless multi-split heat pump systems.

International Journal of Refrigeration, 38 (2014): 30-45.

25. Chi and Didion 1982

Chi J. and Didion D.

A simulation model of the transient performance of a heat pump. International Journal of Refrigeration, 5.3 (1982): 176-184.

26. Chiou et al. 2008

Chiou C. B., Chiou C. H., Chu C. M. and Lin S. L.

The study of energy-saving strategy for direct expansion air conditioning system. Energy and Buildings, 40.9 (2008): 1660-1665.

27. Chiou et al. 2009

Chiou C. B., Chiou C. H., Chu C. M. and Lin S. L.

The application of fuzzy control on energy saving for multi-unit room air-conditioners. Applied Thermal Engineering, 29.2 (2009): 310-316.

28. Cleland 1986

Cleland A. C.

Computer subroutines for rapid evaluation of refrigerant thermodynamic properties. International Journal of Refrigeration, 9.6 (1986): 346-351.

29. Choi and Kim 2003

Choi J. M. and Kim Y. C.

Capacity modulation of an inverter-driven multi-air conditioner using electronic

expansion valves. Energy, 28.2 (2003): 141-155.

30. Cuevas and Lebrun 2009

Cuevas C. and Lebrun J.

Testing and modelling of a variable speed scroll compressor. Applied Thermal Engineering, 29.2 (2009): 469-478.

31. DAIKIN 2015

DAIKIN VRV catalogue

http://www.daikin.co.uk/binaries/Daikin%20VRV%20Catalogue%202015_tcm511-370435.pdf. 2015.

32. Damasceno et al. 1990

Damasceno G. S., Goldschmidt V. W. and Rooke S. P.

Comparison of three steady-state heat pump computer models. ASHRAE Transactions, (1990).

33. Deng 2000

Deng S. M.

A dynamic mathematical model of a direct expansion (DX) water-cooled air-conditioning plant. Building and Environment, 35.7 (2000): 603-613.

34. Deng 2002

Deng S. M.

The application of feedforward control in a direct expansion (DX) air

conditioning plant. Building and Environment, 37.1 (2002): 35-40.

35. Deng et al. 2009

Deng S. M., Li Z. and Qu M. L.

Indoor thermal comfort characteristics under the control of a direct expansion air conditioning unit having a variable-speed compressor and a supply air fan. Applied Thermal Engineering, 29.11 (2009): 2187-2193.

36. Ding 2007

Ding G. L.

Recent developments in simulation techniques for vapour-compression refrigeration systems. International Journal of Refrigeration, 30.7 (2007): 1119-1133.

37. Dyer 2006

Dyer M. J.

Approaching 20 years of VRF in the UK. Modern Building Services, http://www.modbs.co.uk/news/fullstory.php/aid/2127/Approaching_20_years_of_VRF_in_the_UK.html, June, (2006).

38. Elliott and Rasmussen 2009

Elliott M. S. and Rasmussen B. P.

A model-based predictive supervisory controller for multi-evaporator HVAC systems. In American Control Conference, (2009): 3669-3674.

39. Elliott and Rasmussen 2013

Elliott M. S. and Rasmussen B. P.

Decentralized model predictive control of a multi-evaporator air conditioning system. Control Engineering Practice, 21.12 (2013): 1665-1677.

40. Elsarrag et al. 2005

Elsarrag E., M. Ali E. E. and Jain S.

Design guidelines and performance study on a structured packed liquid desiccant air-conditioning system. HVAC&R Research, 11.2 (2005): 319-337.

41. Fanger 1982

Fanger P. O.

Thermal comfort: analysis and applications in environmental engineering. (1982).

42. Fujimoto et al. 2011a

Fujimoto, I., Takemura K., Ueno K., Saito K. and Ohno K.

Performance evaluation of VRF systems using refrigerant enthalpy method. International Congress of Refrigeration, Prague, August 21–26, 2011.

43. Fujimoto et al. 2011b

Fujimoto I., Ueno K., Saito K., Ohno K., Murata H. and Nakamura H.

Performance evaluation of VRF systems. International Congress of Refrigeration, Prague, August 21–26, 2011.

44. Fujita et al. 1992

Fujita Y., Kubo T. and Suma S.

Multi-air conditioner with two indoor units. Refrigeration, 67.772 (1992): 171-176.

45. Goetzler 2007

Goetzler W.

Variable refrigerant flow systems. ASHRAE Journal, 49.4 (2007): 24-31.

46. Gordon et al. 1999

Gordon B. W., Liu S. and Asada H. H.

Dynamic modeling of multiple-zone vapor compression cycles using variable order representations. American Control Conference, 1999. Proceedings of the 1999. Vol. 6. IEEE.

47. Hai et al. 2006

Hai X. H., Jun S., Hang Z. and Bin T.

Design and research of the digital VRV multi-connected units with three pipes type heat recovery system. International Refrigeration and Air Conditioning Conference, (2006): Paper 786.

48. Harriman et al. 2000

Harriman L. G., Lstiburek J. and Kittler R.

Improving humidity control for commercial buildings. ASHRAE Journal, 42.11

(2000): 24-32.

49. He et al. 1997

He X. D., Liu S. and Asada H. H.

Modeling of vapor compression cycles for multivariable feedback control of HVAC systems. Journal of Dynamic Systems, Measurement and Control, 119.2 (1997): 183-191.

50. He et al. 1998

He X. D., Liu S., Asada H. H. and Itoh H.

Multivariable control of vapor compression systems. HVAC&R Research, 4.3 (1998): 205-230.

51. He and Asada 2003

He X. D., and Asada H. H.

A new feedback linearization approach to advanced control of multi-unit HVAC systems. American Control Conference, Vol. 3 (2003): 2311-2316

52. Henderson et al. 1993

Henderson H. I., Rengarajan K. and Shirey D. B.

The impact of comfort control on air conditioner energy use in humid climates. Transactions-American Society of Heating Refrigerating and Air Conditioning Engineers, 98 (1993): 104.

53. Hirao et al. 1992

Hirao T., Ohzeki S., Imaiida T. and Kobayashi S.

Prediction of performance and stability of heat pump systems with long pipes and high head. ASHRAE Winter Meeting, Anaheim, CA, USA, (1992): 411-419.

54. Hong and Webb 1996

Hong K. T. and Webb R. L.

Calculation of fin efficiency for wet and dry fins. HVAC&R Research, 2.1 (1996): 27-41.

55. Hu and Yang 2005

Hu S. C. and Yang R. H.

Development and testing of a multi-type air conditioner without using AC inverters. Energy Conversion and Management, 46.3 (2005): 373-383.

56. Huang et al. 2008

Huang H., Li Q., Yuan D., Qin Z. and Zhang Z.

An experimental study on variable air volume operation of ducted air-conditioning with digital scroll compressor and conventional scroll compressor. Applied Thermal Engineering, 28.7 (2008): 761-766.

57. Huh and Brandemuehl 2008

Huh J. H. and Brandemuehl M. J.

Optimization of air-conditioning system operating strategies for hot and humid

climates. Energy and Buildings, 40.7 (2008): 1202-1213.

58. Jia et al. 1995

Jia X., Tso C. P., Chia P. K. and Jolly P.

A distributed model for prediction of the transient response of an evaporator. International Journal of Refrigeration, 18.5 (1995): 336-342.

59. Jiang et al. 2006

Jiang W., Khan J. and Dougal R. A.

Dynamic centrifugal compressor model for system simulation. Journal of Power Sources, 158.2 (2006): 1333-1343.

60. Joo et al. 2011

Joo Y., Kang H., Ahn J. H., Lee M. and Kim Y.

Performance characteristics of a simultaneous cooling and heating multi-heat pump at partial load conditions. International Journal of Refrigeration, 34.4 (2011): 893-901.

61. Kang et al. 2009

Kang H., Joo Y., Chung H., Kim Y. and Choi J.

Experimental study on the performance of a simultaneous heating and cooling multi-heat pump with the variation of operation mode. International Journal of Refrigeration, 32.6 (2009): 1452–1459.

62. Kandlikar 1990

Kandlikar S. G.

A general correlation for saturated two-phase flow boiling heat transfer inside horizontal and vertical tubes. Journal of Heat Transfer, 112.1 (1990): 219-228.

63. Karunakaran et al. 2010

Karunakaran R., Iniyan S. and Goic R.

Energy efficient fuzzy based combined variable refrigerant volume and variable air volume air conditioning system for buildings. Applied Energy, 87.4 (2010): 1158-1175.

64. Kasahara 2000

Kasahara M.

Physical model of an air-conditioned space for control analysis. ASHRAE Transactions: Research, 106 (2000): 304-317.

65. Kishi et al. 2009

Kishi R., Saijo Y., Kanazawa A., Tanaka M., Yoshimura T., Chikara H., Takigawa T., Morimoto K., Nakayama K. and Shibata E.

Regional differences in residential environments and the association of dwellings and residential factors with the sick house syndrome: a nationwide cross‐sectional questionnaire study in Japan. Indoor Air, 19.3 (2009): 243-254.

66. Koeln et al. 2012

Koeln J. P., Kania M. D., Jain N. and Alleyne A. G.

Experimental Load Emulation for Multi-Evaporator Air Conditioning and Refrigeration Systems. International Refrigeration and Air Conditioning Conference, (2012): Paper 1284.

67. Koeln and Alleyne 2013

Koeln J. P. and Alleyne A. G.

Decentralized controller analysis and design for multi-evaporator vapor compression systems. In American Control Conference, (2013): 437-442.

68. Kosar 2006

Kosar D.

Dehumidification system enhancements. ASHRAE Journal, 48.2 (2006): 48-58.

69. Kwon et al. 2014

Kwon L., Lee H., Hwang Y., Radermacher R. and Kim B.

Experimental investigation of multifunctional VRF system in heating and shoulder seasons. Applied Thermal Engineering, 66.1 (2014): 355–364.

70. Lam 2000

Lam C. J.

Energy analysis of commercial buildings in subtropical climates. Building and Environment, 35.1 (2000): 19-26.

71. Lee et al. 2002

Lee G., Kim M. S. and Cho Y. M.

An experimental study of the capacity control of multi-type heat pump system using predictive control logic. 7th International Energy Agency Heat Pump Conference, (2002): 158-165.

72. Lee et al. 2011

Lee I. H., Choi J. W. and Kim M. S.

Studies on the heating capacity control of a multi-type heat pump system applying a multi-input multi-output (MIMO) method. International Journal of Refrigeration, 34.2 (2011): 416-428.

73. Li and Deng 2007a

Li Z. and Deng S. M.

An experimental study on the inherent operational characteristics of a direct expansion (DX) air conditioning (A/C) unit. Building and Environment, 42.1 (2007): 1-10.

74. Li and Deng 2007b

Li Z. and Deng S. M.

A DDC-based capacity controller of a direct expansion (DX) air conditioning (A/C) unit for simultaneous indoor air temperature and humidity control–Part I: Control algorithms and preliminary controllability tests. International Journal of

Refrigeration, 30.1 (2007): 113-123.

75. Li and Deng 2007c

Li Z. and Deng S. M.

A DDC-based capacity controller of a direct expansion (DX) air conditioning (A/C) unit for simultaneous indoor air temperature and humidity control–Part II: Further development of the controller to improve control sensitivity. International Journal of Refrigeration, 30.1 (2007): 124-133.

76. Li and Wu 2010

Li Y. M. and Wu J. Y.

Energy simulation and analysis of the heat recovery variable refrigerant flow system in winter. Energy and Buildings, 42.7 (2010): 1093–1099.

77. Li et al. 2009

Li Y. M., Wu J. Y. and Shiochi S.

Modeling and energy simulation of the variable refrigerant flow air conditioning system with water-cooled condenser under cooling conditions. Energy and Buildings, 41.9 (2009): 949-957.

78. Li et al. 2010

Li Y. M., Wu J. Y. and Shiochi S.

Experimental validation of the simulation module of the water-cooled variable

refrigerant flow system under cooling operation. Applied Energy, 87.5 (2010): 1513–1521.

79. Li et al. 2013

Li N., Xia L., Deng S. M., Xu X. G. and Chan M. Y.

On-line adaptive control of a direct expansion air conditioning system using artificial neural network. Applied Thermal Engineering, 53.1 (2013): 96-107.

80. Li 2013a

Li W. H.

Simplified steady-state modeling for variable speed compressor. Applied Thermal Engineering, 50.1 (2013): 318-326.

81. Li 2013b

Li W. H.

Simplified modeling analysis of mass flow characteristics in electronic expansion valve. Applied Thermal Engineering, 53.1 (2013): 8-12.

82. Li et al. 2014

Li Z., Xu X. G., Deng S. M. and Pan D. M.

Further study on the inherent operating characteristics of a variable speed direct expansion air conditioning system, Applied Thermal Engineering, 66.1 (2014): 206-215.

83. Li et al. 2015

Li Z., Xu X. G., Deng S. M. and Pan D. M.

A novel neural network aided fuzzy logic controller for a variable speed (VS) direct expansion (DX) air conditioning (A/C) system. Applied Thermal Engineering, 78 (2015): 9-23.

84. Lijima et al. 1991

Lijima H., Tanaka N., Sumida Y. and Nakamura T.

Development of a new multi-system air conditioner with concurrent heating and cooling operation. ASHRAE Transactions, 97.2 (1991): 309-315.

85. Lin and Yeh 2007a

Lin J. L. and Yeh T. J.

Modeling, identification and control of air-conditioning systems. International Journal of Refrigeration, 30 (2007): 209-220.

86. Lin and Yeh 2007b

Lin J. L. and Yeh T. J.

Identification and control of multi-evaporator air-conditioning systems. International Journal of Refrigeration, 30.8 (2007): 1374-1385.

87. Lin and Yeh 2009a

Lin J. L. and Yeh T. J.

Control of multi-evaporator air-conditioning systems for flow distribution.

Energy Conversion and Management, 50.6 (2009): 1529-1541.

88. Lin and Yeh 2009b

Lin J. L. and Yeh T. J.

Identification and control of multi-evaporator air conditioning systems. International Journal of Refrigeration, 30.8 (2007): 1374-1385.

89. Ling et al. 2011

Ling J., Kuwabara O., Hwang Y. and Radermacher R.

Experimental evaluation and performance enhancement prediction of desiccant assisted separate sensible and latent cooling air-conditioning system. International Journal of Refrigeration, 34.4 (2011): 946-957.

90. Lu et al. 2009

Lu H. L., Chen H. X., Xie J. L. Tao H. G. and Hu Y. P.

Refrigerant flow distributary disequilibrium caused by configuration of two phase fluid pipe network. Energy Conversion and Management, 50.3 (2009): 730-738.

91. MacArthur and Grald 1987

MacArthur J. W. and Grald E. W.

Prediction of cyclic heat pump performance with a fully distributed model and a comparison with experimental data. ASHRAE Transactions, (1987):1159-1178.

92. Masuda et al. 1991

Masuda M., Wakahara K. and Marsuki K.

Development of a multi-system air conditioner for residential use. ASHRAE Transactions, 97 (1991): 127-131.

93. McGahey 1998

McGahey K.

New commercial applications for desiccant-based cooling. ASHRAE Journal, 40.7 (1998): 41-45.

94. Meissner et al. 2014

Meissner J. W., Abadie M. O., Moura L. M., Mendonça K. C. and Mendes N.

Performance curves of room air conditioners for building energy simulation tools. Applied Energy, 129 (2014): 243-252.

95. Mei and Levermore 2002

Mei L. and Levermore G. J.

Simulation and validation of a VAV system with an ANN fan model and a non-linear VAV box model. Building and environment, 37.3 (2002): 277-284.

96. Moody 1944

Moody L. F.

Friction factors for pipe flow. Trans. Asme, 66.8 (1944): 671-684.

97. Nagaya et al. 2006

Nagaya K., Senbongi T., Li Y., Zheng J. and Murakami I.

High energy efficiency desiccant assisted automobile air-conditioner and its temperature and humidity control system. Applied thermal engineering, 26.14 (2006): 1545-1551.

98. Okuzawa 1992

Okuzawa Y.

One system family air conditioning: multi-system air conditioner for 4-6 rooms. Refrigeration, 67 (1992): 149-56.

99. Olesen and Brager 2004

Olesen B. W. and Brager G. S.

A better way to predict comfort: The new ASHRAE standard 55-2004. ASHRAE Journal, 8 (2004).

100. Osanyintola and Simonson 2006

Osanyintola O. F. and Simonson C. J.

Moisture buffering capacity of hygroscopic building materials: Experimental facilities and energy impact. Energy and Buildings, 38.10 (2006): 1270-1282.

101. Otten 2010

Otten R. J.

Superheat control for air conditioning and refrigeration systems: Simulation and

experiments. M. S. Thesis, University of Illinois at Urbana-Champaign, (2010).

102. Paasi et al. 2001

Paasi J., Nurmi S., Vuorinen R., Strengell S. and Maijala P.

Performance of ESD protective materials at low relative humidity. Journal of Electrostatics, 51 (2001): 429-434.

103. Pan et al. 2012

Pan Y., Xu X. G., Xia L. and Deng S. M.

A modeling study on the effects of refrigerant pipeline length on the operational performance of a dual-evaporator air conditioning system. Applied Thermal Engineering, 39 (2012): 15-25.

104. Pan et al. 2014

Pan Y., Lorente S., Bejan A., Xia L. and Deng S. M.

Distribution of size in multi‐evaporator air conditioning systems. International Journal of Energy Research, 38.5 (2014): 652-657.

105. Parameshwaran et al. 2010

Parameshwaran R., Karunakaran R., Kumar C. V. R. and Iniyan S.

Energy conservative building air conditioning system controlled and optimized using fuzzy-genetic algorithm. Energy and Buildings, 42.5 (2010): 745-762.

106. Park et al. 2001

Park Y. C., Young C. K. and Min M. K.

Performance analysis on a multi-type inverter air conditioner. Energy Conversion and Management, 42.13 (2001): 1607-1621.

107. Park et al. 2007

Park C., Cho H., Lee Y. and Kim Y.

Mass flow characteristics and empirical modeling of R22 and R410A flowing through electronic expansion valves. International Journal of Refrigeration, 30.8 (2007): 1401-1407.

108. Pérez-Lombard and Pout 2008

Pérez-Lombard L., Ortiz J. and Pout C.

A review on buildings energy consumption information. Energy and Buildings, 40.3 (2008): 394-398.

109. Qi and Deng 2009

Qi Q. and Deng S.M.

Multivariable control of indoor air temperature and humidity in a direct expansion (DX) air conditioning (A/C) system. Building and Environment, 44.8 (2009): 1659-1667.

110. Qureshi and Tassou 1996

Qureshi T. Q. and Tassou S. A.

Variable-speed capacity control in refrigeration systems. Applied Thermal Engineering, 16.2 (1996): 103-113.

111. Rasmussen and Jakobsen 2000

Rasmussen B. D. and Jakobsen A.

Review of compressor models and performance characterizing variables. International Compressor Engineering Conference, (2000): Paper 1429.

112. Rasmussen and Alleyne 2004

Rasmussen B. P. and Alleyne A. G.

Control-oriented modeling of transcritical vapor compression systems. Journal of Dynamic Systems, Measurement, and Control, 126.1 (2004): 54-64.

113. Raustad 2013

Raustad R.

A variable refrigerant flow heat pump computer model in EnergyPlus. ASHRAE Transactions, 119 (2013): 299–308.

114. Reinikainen and Jaakkola 2003

Reinikainen L. M. and Jaakkola J. J. K.

Significance of humidity and temperature on skin and upper airway symptoms. Indoor Air, 13.4 (2003): 344-352.

115. Shah et al. 2003

Shah R., Alleyne A.G. and Bullard C.W.

Dynamic modeling and control of single and multi-evaporator subcritical vapor compression systems, Air Conditioning and Refrigeration Center. College of

Engineering, University of Illinois at Urbana-Champaign, (2003).

116. Shah et al. 2004

Shah R., Alleyne A. G. and Bullard C. W.

Dynamic Modeling and Control of Multi-Evaporator Air-Conditioning Systems. ASHRAE Transactions, 110.1 (2004): 109-119.

117. Shao et al. 2008

Shao S., Shi W., Li X. and Yan Q.

Simulation model for complex refrigeration systems based on two-phase fluid network–Part I: Model development. International Journal of Refrigeration, 31.3 (2008): 490-499.

118. Shao et al. 2012

Shao S., Xu H. and Tian C.

Dynamic simulation of multi-unit air conditioners based on two-phase fluid network model. Applied Thermal Engineering, 40 (2012): 378–388.

119. Shen and Rice 2012

Shen B. and Rice C. K.

Multiple-zone variable refrigerant flow system modeling and equipment performance mapping. ASHRAE Winter Conference, Chicago, IL, January 21–25, 2012.

120. Shen et al. 2013

Shen B., Rice C. K., Mcdowell T. P. and Baxter V. D.

Energy simulation of integrated multiple- zone variable refrigerant flow system. ASHARE Annual Conference, Denver, CO, (2013): 22–26.

121. Shi et al. 2003

Shi W., Shao S., Li X., Peng X. and Yang X.

A Network Model to Simulate Performance of Variable Refrigerant Volume Refrigeration Systems. ASHRAE Transactions-American Society of Heating Refrigerating Air Conditioning Engineers, 109.2 (2003): 61-68.

122. Shi et al. 2008

Shi W., Shao S., Li X. and Yan Q.

Simulation model for complex refrigeration systems based on two-phase fluid network–Part II: Model application. International Journal of Refrigeration, 31.3 (2008): 500-509.

123. Shirey et al. 2003

Shirey III D. B. and Raustad R. A.

Understanding the Dehumidification Performance of Air-Conditioning Equipment at Part-Load Conditions. Presented at the CIBSE/ASHRAE Conference, 9.1 (2003): 24-26.

124. Sunwoo et al. 2006

Sunwoo Y., Chou C., Takeshita J., Murakami M. and Tochihara Y.

Physiological and subjective responses to low relative humidity in young and elderly men. Journal of Physiological Anthropology, 25.3 (2006): 229-238.

125. Toftum et al. 1998a

Toftum J., Jørgensen A. S. and Fanger P. O.

Upper limits for indoor air humidity to avoid uncomfortably humid skin. Energy and Buildings, 28.1 (1998): 1-13.

126. Toftum et al. 1998b

Toftum J., Jørgensen A. S. and Fanger P. O.

Upper limits of air humidity for preventing warm respiratory discomfort. Energy and Buildings, 28.1 (1998): 15-23.

127. Toftum and Fanger 1999

Toftum J. and Fanger P. O.

Air humidity requirements for human comfort. ASHRAE Transactions, 99 (1999).

128. Tu et al. 2011

Tu Q., Dong K., Zou D. and Lin Y.

Experimental study on multi-split air conditioner with digital scroll compressor. Applied Thermal Engineering, 31.14 (2011): 2449-2457.

129. Vakiloroaya et al. 2014

Vakiloroaya V., Samali B., Fakhar A. and Pishghadam K.

A review of different strategies for HVAC energy saving, Energy Conversion and Management, 77 (2014): 738-754.

130. Wang 1997

Wang S. J.

Power consumption comparison of air cooled and water-cooled chiller units. HV and AC, 27.3 (1997): 24-25.

131. Wang et al. 1999

Wang C. C., Lee C. J., Chang C. T. and Lin S. P.

Heat transfer and friction correlation for compact louvered fin-and-tube heat exchangers. International Journal of Heat and Mass Transfer, 42.11 (1999): 1945-1956.

132. Wang et al. 2000

Wang C. C., Lin Y. T. and Lee C. J.

Heat and momentum transfer for compact louvered fin-and-tube heat exchangers in wet conditions. International Journal of Heat and Mass Transfer, 43.18 (2000): 3443-3452.

133. Wang 2014

Wang S.

Energy modeling of ground source heat pump vs. variable refrigerant flow systems in representative US climate zones. Energy and Buildings, 72 (2014): 222–228.

134. Welsby et al. 1988

Welsby P., Devotta S. and Diggory P. J.

Steady-and dynamic-state simulations of heat-pumps. Part I: Literature review, Applied energy, 31.3 (1988): 189-203.

135. Winkler et al. 2008

Winkler J., Aute V. and Radermacher R.

Comprehensive investigation of numerical methods in simulating a steady-state vapor compression system. International Journal of Refrigeration, 31 (2008): 930-942.

136. Winterton 1998

Winterton R. H. S.

Where did the Dittus and Boelter equation come from? International Journal of Heat and Mass Transfer, 41.4 (1998): 809-810.

137. Xia et al. 2002

Xia J., Winandy E., Georges B. and Lebrun J.

Testing methodology for VRF systems. International Refrigeration and Air Conditioning, (2002): Paper 542.

138. Xia et al. 2003

Xia J., Zhou X., Jin X. and Wu Y.

Simulation study on operating characteristics of multi-evaporator VRV air conditioner, (2003) 1-7.

139. Xia et al. 2004

Xia J., Winandy E., Georges B. and Lebrun J.

Experimental analysis of the performances of variable refrigerant flow systems. Building Services Engineering Research and Technology, 25.1 (2004): 17-23.

140. Xu et al. 2008

Xu X. G., Deng S. M. and Chan M. Y.

A new control algorithm for direct expansion air conditioning systems for improved indoor humidity control and energy efficiency. Energy Conversion and Management, 49.4 (2008): 578-586.

141. Xu et al. 2010

Xu X. G., Xia L., Chan M. Y. and Deng S. M.

Inherent correlation between the total output cooling capacity and equipment sensible heat ratio of a direct expansion air conditioning system under variable-speed operation (XXG SMD SHR DX AC unit). Applied Thermal Engineering, 30.13 (2010): 1601-1607.

142. Xu et al. 2013a

Xu X. G., Shen C. and Deng S. M.

Using two parallel connected compressors to implement a novel control algorithm for improved indoor humidity at a low cost. Building Services Engineering Research and Technology, 34.3 (2013): 349-354.

143. Xu et al. 2013b

Xu X. G., Pan Y., Deng S. M. and Xia L.

Experimental study of a novel capacity control algorithm for a multi-evaporator air conditioning system. Applied Thermal Engineering, 50.1 (2013): 975-984.

144. Yao et al. 2013

Yao Y., Yang K., Huang M. and Wang L.

A state-space model for dynamic response of indoor air temperature and humidity. Building and Environment, 64 (2013): 26-37.

145. Zhang and Zhang 2006

Zhang W. J. and Zhang C. L.

A generalized moving-boundary model for transient simulation of dry-expansion evaporators under larger disturbances. International Journal of Refrigeration, 29.7 (2006): 1119-1127.

146. Zhang and Zhang 2011

Zhang W. J. and Zhang C. L.

Transient modeling of an air conditioner with a rapid cycling compressor and multi-indoor units, Energy conversion and management, 52.1 (2011): 1-7.

147. Zhao et al. 2011

Zhao K., Liu X. H., Zhang T. and Jiang Y.

Performance of temperature and humidity independent control air-conditioning system in an office building. Energy and Buildings, 43.8 (2011): 1895-1903.

148. Zhou et al. 2007

Zhou Y. P., Wu J. Y., Wang R. Z. and Shiochi S.

Energy simulation in the variable refrigerant flow air-conditioning system under cooling conditions. Energy and Buildings, 39.2 (2007): 212-220.

149. Zhou et al. 2008

Zhou Y. P., Wu J. Y., Wang R. Z., Shiochi S. and Li Y. M.

Simulation and experimental validation of the variable-refrigerant-volume (VRV) air-conditioning system in EnergyPlus. Energy and Buildings, 40.6 (2008): 1041–1047.

150. Zhu et al. 2013

Zhu Y., Jin X., Du Z., Fan B. and Fu S.

Generic simulation model of multi-evaporator variable refrigerant flow air conditioning system for control analysis. International Journal of Refrigeration, 36.6 (2013): 1602–1615.

151. Zhu et al. 2014a

Zhu Y., Jin X., Du Z., Fan B. and Fang X.

Simulation of variable refrigerant flow air conditioning system in heating mode combined with outdoor air processing unit. Energy and Buildings, 68 (2014): 571-579.

152. Zhu et al. 2014b

Zhu Y., Jin X., Du Z., Fang X. and Fan B.

Control and energy simulation of variable refrigerant flow air conditioning system combined with outdoor air processing unit. Applied Thermal Engineering, 64.1 (2014): 385–95.

153. Zivi 1964

Zivi S. M.

Estimation of steady-state steam void-fraction by means of the principle of minimum entropy production. Journal of Heat Transfer, 86.2 (1964): 247-251.